

action
4021

UM-HSRI-77-39-1

**WHOLE BODY RESPONSE
RESEARCH PROGRAM**

**N. M. Alem
J. W. Melvin
B. M. Bowman
J. B. Benson**

**FINAL REPORT
APRIL 1978**



**THE UNIVERSITY OF MICHIGAN
HIGHWAY SAFETY RESEARCH INSTITUTE**

UM-HSRI-77-39-1

WHOLE BODY RESPONSE RESEARCH PROGRAM

Final Report

By

Nabih M. Alem
John W. Melvin
Bruce M. Bowman
Joseph B. Benson

prepared for

Biomedical Science Department
General Motors Research Laboratories
Warren, Michigan 48090

April 25, 1978

Biomechanics Department
Highway Safety Research Institute
The University of Michigan
Ann Arbor, Michigan 48109

Technical Report Documentation Page

1. Report No. UM-HSRI-77-39-1	2. Government Accession No.	3. Recipient's Catalog No.	
4. Title and Subtitle Whole Body Response Research Program		5. Report Date April 25, 1978	
		6. Performing Organization Code	
7. Author(s) N.M. Alem, J.W. Melvin, B.M. Bowman, J.B. Benson		8. Performing Organization Report No. UM-HSRI-77-39-1	
9. Performing Organization Name and Address Highway Safety Research Institute The University of Michigan Huron Parkway and Baxter Road Ann Arbor, Michigan 48109		10. Work Unit No. (TRAIS) 320316	
		11. Contract or Grant No. 77-375-KE1	
12. Sponsoring Agency Name and Address General Motors Research Laboratories GM Tech Center 12 Mile and Mound Roads Warren, Michigan 48042		13. Type of Report and Period Covered Final 7-1-73 to 8-31-77	
		14. Sponsoring Agency Code	
15. Supplementary Notes			
16. Abstract The general objective of this program was to generate data on the kinematics and response of human surrogates in a realistic automobile impact environment. The program used a test configuration consisting of an idealized hard seat representation of a car seat with a three-point harness restraint system. Three different severity levels of crash test conditions were used. The human surrogates tested in this program were fifteen male cadavers, a Hybrid II (Part 572) Anthropomorphic Test Device and a Hybrid III ATD recently developed by GM. In addition, mathematical simulations of the response and kinematics of a 50th percentile male occupant were performed at the three levels of crash severity, using the MVMA Two-Dimensional Crash Victim Simulator. The data that has been produced by this program represents one of the most comprehensive and extensive documentations of whole-body response to date. The primary utility of the data is for comparing the similarities and differences in response and kinematics of the various types of human surrogates and in pointing out areas that need improvement in both anthropomorphic test devices and mathematical models.			
17. Key Words Whole-Body Kinematics; Cadaver Anthropometry; 3-D Motion; X-Ray Measurements; Head Injury Criterion; Digital Filtering & Processing.		18. Distribution Statement Unlimited	
19. Security Classif. (of this report) Unclassified	20. Security Classif. (of this page) Unclassified	21. No. of Pages 108	22. Price

ACKNOWLEDGEMENTS

The authors wish to acknowledge the contributions and efforts of the entire Biomechanics Department team at HSRI, who made it possible to carry out the Whole Body Response research program.

In particular, we wish to thank Mr. Guy Nusholtz for his assistance in the development of the surgical techniques and performing the surgery, Dr. Richard Stalnaker for his help in development of experimental and surgical methods, Mr. Max Bender for his radiology work, Dr. Mac Reynolds for the anthropometry work, Mr. Marv Dunlap for the instrumentation and electronics development, Mr. Jean Brindamour for the photography, Mr. Don Erb for machining the hardware, Mr. Roger Culver for his assistance in sled preparation and help during and after each test, Mr. Garry Holstein for diligent computer programming, and finally, Mrs. Kay Saucier for the secretarial duties and her patience in dealing with all of us.

The guidance and advice offered by the staff of the GMRL's Biomedical Science Department has been most appreciated. Most helpful were the encouragement and understanding of Drs. Gerald Nyquist and Harold Mertz during the rough initial phases of the program. The continuing support and guidance of Dr. J. Vostal, Mr. John Horsch and Dr. David Viano to carry out the goals of this research effort are greatly appreciated.

TABLE OF CONTENTS

<u>CHAPTER</u>	<u>PAGE</u>
1. INTRODUCTION	1
1.1. Program Objectives	1
1.2. General Approach	2
1.3. Progress Review	3
1.3.1. Review Of 1973-74 Year	4
1.3.2. Review Of 1974-75 Year	4
1.3.3. Review Of 1975-76 Year	5
1.3.4. Review Of 1976-77 Year	5
1.4. Report Outline	6
2. TESTING AND ANALYSIS METHODS	9
2.1. Surgical Techniques	10
2.1.1. Head Accelerometer Mounting	10
2.1.2. Thoracic Accelerometer Mounting	11
2.1.3. Pelvic Accelerometer Mounting	11
2.1.4. Photographic Targets	11
2.2. Digital Signal Processing	12
2.2.1. A-to-D Conversion	13
2.2.2. Digital Filtering	15
2.3. Analytical Measurement Methods	16
2.3.1. 3-D Accelerometry	16
2.3.2. 3-D Photogrammetry	17
2.3.3. Fast HIC Computation	18
3. DESCRIPTION OF TESTS	19
3.1. Test Conditions	19
3.2. Cadaver Selection And Description	22
3.3. Anthropomorphic Test Devices	26

TABLE OF CONTENTS (continued)

<u>CHAPTER</u>	<u>PAGE</u>
4. EXPERIMENTAL RESULTS	27
4.1. Thoracic Damage	27
4.2. Kinematic Responses	30
5. COMPUTER SIMULATIONS	69
5.1. Description Of Simulations	70
5.1.1. Cadaver Model	70
5.1.2. Restraint System Model	71
5.1.3. Initial Configuration	71
5.1.4. Sled Accelerations	72
5.2. Results Of Simulations	73
5.2.1. Printer-Plot Sequence	74
5.2.2. Low-Severity Results	75
5.2.3. Medium-Severity Results	78
5.2.4. High-Severity Results	78
5.3. Discussion Of Simulations	79
6. DISCUSSION OF RESULTS	93
6.1. Factors Influencing The Experimental Results	93
6.1.1. Effects Of Repeated Tests	93
6.1.2. Effects Of Embalming	96
6.2. Comparison Of Human Surrogate Test Results	97
6.2.1. Head-Neck Response	97
6.2.2. Chest Response	100
6.2.3. Pelvis Response	101
6.2.4. Restraint System Loads	101

TABLE OF CONTENTS (continued)

<u>CHAPTER</u>	<u>PAGE</u>
7. CONCLUSIONS	103
7.1. Experimental Methods	103
7.2. Analytical Methods	104
7.3. Computer Simulations	104
7.4. Some Aspects Of The Results	105
8. REFERENCES	107

LIST OF FIGURES

<u>FIGURE</u>	<u>PAGE</u>
1. Flow-Chart of Data Handling System in Operation at HSRI for Biomechanical Experiments.	13
2. Diagram of Seating and Positioning in All Whole- Body Response Tests.	20
3. Typical Sled Deceleration Profiles at Three Severity Levels Used in the WBR Testing Program.	21
4. Resultant Head Angular Acceleration Low-Severity Sled Runs -- A Composite Plot.	32
5. Resultant Head Angular Acceleration Mid-Severity Sled Runs -- A Composite Plot.	33
6. Resultant Head Angular Acceleration High-Severity Sled Runs -- A Composite Plot.	34
7. Resultant Head Angular Velocity Low-Severity Sled Runs -- A Composite Plot.	35
8. Resultant Head Angular Velocity Mid-Severity Sled Runs -- A Composite Plot.	36
9. Resultant Head Angular Velocity High-Severity Sled Runs -- A Composite Plot.	37
10. Resultant Head Center-of-Mass Acceleration. Low-Severity Sled Runs -- A Composite Plot.	38
11. Resultant Head Center-of-Mass Acceleration. Mid-Severity Sled Runs -- A Composite Plot.	39
12. Resultant Head Center-of-Mass Acceleration. High-Severity Sled Runs -- A Composite Plot.	40
13. Resultant Head Center-of-Mass Velocity. Low-Severity Sled Runs -- A Composite Plot.	41
14. Resultant Head Center-of-Mass Velocity. Mid-Severity Sled Runs -- A Composite Plot.	42

LIST OF FIGURES (continued)

<u>FIGURE</u>	<u>PAGE</u>
15. Resultant Head Center-of-Mass Velocity. High-Severity Sled Runs -- A Composite Plot.	43
16. Internal Chest A-P Acceleration. Low-Severity Sled Runs -- A Composite Plot.	44
17. Internal Chest A-P Acceleration. Mid-Severity Sled Runs -- A Composite Plot.	45
18. Internal Chest A-P Acceleration. High-Severity Sled Runs -- A Composite Plot.	46
19. External Chest A-P Acceleration. Low-Severity Sled Runs -- A Composite Plot.	47
20. External Chest A-P Acceleration. Mid-Severity Sled Runs -- A Composite Plot.	48
21. External Chest A-P Acceleration. High-Severity Sled Runs -- A Composite Plot.	49
22. Internal Pelvis A-P Acceleration. Low-Severity Sled Runs -- A Composite Plot.	50
23. Internal Pelvis A-P Acceleration. Mid-Severity Sled Runs -- A Composite Plot.	51
24. Internal Pelvis A-P Acceleration. High-Severity Sled Runs -- A Composite Plot.	52
25. External Pelvis A-P Acceleration. Low-Severity Sled Runs -- A Composite Plot.	53
26. External Pelvis A-P Acceleration. Mid-Severity Sled Runs -- A Composite Plot.	54
27. External Pelvis A-P Acceleration. High-Severity Sled Runs -- A Composite Plot.	55
28. Upper Shoulder Harness Force. Low-Severity Sled Runs -- A Composite Plot.	56

LIST OF FIGURES (continued)

<u>FIGURE</u>	<u>PAGE</u>
29. Upper Shoulder Harness Force. Mid-Severity Sled Runs -- A Composite Plot.	57
30. Upper Shoulder Harness Force. High-Severity Sled Runs -- A Composite Plot.	58
31. Lower Shoulder Harness Force. Low-Severity Sled Runs -- A Composite Plot.	59
32. Lower Shoulder Harness Force. Mid-Severity Sled Runs -- A Composite Plot.	60
33. Lower Shoulder Harness Force. High-Severity Sled Runs -- A Composite Plot.	61
34. Left Lap Belt Load. Low-Severity Sled Runs -- A Composite Plot.	62
35. Left Lap Belt Load. Mid-Severity Sled Runs -- A Composite Plot.	63
36. Left Lap Belt Load. High-Severity Sled Runs -- A Composite Plot.	64
37. Right Lap Belt Load. Low-Severity Sled Runs -- A Composite Plot.	65
38. Right Lap Belt Load. Mid-Severity Sled Runs -- A Composite Plot.	66
39. Right Lap Belt Load. High-Severity Sled Runs -- A Composite Plot.	67
40. Printer-Plot Time Sequence from Simulation of Test A-869 (t=0 and t=70 ms).	75
41. Printer-Plot Time Sequence from Simulation of Test A-869 (t=110 and t=130 ms).	76
42. Printer-Plot Time Sequence from Simulation of Test A-869 (t=160 and t=200 ms).	77

LIST OF FIGURES (continued)

<u>FIGURE</u>		<u>PAGE</u>
43.	Head Pitch Velocities and Accelerations for Low-Severity Test, A-926.	79
44.	Anatomical Components of Head Center-of-Mass Acceleration for Low-Severity Test, A-926.	80
45.	Simulation and Actual Torso Belt Loads for Low-Severity Test, A-926.	81
46.	Head Pitch Velocities and Accelerations for Mid-Severity Test, A-869.	82
47.	Anatomical Components of Head Center-of-Mass Acceleration for Mid-Severity Test, A-869.	83
48.	Simulation and Actual Torso Belt Loads for Mid-Severity Test, A-869.	84
49.	Head Pitch Velocities and Accelerations for High-Severity Test, A-866.	85
50.	Anatomical Components of Head Center-of-Mass Acceleration for High-Severity Test, A-866.	86
51.	Simulation and Actual Torso Belt Loads for High-Severity Test, A-866.	87

LIST OF TABLES

<u>TABLE</u>		<u>PAGE</u>
1.	Matrix of Sled Runs Conducted During the Whole-Body Response Research Program.	22
2.	Selected Anthropometric Measurements of Tested Cadavers.	24
3.	Whole-Body Response Cadaver Tests Record.	25
4.	Summary of WBR test Cadavers Injuries.	28
5.	Variables Used to Characterize the Whole-Body Response Kinematics.	30
6.	Velocity Changes and Average (Plateau) Accelerations of Three Simulated Sled Profiles.	73
7.	Weights and Heights of Simulation "Cadaver" and the Cadavers of Three Simulated Tests.	73
8.	Peak Values for Accelerations Responses and Belt Loads.	89
9.	Magnitudes and Phases of Head Responses.	92
10.	Comparison of Mid-Severity Chest Acceleration Peak Data.	94

Chapter 1

I N T R O D U C T I O N

1.1. Program Objectives

The Whole-Body Response (WBR) research program was conducted over the past four years (September 1973 to August 1977) at the Highway Safety Research Institute (HSRI) of the University of Michigan, under the sponsorship of the Biomedical Science Department of the General Motors Research Laboratories (GMRL).

The general objective of the program was to generate data on the kinematic response of human surrogates, restrained by a three-point belt system, and subjected to a realistic automotive impact environment. Ultimately, the generated data is to be utilized in identifying similarities and differences in kinematic response of the various types of surrogates, and in pointing out areas that need improvement in anthropomorphic test devices (dummies) and in the development of mathematical models.

The immediate objectives of the WBR research program were to develop and employ the techniques necessary for obtaining the desired whole-body kinematic responses, conduct sled tests with fully instrumented and properly selected subjects, then analyze the resulting data and present it in a most useful format.

1.2. General Approach

Full-scale sled tests were conducted at the HSRI Sled Facility with a test configuration consisting of an idealized hard seat representation of a car seat with a three-point harness restraint system.

Three severity levels of crash tests were used:

- 1) LOW ... 16-mph velocity change, 10-G deceleration,
- 2) MID ... 20-mph velocity change, 10-G deceleration,
- 3) HIGH ... 32-mph velocity change, 20-G deceleration.

Four human surrogates were used in this program, all approximating the 50th percentile male in size:

- 1) Unembalmed male cadavers*, selected on the basis of their size and skeletal integrity,
- 2) A certified Part 572 (Hybrid II) Anthropometric Test Device (ATD),
- 3) Hybrid III ATD, recently developed by GM and which includes additional built-in instrumentation,
- 4) MVMA-2D Crash Victim Simulator, which is a two-dimensional mathematical model of a car occupant.

* The protocol for the use of cadavers in this study was reviewed by the Committee to Review Grants for Clinical Research and Investigation Involving Human Beings of the University of Michigan Medical Center and follows guidelines established by the U.S. Public Health Service and recommended by the National Academy of Sciences/National Research Council.

The test procedures for the cadavers involved the following features: detailed anthropometric description of the subject, extensive pre- and post-test radiographic documentation of the skeletal structure, mounting nine accelerometers on the head for three-dimensional motion measurement, mounting of accelerometers on the thoracic spine and the pelvis, targeting the body segments for photographic motion analysis, and finally, measurement of restraint system loads.

The test setups and subjects were suitably instrumented and fully documented for subsequent data analysis. Standard methods of analysis were applied where possible, but additional new techniques were developed as needed.

This final report culminates the research efforts of this four-year program, and presents an overview of what was accomplished. Detailed results were either presented in earlier reports [1,2,3]*, or are included in Appendices A, B, and C of this report.

1.3. Progress Review

The data that has been produced by this program represents one of the most comprehensive and extensive documentations of whole body response to date. This research effort pioneered many of the methods considered today to be the state-of-the-art. The following is a year-by-year review of the progress of this program.

* Numbers in [] are references given at end of report.

1.3.1. Review of 1973-74 Year. Much of the first year of the WBR research program was spent in initial development. This included instrumentation hardware design and fabrication, data processing software development and implementation, and development of an overall test procedure and cadaver handling protocol.

Since many kinematic responses (e.g., 3-D motion of the head) were being measured for the first time anywhere, new original and sophisticated measurement techniques and data processing methods had to be developed and tested. This revealed some deficiencies in the industry-wide standard data acquisition system being used at HSRI, and necessitated the introduction of new data handling equipment and methods which will be described later. As a result, the first two cadavers tested were only partially used in subsequent data analyses, and only a total of four cadavers were tested during this period.

1.3.2. Review of 1974-75 Year. During the second contract year, the surgical techniques were refined, the photographic coverage improved, the instrumentation hardware redesigned and improved, nine accelerometers were mounted on the head instead of the original six, and generally, experience from the first year resulted in the refinement of the test protocol.

A total of twenty-five tests were conducted during this period. Four cadavers were subjected to two tests each for a total of 8 cadaver tests, and a certified Part 572 dummy with two types of instrumentation was subjected to 17 tests at the three different

severity levels.

Development of data analysis methods, initiated in the first year, continued during this year, and were validated towards the end of this period.

1.3.3. Review of 1975-76 Year. By the third contract year of the WBR program, instrumenting and testing of cadavers and dummies became a well refined routine operation. Data analysis of previous dummy runs revealed instrumentation failures which were not apparent at the time tests were conducted. Thus a third series of 9 tests (3 at each severity) was conducted on the Part 572 dummy. The GM Hybrid-III was also subjected to the same matrix of tests. Finally, nine additional cadavers were subjected to a total of 11 tests at various severity levels to fill the voids in the matrix of results.

1.3.4. Review of 1976-77 Year. The fourth and final year was devoted to processing of all the data generated during the previous three, and to analyzing those results.

Data processing consisted of organizing the written data sheets in uniform and consistent formats, converting the transducers' recorded analog signals to digital ones, and finally, applying appropriate computer programs to the converted digital signals to produce direct and calculated measurements of kinematic responses.

Data analysis consisted of examination of the processed data to point out unusual results, tabulation of results by variables, subjects and severity levels, limited statistical analyses of these

results, and finally, drawing conclusions about the kinematic responses variations between subjects at various impact severity levels.

1.4. Report Outline

The remainder of this final report is organized in the following chapters:

CHAPTER 2, which describes the test setup and hardware, the general protocol for handling subjects and conducting a typical WBR test, and outlines briefly the new techniques developed for processing and analyzing the data generated by the WBR program;

CHAPTER 3, where test conditions (i.e., initial configuration, restraint system, crash severity) and test subjects (i.e., cadavers, dummies, computer models) are described;

CHAPTER 4, in which summaries of the test results are presented, and includes condensed graphs and tables from the experimental phase of the program;

CHAPTER 5, which describes the computer simulations and presents and discusses their results;

CHAPTER 6, where these results are discussed to point out similarities and differences between various responses, offer possible interpretations and explain discrepancies, and discuss the significance of the results;

CHAPTER 7, where conclusions are drawn based on the lessons learned from this program and recommendations are made for future research programs.

1. INTRODUCTION

In addition to its main body, this report includes (in separate volumes) three appendices which constitute one of the most comprehensive and detailed documentation of a whole-body testing program. The 3 appendices are:

A: METHODOLOGY appendix which describes the analytical and experimental methods developed for the WBR program but may be applied in a wide range of situations.

B: RAW DATA appendix which is a complete test-by-test documentation of all the generated data before it was processed.

C: PROCESSED DATA appendix which includes tabular and graphical details of all recorded and computed variables.

Chapter 2

T E S T I N G A N D A N A L Y S I S M E T H O D S

Most of the experimental techniques and procedures employed in testing the cadavers were developed by HSRI specifically for this research program, since no standards had been established for dealing with instrumentation and handling requirements for this type of testing. Since then, the use of cadavers as surrogates for the living human has gained enough acceptance that special guidelines and standards have been suggested.

In contrast to cadavers, testing standards for anthropomorphic dummies are well established so that most of the procedures followed in preparing the dummy for a WBR sled test and the subsequent data processing were standard and accepted ones.

This chapter, therefore, focuses on those methods which were developed and employed throughout the cadaver testing part of this program. The adopted procedures described below are the last "version", since many of them evolved over the past four years to the level of sophistication necessary for producing satisfactory results.

2.1. Surgical Techniques

Several types of transducers were rigidly attached to the bony structure of each cadaver at various locations. Triaxial accelerometers were mounted on the skull, thoracic spine and pelvic complex. All these mounts had provision for mounting three-dimensional photographic targets. Simple photographic targets (balls or discs) were also mounted on the two acromions and two femurs.

During the development phase of each surgery technique, and during its actual application, primary consideration was given to three basic requirements: 1) simplicity and speed of surgery and hardware mounting, 2) strength and rigidity of the mount-bone structure and 3) repeatability of locating transducer from one cadaver to another. Other considerations were also given to avoiding significant alterations of the whole-body mechanical properties, clearances between seat and hardware during the test, ability to precisely determine locations and orientations of transducers relative to "standard" anatomical reference frames and facility of transducer removal after the test is completed.

2.1.1. Head Accelerometer Mounting. Three sites on the skull are selected so that they provide maximum separation between the three triaxial accelerometers. The scalp is removed exposing the skull which is then cleaned and dried. For each mount, 3 pilot holes are drilled in the skull to allow three screws to be placed into the outer layer of the skull bone. A steel wire is wrapped around the three partially-exposed screws forming an triangular area

2. TESTING AND ANALYSIS METHODS

where the mount is placed and secured to the wire and screws with dental acrylic. The acrylic is allowed to harden before removing the special alignment jig and leaving the three mounts rigidly attached to the skull in an orthogonal formation.

2.1.2. Thoracic Accelerometer Mounting. The basic principle of attaching hardware to the vertebral body (T7 in this case) is to secure a U-shaped aluminum mount over the spinous process with a long sheet-metal screw through and along the process into the body of the vertebra. To add rigidity and reinforcement and to stop any looseness, dental acrylic is used to pot the U-shaped mount over the process and to fill the voids between the bone and metal.

2.1.3. Pelvic Accelerometer Mounting. To attach the pelvic mount, which consists of a long machined aluminum bar, two incisions are made down to the superior-posterior pelvic crests, a pilot hole drilled in each crest in the A-P direction, and a long coarse lag bolt threaded in until flush with the skin. The heads of these two bolts form a strong support for the aluminum bar, at the center of which the pelvic biaxial accelerometer is mounted.

2.1.4. Photographic Targets. The femur target consisted of a flat disc, while the acromion target was a styrofoam ball. Each was mounted to the bone with a long, coarse screw into which a small machine screw holding the target was threaded. It was found that a screw threaded into a thick or strong bone provides a sufficiently

strong and rigid support for light-weight hardware. Dental acrylic was not necessary in mounting these targets, since they are light in weight, and since the femur and the acromion are sufficiently strong for their support.

2.2. Digital Signal Processing

The complexity of experimental measurement methods, developed and employed during the WBR research program, requires a well organized data handling protocol, capable of transforming laboratory records into clear final presentations. Such protocol is followed at HSRI, as illustrated in the flowchart of Figure 1. An Essential requirement in this system is a sophisticated signal processing procedure. With the availability of digital computers, this task is greatly simplified, but new signal processing methods had to be developed and implemented.

Traditionally, analog signals have been the primary form of describing measured transducer output. Standards and guidelines for dealing with analog signals, such as SAE-J211, are therefore well established and widely applied. In contrast, no guidelines for dealing with digital signals are available, since this form of data is relatively new, particularly in biomechanics applications. It was therefore necessary to develop and adopt new guidelines for converting analog signals to digital form, and for digital filtering of these signals, to be specifically applied to impact testing.

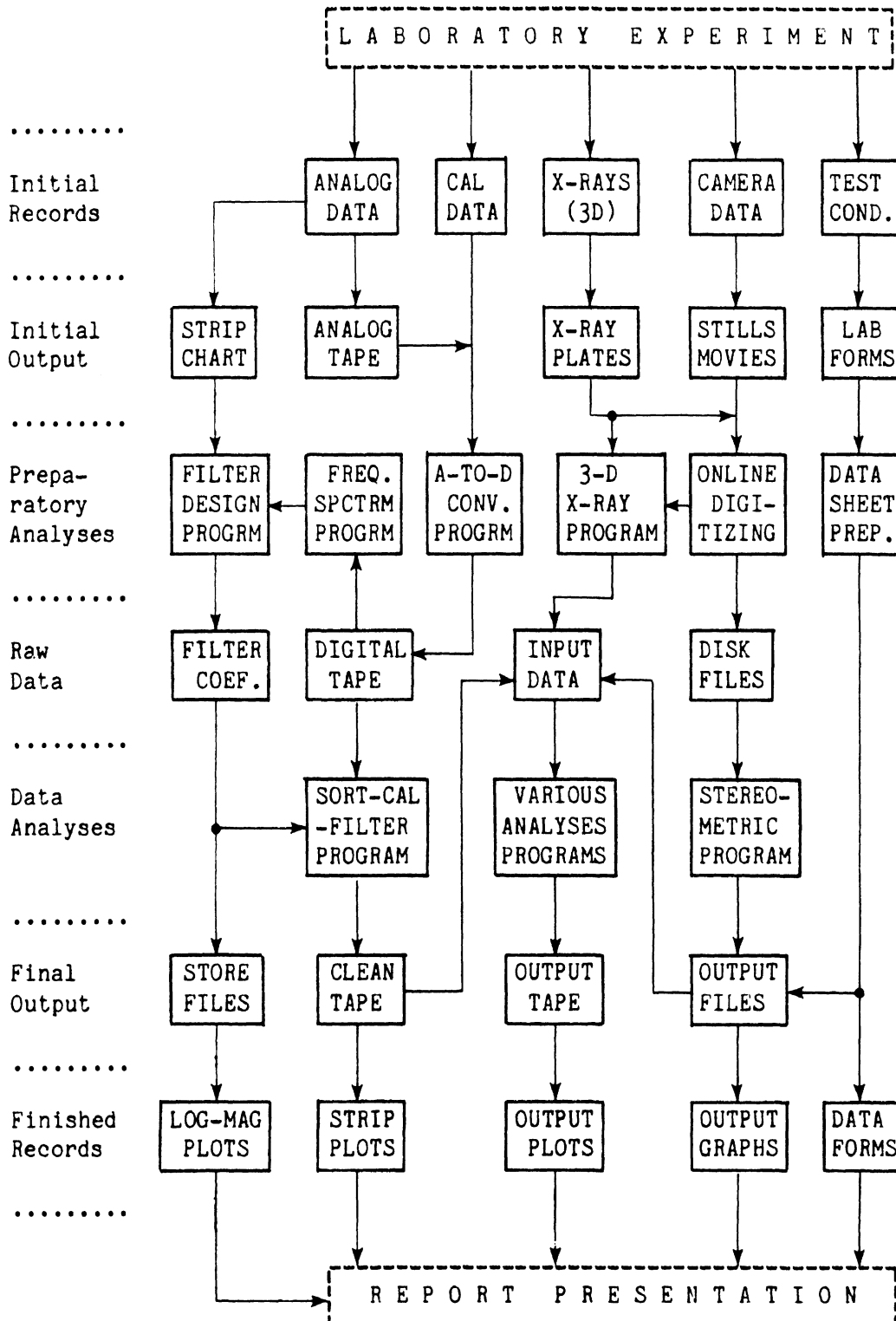


FIGURE 1. Flow-Chart of Data Handling System in Operation at HSRI for Biomechanical Experiments.

2.2.1. A-to-D Conversion. The first operation in digital signal processing is to convert the analog data to digital form. Results from this operation (tables of sampled values of the analog signal) are affected by two interrelated factors: 1) the sampling rate, i.e., the time interval between two consecutive samples, and 2) the bandwidth of the analog signal being digitized. A proper choice of the sampling rate and the proper bandlimiting of the analog signal determines the validity and usefulness of the digital signal in later analytical applications.

The sampling rate used in this program was 1600 Hz to allow the exact mathematical reconstruction of all frequencies below 800 Hz. It was judged that no frequencies higher than the 800-Hz Nyquist rate are of interest as far as the types of measurements being made. The A-to-D conversion unit at HSRI has a fixed sampling rate of 400 Hz per channel, so that time-expansion of the taped signals was necessary to attain the desired sampling rate of the actual signals.

In order to eliminate any distortions (aliasing errors) in the digitized signals, which result from the sampling process, the time-expanded analog signals were bandlimited to 200 Hz by using anti-aliasing analog filters, inserted between the tape output and the input the the A-to-D unit. These were active linear-phase filters with corner frequencies at 100 Hz, so that all frequencies above 200 Hz were attenuated by at least 24 dB. The digital signal processing methods are described in Appendix A of this report.

2.2.2. Digital Filtering. Early work on digital filtering was concerned with the ways analog filters could be approximated on digital computers. With the introduction of the Fast Fourier Transform (FFT) in 1965, many signal processing concepts had to be reformulated to conform to the exact mathematics of the FFT. The implication of these conceptual changes is that many industry and government standards cannot be intelligently be applied to digital filters.

An example is the SAE-J211b instrumentation guideline which specifies the channel class filters to be used on transducer signals in the impact testing of anthropomorphic dummies. In this guideline, it is recommended that filters have a passband ripple of 0.5 dB, a common tolerance in commercial analog filters, which can easily be reduced to 0.01 dB in a digital filter. Another recommended practice, also based on analog filters, is to allow the corner frequency (-3 dB point) to be as much as 65% of the cutoff frequency where the gain begins to drop. In digital filters, the corner frequency may be made as low as 5% of the cutoff frequency, which means that the digital filter may be designed to have a much sharper corner than its analog counterpart.

Currently, there is no "standard" for specifying digital filter characteristics for applications in biomechanics instrumentation. Until such a guideline is established, HSRI has been following a practice that it has developed based on its experience in this field. This practice is fully documented in Appendix A.

2.3. Analytical Measurement Methods

Innovative methods were developed for monitoring the kinematics of whole-body response. Most of these methods are concerned with the three-dimensional motion of the head, using accelerometry and photogrammetry. They required the refinement and/or development of signal digitizing and filtering methods, the development of experimental procedures for transducer installation and design of associated hardware, the development of analytical methods for determining their locations on the body, and the development of analytical methods to extract the desired kinematic information from digitized signals and from photographic sequences.

This section describes briefly some of these procedures, which were developed during this program, but which are considered to be most useful for general applications. All of these are fully documented in Appendix A, or references to their detailed description are given.

2.3.1. 3-D Accelerometry. Three-dimensional rigid-body motion measurement of the head dominated the analytical efforts in this research program. At the onset of the program (1973), it was believed that six accelerometers are necessary and sufficient for complete description of the 6 degrees of freedom of the motion. Subsequent work at HSRI and elsewhere [4,5] showed that the mathematical formulation using only six acceleration readings is numerically unstable, and cannot be reliably used for complete 3-D motion determination.

The use of redundant accelerometers was therefore necessary to maintain the stability of the numerical integration procedure. Several configurations were suggested, including the HSRI 3-3-3 and the Wayne State 3-2-2-2 ones. Since experimental procedures were already developed at HSRI for mounting a 2-2-2 configuration of six accelerometers, the choice of the new 3-3-3 configuration was a natural one, and required the addition of only one more accelerometer at each of the three locations. The computational procedure for this configuration, which has been proven stable, is described in Appendix A and has been presented elsewhere [6,7,8].

2.3.2. 3-D Photogrammetry. The use of high-speed movies in crash testing has been and today remains the primary means of documenting the motion of the test subject. This photographic documentation is qualitative in nature, since most of the attempts to extract quantitative time-histories from these films have consistently resulted in distorted, partial or, at best, approximate answers.

Although each WBR sled test was covered from the top, front, right and left sides with high-speed cameras, early attempts to calibrate the field of view and to extract 3-D motion of body segments (particularly the head) were not very successful.

It was not until the middle of the final contract year that a three-dimensional technique [9] using the Direct Linear Transformation was implemented and successfully tried out at HSRI. It is anticipated that most future tests conducted at HSRI which call for

photographic coverage will employ this method. The method is general and simple, and requires no special or expensive equipment, and may be applied in high-speed motion or still photogrammetry or radiogrammetry.

One of the stereometric methods developed and successfully implemented in this program was the x-ray technique, described in Appendix A, to obtain the orthogonal transformation matrix between the instrumentation and anatomical reference frames. The matrix is essential in transforming the kinematic data from the arbitrarily chosen accelerometer's frame to a standard one.

2.3.3. Fast HIC Computation. Evaluation of head response is currently done by calculating the Head Injury Criterion (HIC), as required by FMVSS-208 [10]. If approached in a straightforward manner, this computation can be a costly and lengthy proposition, even using today's fast digital computers.

The HIC properties have been studied [11] so that time-saving procedures may be implemented. An additional study was carried out at HSRI and new properties of the HIC uncovered. Using this cumulative knowledge, a new, fast algorithm for computing the HIC was developed, and is fully documented in Appendix A of this report.

Chapter 3

DESCRIPTION OF TESTS

3.1. Test Conditions

The test environment at the onset of impact is described in terms of seating configuration, restraint system, direction and severity of impact and the type of surrogate used as test subject.

In all of the WBR testing program, the subject was seated for frontal impact in a GM-supplied test fixture (buck) which is an idealized hard seat representation of a car seat. The subject was positioned as close as possible to the diagram of Figure 2, which represents a "natural" seating position of a typical car driver.

The restraint system used was a three-point system in a driver's side configuration and instrumented with load transducers to monitor the upper and lower forces in the shoulder harness, and the left and right forces in the lap belt. All the belts were tensioned to a 10-lb preload, then a 3-inch slack was introduced in the shoulder harness.

The sled deceleration profiles were selected to provide three levels of crash severities. The low-severity level corresponds to a 16-mph velocity change and a 10-G average deceleration, or an equivalent stopping distance of 11 inches. The intermediate-severity level has twice the kinetic energy of the low severity one, and corresponds to 20 mph and 10 G. Finally, the high-severity level with twice the energy of the mid-severity one but the same stopping

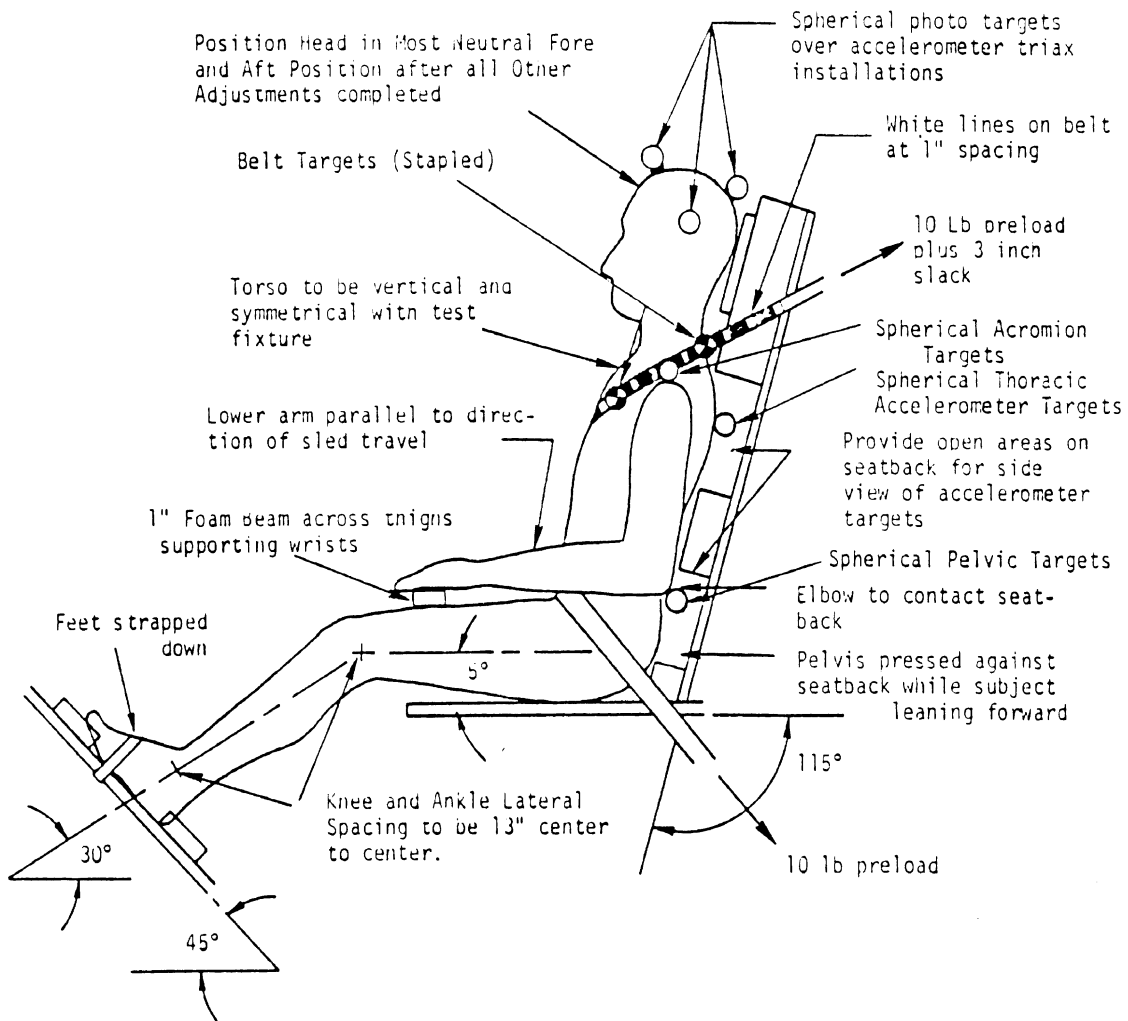


FIGURE 2. Diagram of Seating and Positioning in All Whole-Body Response Tests.

SLED DECELERATION, G'S

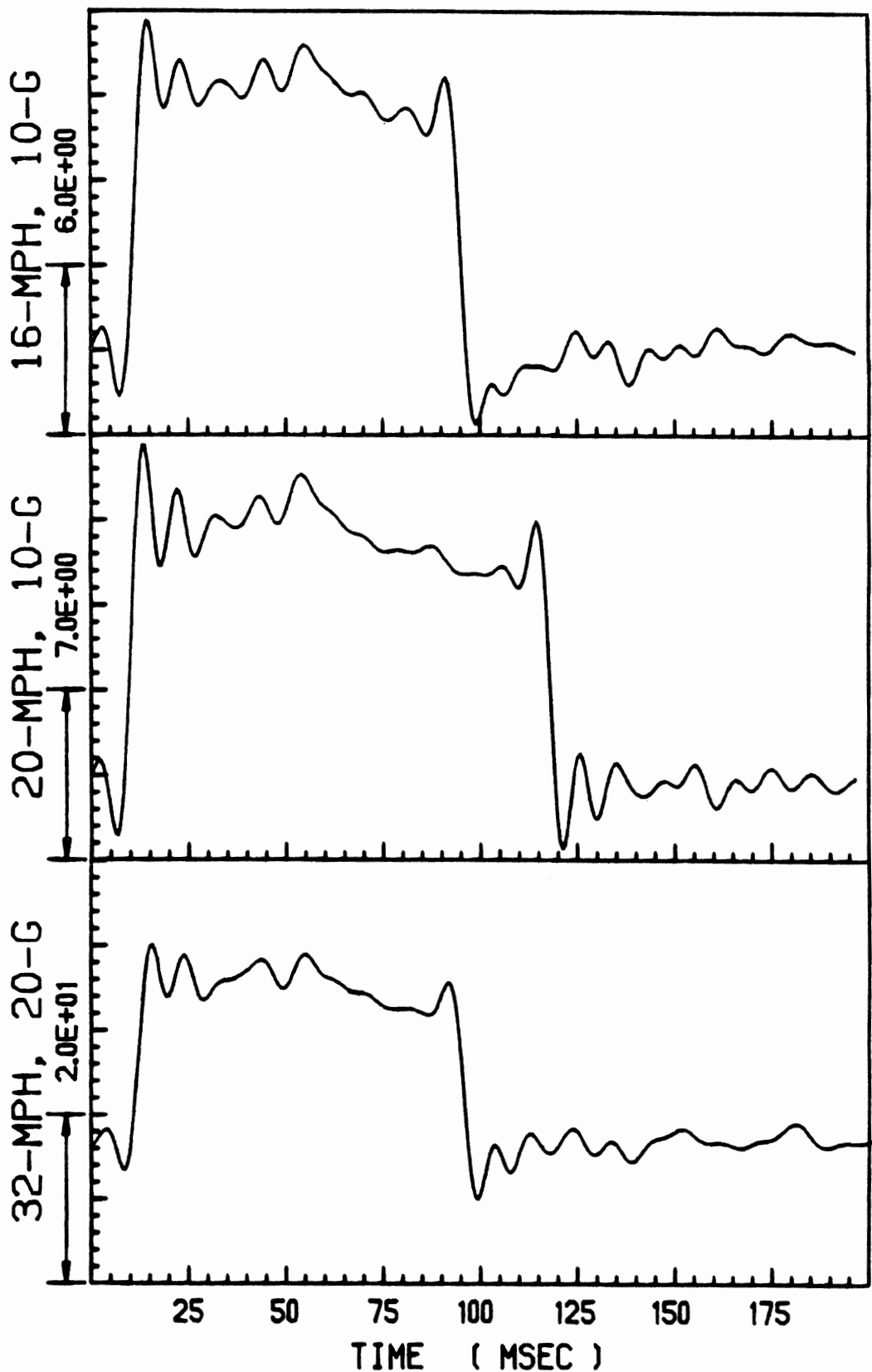


FIGURE 3. Typical Sled Deceleration Profiles at Three Severity Levels Used in the WBR Testing Program.

distance of 22 inches, corresponds to a 32-mph velocity change and 20-G average deceleration. All the sled deceleration pulses were approximately "square" and typical ones are shown in Figure 3.

The surrogates used in this program were cadavers, anthropomorphic test devices and computer models. These test subjects are described below, along with their associated instrumentation and special handling requirements. The number of sled runs conducted on each of the surrogates is given in Table 1.

TABLE 1. Matrix of Sled Runs Conducted During the Whole-Body Response Research Program.

<u>SEVERITY</u>	<u>CADAVERS</u>	<u>PART 572</u>	<u>HYBRID-3</u>	<u>TOTAL</u>
low	4	11	3	18
medium	13	8	3	24
high	6	7	3	16
TOTAL	23	26	9	58

3.2. Cadaver Selection and Description

Fifteen male cadavers, designated WBR-1 through WBR-15, were selected as human surrogates for testing in this research program, all approximating the 50th percentile in size. All but two were unembalmed, since embalming has been established to alter the mechanical properties of both soft tissue and bone.

3. DESCRIPTION OF TESTS

Surgery was performed for the purpose of mounting the instrumentation necessary for monitoring the three-dimensional motion of the head, the accelerations of the thorax and pelvis, and for photographic coverage of the motions of the head, shoulders, torso and legs. Locations of thorax and pelvis accelerometers were selected to correspond approximately to those built in test dummies.

Detailed anthropometric measurements were taken before surgery. In addition, a complete x-ray record was made of each cadaver skeletal structure, both in a lateral seated view that simulates the test configuration and in a prone frontal view after surgery has been completed.

In order to completely describe the tested cadavers, some 75 anthropometric measurements were taken on each cadaver. These measurements, given in detail in Appendix B, are essential to data analysts for interpretation of the results, and provide mathematical modelers with the necessary data for computer simulation of individual tests. To give an idea about some of the physical characteristics of the sample of cadavers, Table 2 presents selected measurements and their statistical variations.

During the first two years of the WBR program, each cadaver was subjected to two sled tests, one at the intermediate crash severity level, followed by a second one at the high level. It was consistently observed that the tested cadavers were sustaining considerable damage in the thoracic region, including rib, sternum and clavicle fractures.

TABLE 2. Selected Anthropometric Measurements of Tested Cadavers.

<u>MEASUREMENT (cm)</u>	<u>N</u>	<u>MEDIAN</u>	<u>MEAN</u>	<u>S.D.</u>
Age (years)	13	67.5	67.9	14.8
Weight (kg)	14	62.8	66.9	11.5
Stature	13	171.	172.	3.51
Head A-P length	12	19.6	19.4	0.74
Head L-R Breadth	12	15.2	15.4	0.64
Head Circumference	11		56.7	0.69
Vertex to Acromion	6	23.8	23.9	0.88
Vertex to Mid-Chest	12	40.9	40.9	6.70
Vertex to Trochanterion	12	82.3	81.7	3.93
Mid-Chest A-P Depth	14	22.3	22.1	2.46
Mid-Chest L-R Breadth	14	29.9	30.5	1.63
Hip Breadth at Iliocristale	12	29.2	28.8	3.15
Upper Arm (Acrom.-Radiale)	13	18.4	18.6	0.90
Lower Arm (Rad.-Stylon)	12	25.0	25.9	1.47
Upper Leg (Troch.-Fibulare)	13	42.2	43.1	3.29
Lower Leg (Fib.-L.Malleus)	12	39.0	39.8	1.96

Since significant thoracic and clavical bone damage may alter significantly the kinematics of the subject, and to avoid the risk of degrading the skeletal structure during the first test, each of the cadavers subsequently tested in the third contract year was subjected to a single test at a severity level determined to fill the voids in the matrix of runs. The sled runs distribution for the tested cadavers is given in Table 3, along with the cause of death and age at death of each cadaver.

3. DESCRIPTION OF TESTS

TABLE 3. Whole-Body Response Cadaver Tests Record.

TEST DATE	RUN ID AND SEVERITY LOW MID HIGH	CADAVER ID & NO	HGHT cm	WGHT kg	AGE yrs	CAUSE OF DEATH
03-21-74	A-720	WBR-1				
05-09-74	... A-725 A-726	WBR-2 (#19942)	167.3	47.7	78	coronary pulmonary
04-11-75	... A-865 A-866	WBR-3 (#20150)	173.7	57.3	59	ruptured aortic aneurism in abdomen
06-03-75	... A-869 ... A-870	WBR-4 (#20194)	165.5	61.5	82	pneumonia
06-17-75	... A-874 ... A-875	WBR-5 (#20208)	170.6	83.9	49	cardiac arrest
07-01-75	A-881 A-882 ...	WBR-6 (#20218)	169.7	44.0	60	adeno carcinoma of pancreas
10-03-75	A-925 A-926	WBR-7 (#20281)	178.5	77.9	82	cancer
11-20-75	... A-934 A-936 A-935	WBR-8 (#20287)	172.6	60.1	85	cardiac arrest (embalmed)
12-16-75	... A-938 ...	WBR-9 (#20336)	172.7	62.3	50	natural cirrhosis chronic thrombosis
02-03-76 76B001	WBR-10 (#20372)	174.4	62.8	57?	lung cancer (embalmed)
02-03-76	... 76B002 ...	WBR-11 (#20418)	170.6	73.9	88	septicemia
04-28-76	... 76B003 ...	WBR-12 (#20447)	168.3	61.9	47	cancer of colon, hepatic metastasis
06-09-76 76B004	WBR-13 (#20483)	175.5	75.3	73	cancer of prostate
07-06-76	... 76B005 ...	WBR-14 (#20500)	168.3	75.8	57	lung cancer
07-13-76 76B006	WBR-15 (#20508)	169.3	84.1	72	(unlisted)

3.3. Anthropomorphic Test Devices

Anthropomorphic dummies are generally used as human surrogates in crash testing and allow repeatable and consistent kinematic response measurements to be made. In order to provide a data base for comparing their kinematics to those of cadavers, two series of tests were conducted using two different dummies: a certified Part 572 ATD or "Hybrid-II", and the Hybrid-III dummy, recently developed by GM.

In addition to the transducers built in these dummies, the head was instrumented with the HSRI nine-accelerometer package for measuring the three-dimensional head motion. Since both cadavers and dummies were instrumented with the same head package, the measured 3-D motion would be compatible for comparison. Furthermore, the added weight was considered to be tolerable in comparison to that of the head alone.

Standard instrumentation on the Part 572 ATD and the Hybrid-III consists of triaxial accelerometers at the head, chest and pelvis. The Hybrid-III included an additional neck transducer to measure the neck axial and shear forces and its moment, a chest defelctometer and two femur load cells.

Every effort was made to seat the dummies in the same configuration as the cadavers (see Figure 2), and the same three crash severity levels (Figure 3) were applied.

Chapter 4

E X P E R I M E N T A L R E S U L T S

Complete and detailed documentation of the experimental results are given in Appendix B (Raw Data) and in Appendix C (Processed Data) of this final report, or have already been presented in earlier reports [1,2,3]. In this chapter, attempt is made to condense these results in tabular and graphical summaries, which are most characteristic of the whole-body biomechanical response. Thus, the next section summarizes the autopsy reports on each tested cadaver, followed by graphical summaries section, in which kinematic responses of the three sled-tested surrogates are presented.

4.1. Thoracic Damage

As part of test subject documentation, x-rays and anthropometric measurements were taken on each cadaver prior to each test. Post-test x-rays and autopsy were included in the testing protocol to identify and record thoracic damage due to the three-point belt system being used. Results indicate that all tested cadavers suffered rib cage damage to varying extents. The test injury records are summarized in Table 4.

TABLE 4. Summary of WBR Tests Cadavers Injuries.

TEST NO.	SEVERITY	LUNGS PRESS?	OTHER CONDITIONS AND INJURY RECORD
WBR-3	M,H	no	Fractured ribs #3, 4, 5 and 6 on left side; #1, 3, 4, 5, 6 and 7 on right side. Sternum fractured in three places. Pneumothorax on both sides.
WBR-4	M,M	yes	Fractured ribs #2, 3, 4(two places) and 5 on left side; #2, 3 and 4 on right. Sternum fractured in one place. Left clavicle was fractured.
WBR-5	M,M	no	Fractured ribs #2 and 6 on left side; #3, 4, 5 and 6 on right side. Sternum was fractured in one place. The acromial articular surface was dislocated, as was the head of the humerus.
WBR-6	L,M	yes	Fractured ribs #2(four places), 3(two places) and 4(two places) on left side; ribs #2(two places), 3(two places), 4, 5, 6(two places), 7 and 8 on right side. Pneumothorax. Blood was found inside the pericardium.
WBR-7	L,L	yes	Fractured ribs #2 through #7 on left side; ribs #1 through #7 on right side. Sternum fractured in three places. Pneumothorax on left side.
WBR-8	M,M,H	no	(embalmed specimen) Fractured ribs #1, 2, 3 and 4 on left side; ribs #1 through #7 on right side. Sternum fractured in one place. Clavicle broken.

TABLE 4. Summary of WBR Tests Cadavers Injuries. (continued)

TEST NO.	SEVERITY	LUNGS PRESS?	OTHER CONDITIONS AND INJURY RECORD
WBR-9	M	yes	Fractured ribs #2, 3 and 4 on left side; ribs #4 and 5 on right side.
WBR-10	H	no	(embalmed specimen) Fractured ribs #2 and 3 on left side; ribs #3, 4, 5, 6 and 7 on right side. Sternum fractured in one place.
WBR-11	M	yes	Fractured ribs #3 and 4 on left side; ribs #3, 4, 5, 6 and 7 on right side.
WBR-12	M	yes	Fractured ribs #2 and 3 on right side. Sternum fractured in three places.
WBR-13	H	yes	Fractured ribs #1, 2, 3 and 4 on left side; ribs #1 through #7 on right side. Sternum fractured in one place. Left clavicle dislocated.
WBR-14	M	yes	(cadaver in very good condition prior to sled test) Fractured ribs #3, 4 and 5 on left side; ribs #3, 5, 6, 7 and 8 on right side. Sternum fractured in one place.
WBR-15	H	yes	(also, brain vascular system pressurized and brain vasc. pressure measured.) Fractured ribs #1 through #7 on left side; ribs #1 through #9 on right side. Sternum fractured two places. Complete separation of ribs at fractures. Extensive pericardium hemorrhage.

4.2. Kinematic Responses

The kinematic responses of tested cadavers and dummies may be characterized by accelerations, velocities and displacements of various body segments, as well as the belt forces. For each sled run, data processing produced time-histories of as many as 52 such variables, some of which were directly measured, others resulting from computational procedures described in Appendix A.

To be concise, only the twelve most characteristic variables were selected to be included here. These variables, listed in Table 5, are common to all three tested surrogates, and are the most compatible for comparison purposes.

TABLE 5. Variables Used to Characterize the Whole-Body Response Kinematics.

<u>VARIABLE</u>	<u>LOCATION</u>	<u>TYPE</u>	<u>UNITS</u>
Angular Acc.	Head	Resultant	r/s/s
Angular Vel.	Head	Resultant	r/s
Transl. Acc.	Head C.G.	Resultant	G's
Transl. Vel.	Head C.G.	Resultant	in/s
Acceleration	Int. Thorax	A-P	G's
Acceleration	Ext. Thorax	A-P	G's
Acceleration	Int. Pelvis	A-P	G's
Acceleration	Ext. Pelvis	A-P	G's
Belt Force	Shoulder	Upper	lbs
Belt Force	Shoulder	Lower	lbs
Belt Force	Lap Belt	Left	lbs
Belt Force	Lap Belt	Right	lbs

4. EXPERIMENTAL RESULTS

In the following 36 figures, composite time-history plots of each of the 12 variables are given for the cadavers, Hybrid II and Hybrid III dummies at the three severity levels. It should be noted that these plots include only valid time-histories since, in some tests, data processing was neither possible nor satisfactory because of instrumentation problems.

RESULTANT HEAD ANG ACC, RAD/S/S

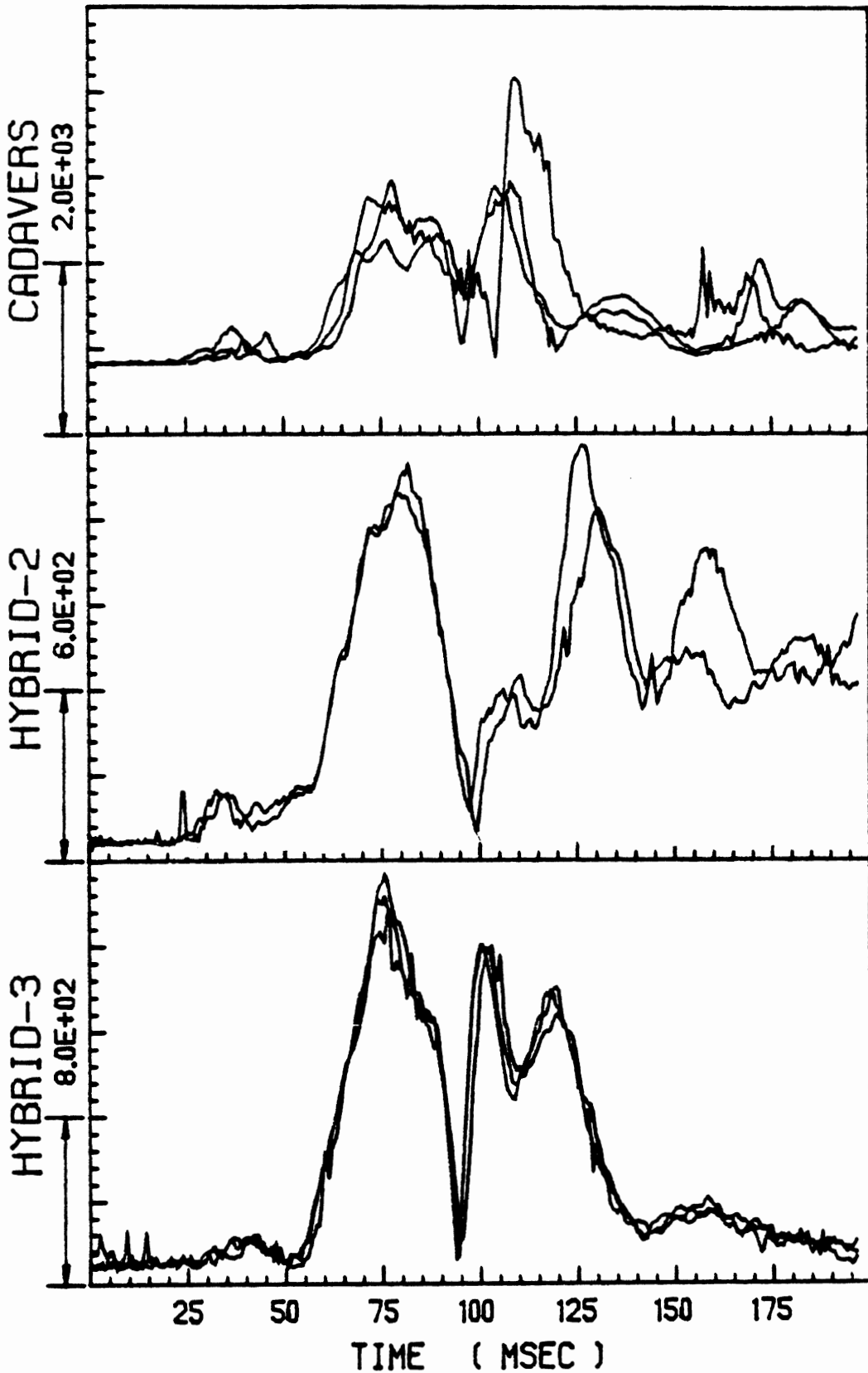


FIGURE 4. Resultant Head Angular Acceleration
Low-Severity Sled Runs -- A Composite Plot.

RESULTANT HEAD ANG ACC, RAD/S/S

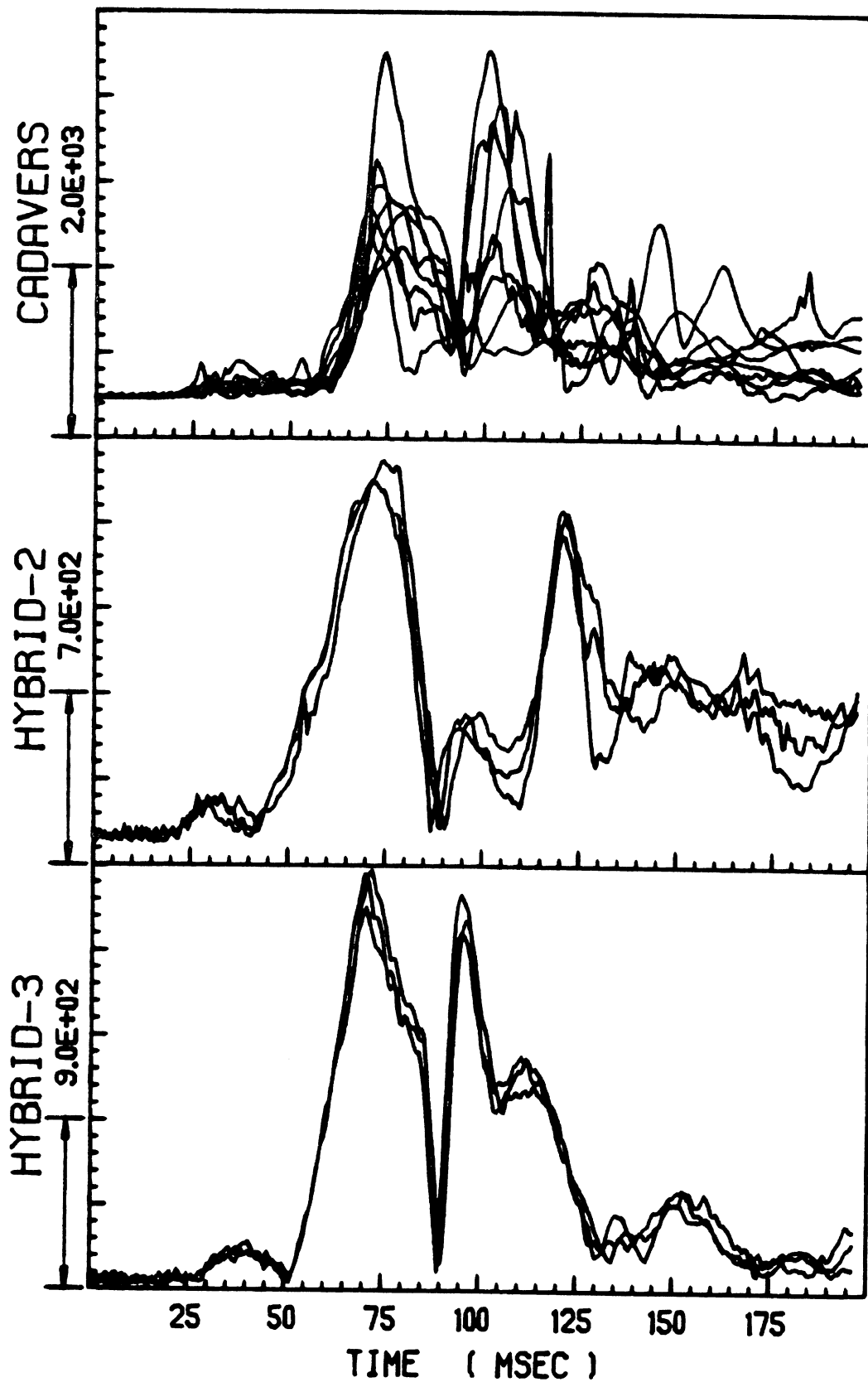


FIGURE 5. Resultant Head Angular Acceleration
Mid-Severity Sled Runs -- A Composite Plot.

RESULTANT HEAD ANG ACC, RAD/S/S

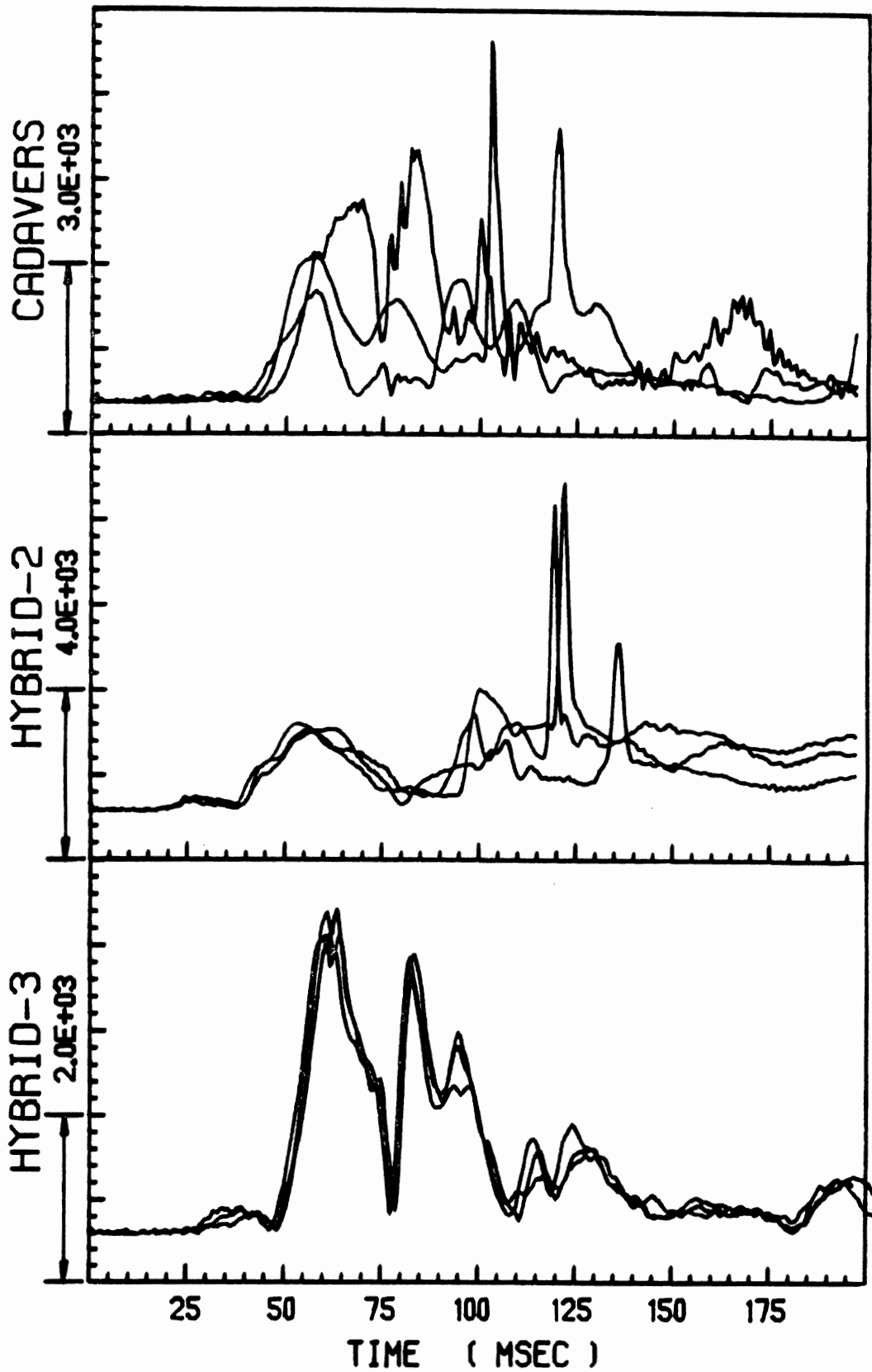


FIGURE 6. Resultant Head Angular Acceleration
High-Severity Sled Runs -- A Composite Plot.

RESULTANT HEAD ANG VEL, RAD/S

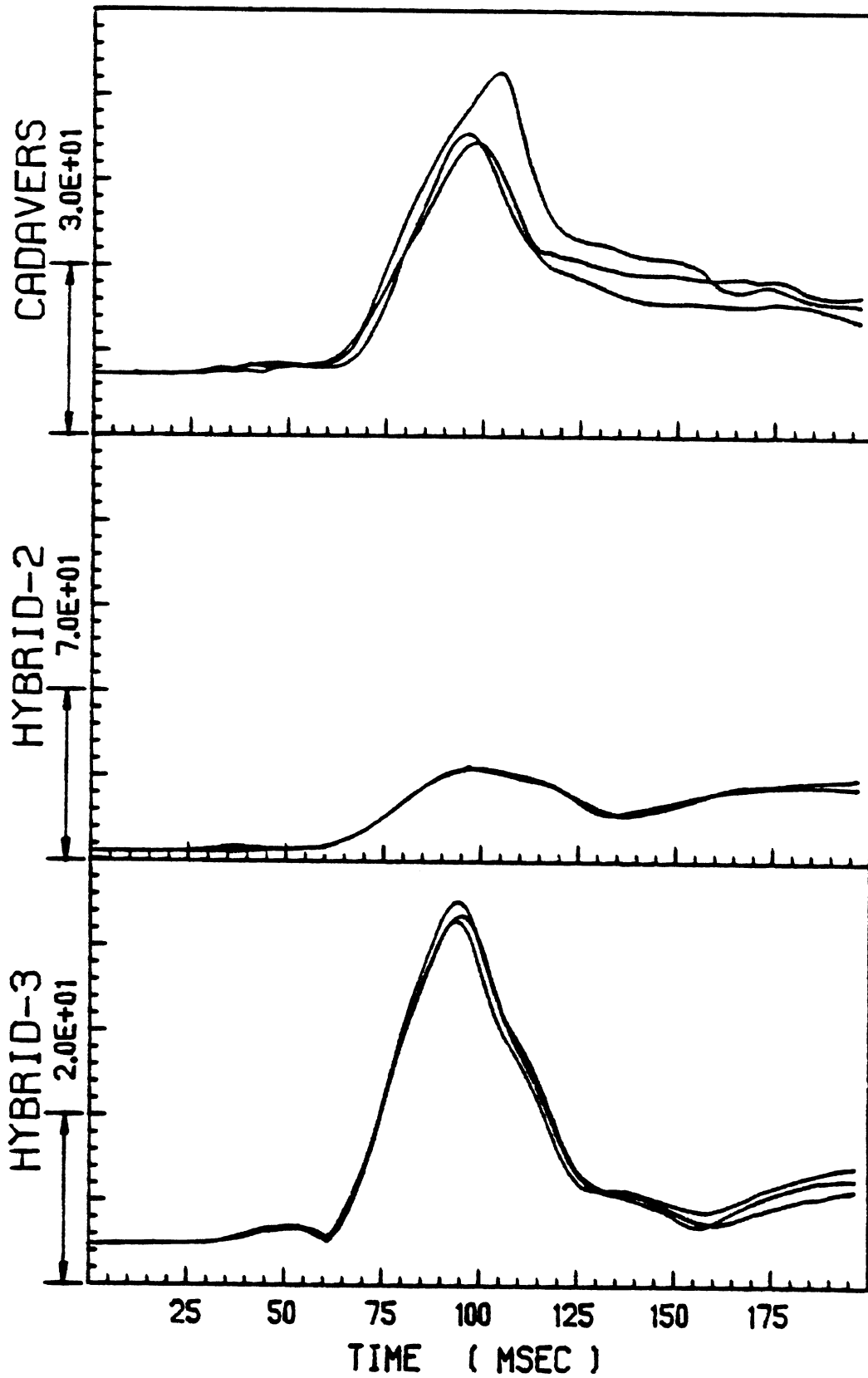


FIGURE 7. Resultant Head Angular Velocity
Low-Severity Sled Runs -- A Composite Plot.

RESULTANT HEAD ANG VEL, RAD/S

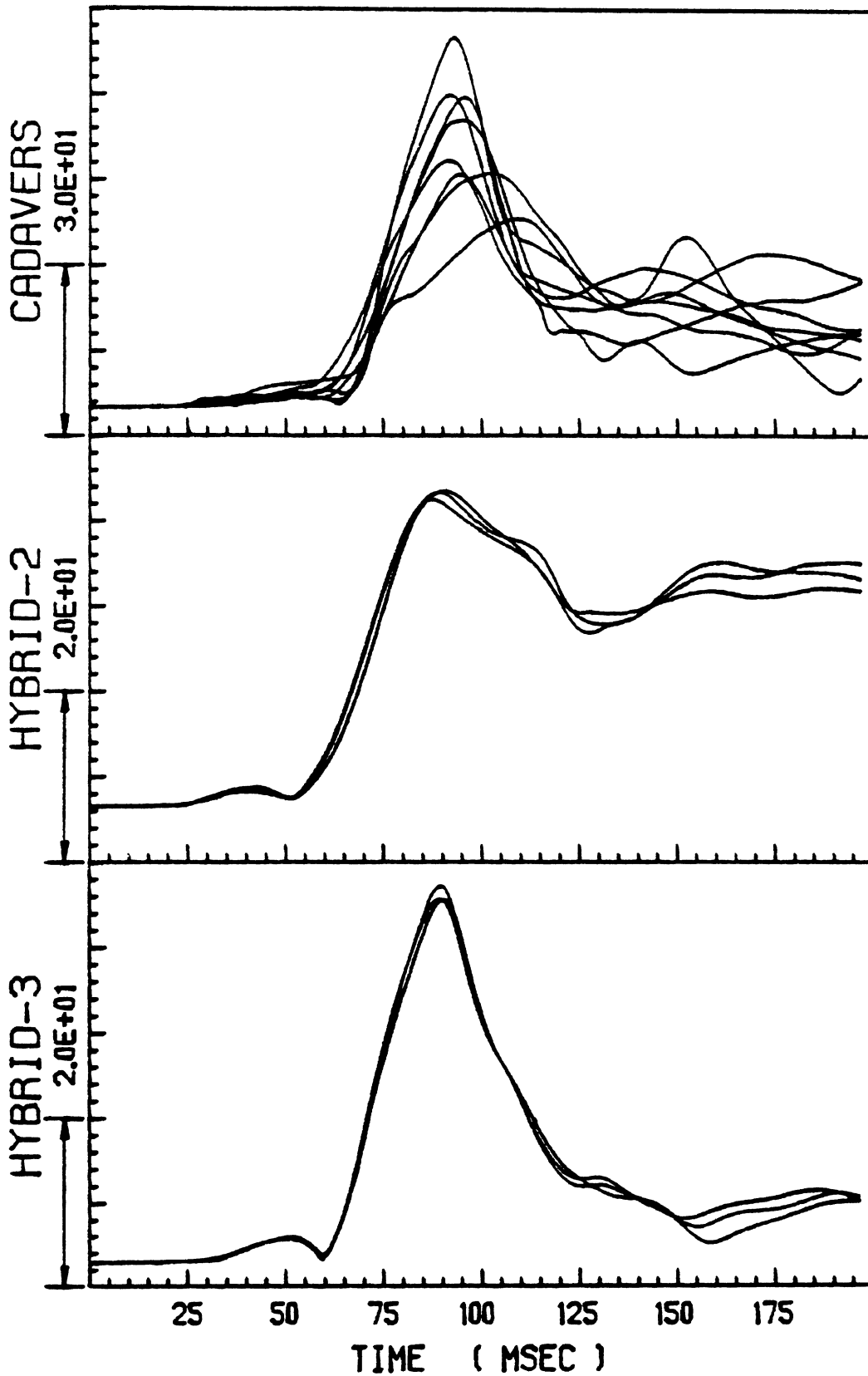


FIGURE 8. Resultant Head Angular Velocity
Mid-Severity Sled Runs -- A Composite Plot.

RESULTANT HEAD ANG VEL, RAD/S

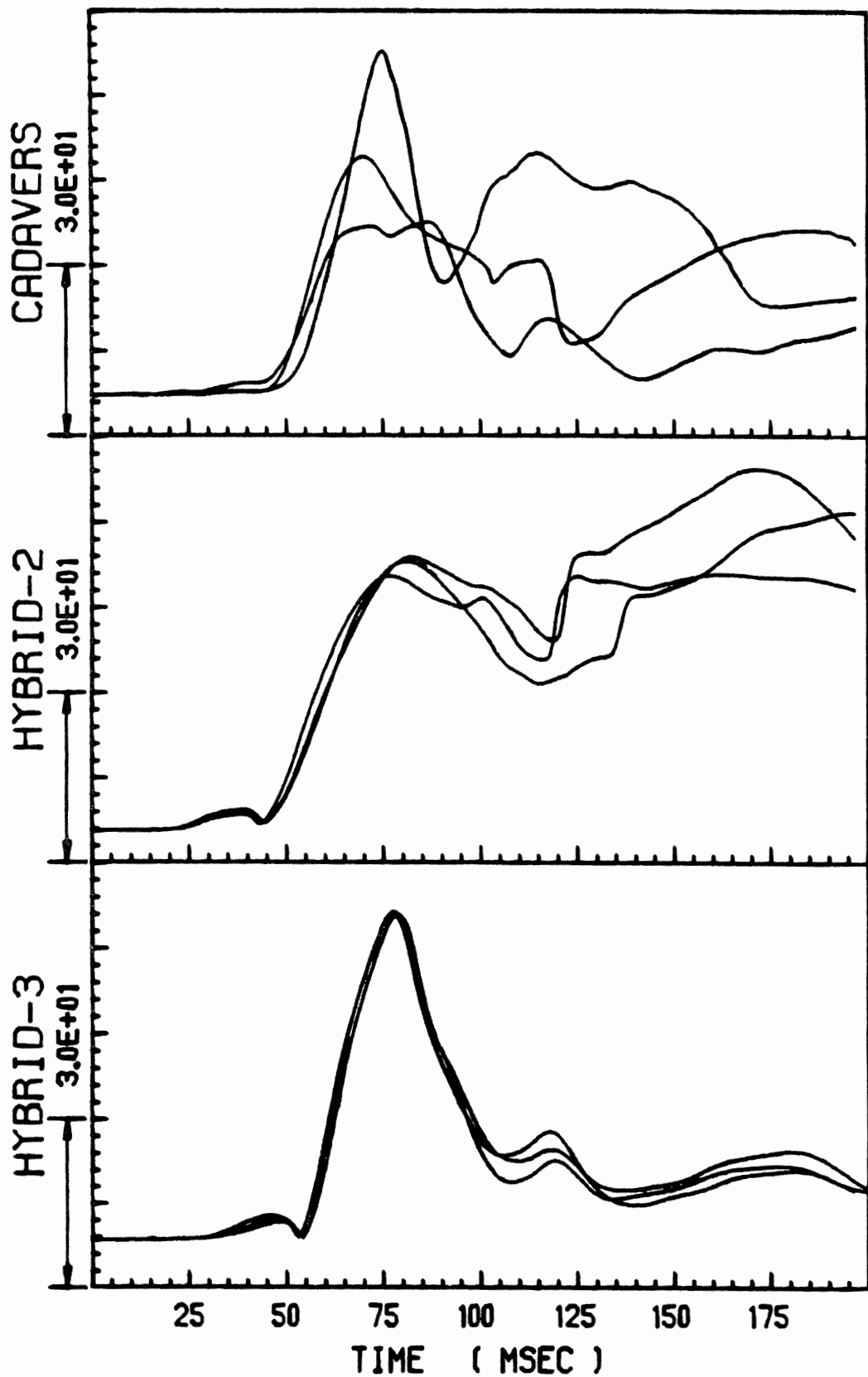


FIGURE 9. Resultant Head Angular Velocity High-Severity Sled Runs -- A Composite Plot.

RESULTANT HEAD C.G. ACC, G'S

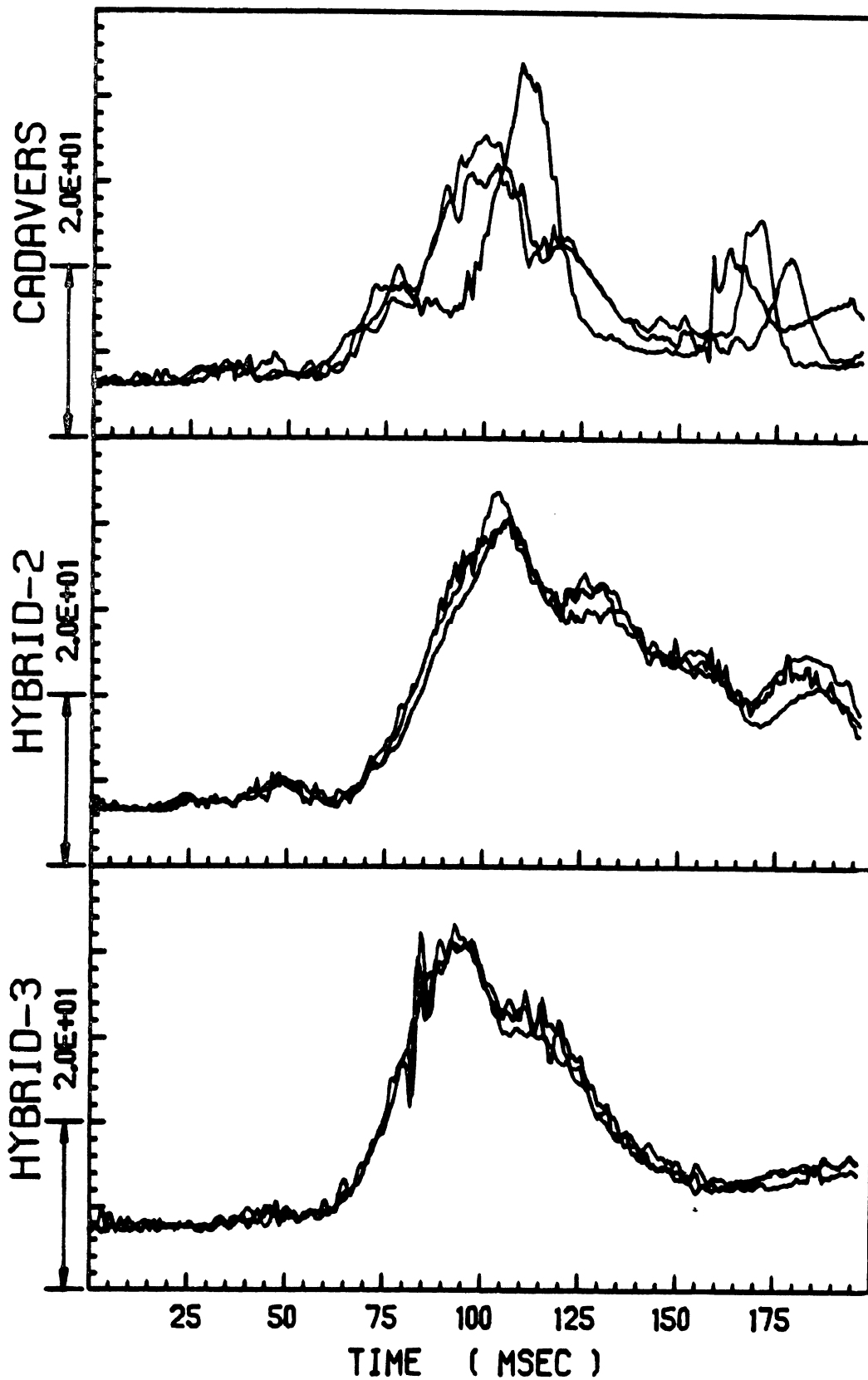


FIGURE 10. Resultant Head Center-of-Mass Acceleration.
Low-Severity Sled Runs -- A Composite Plot.

RESULTANT HEAD C.G. ACC, G'S

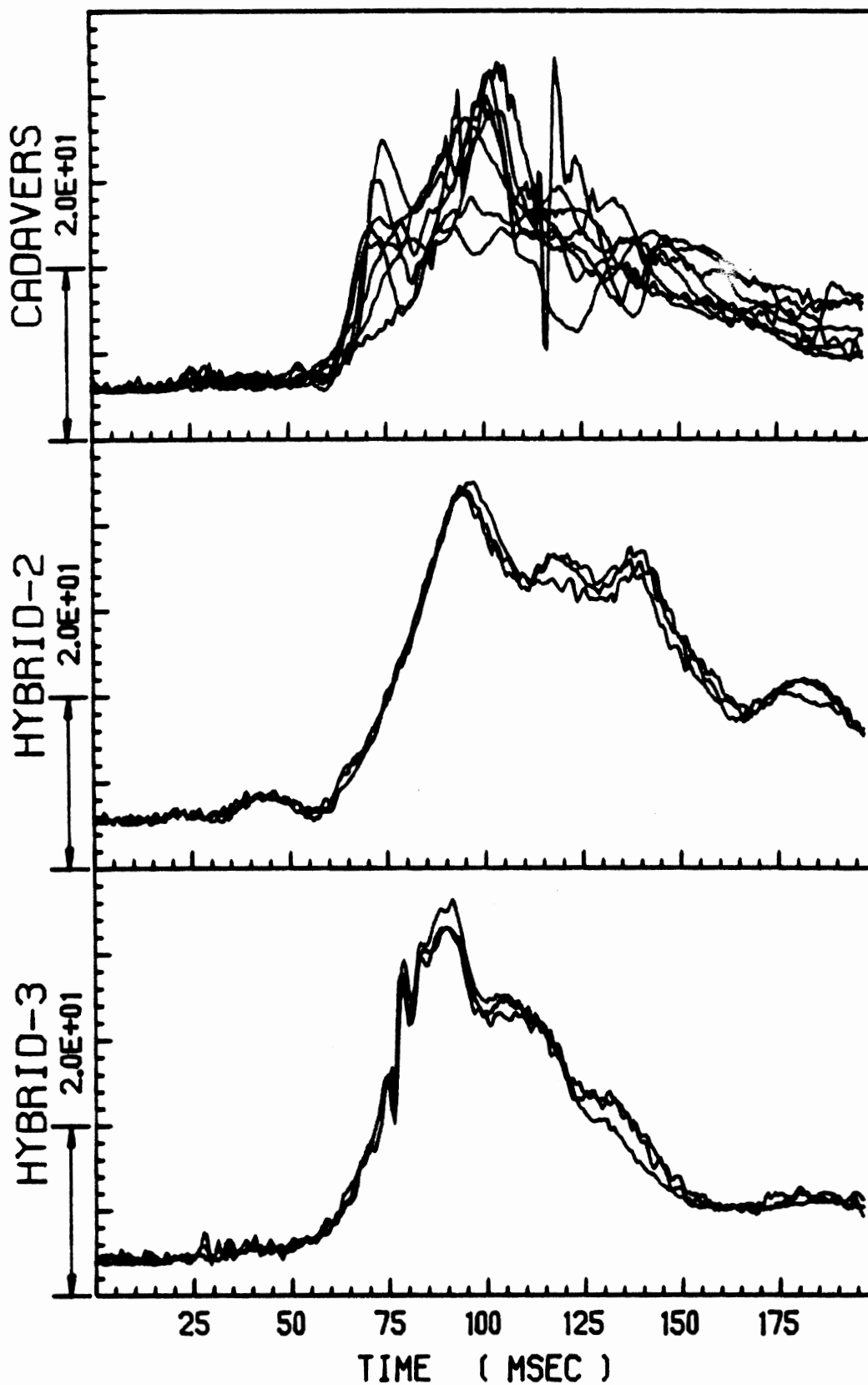


FIGURE 11. Resultant Head Center-of-Mass Acceleration. Mid-Severity Sled Runs -- A Composite Plot.

RESULTANT HEAD C.G. ACC, G'S

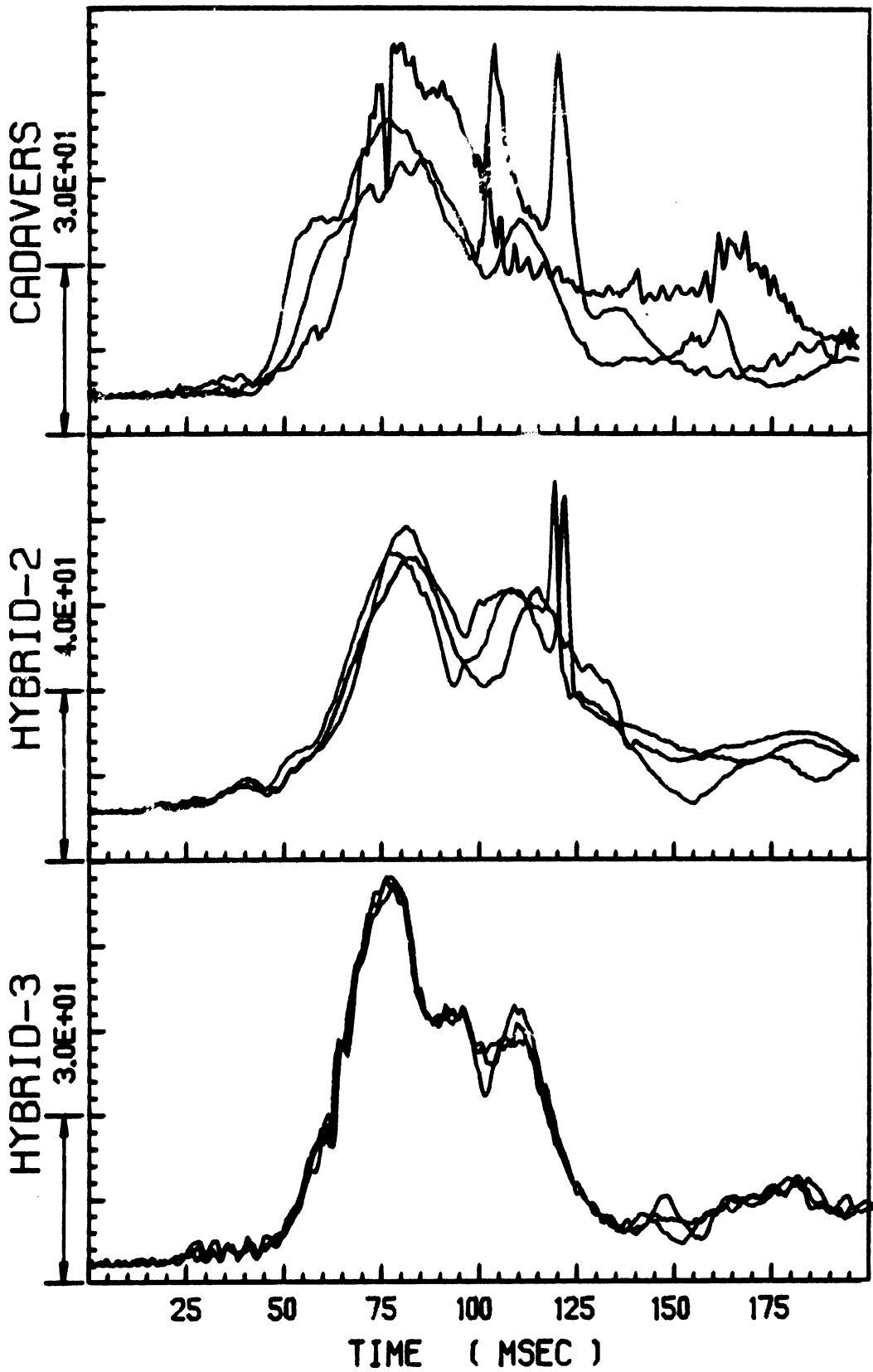


FIGURE 12. Resultant Head Center-of-Mass Acceleration.
High-Severity Sled Runs -- A Composite Plot.

RESULTANT HEAD C.G. VEL, IN/S

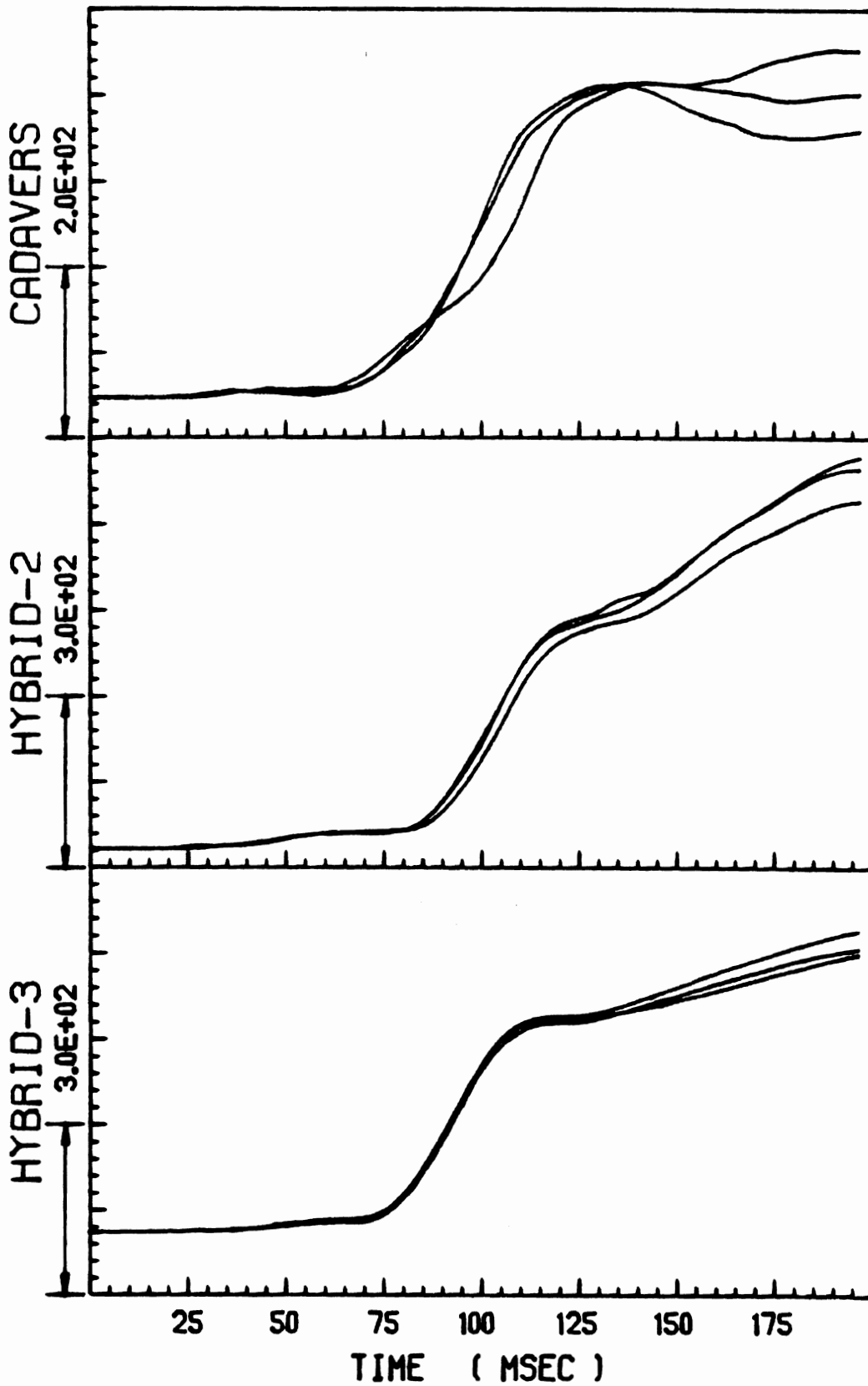


FIGURE 13. Resultant Head Center-of-Mass Velocity.
 Low-Severity Sled Runs -- A Composite Plot.

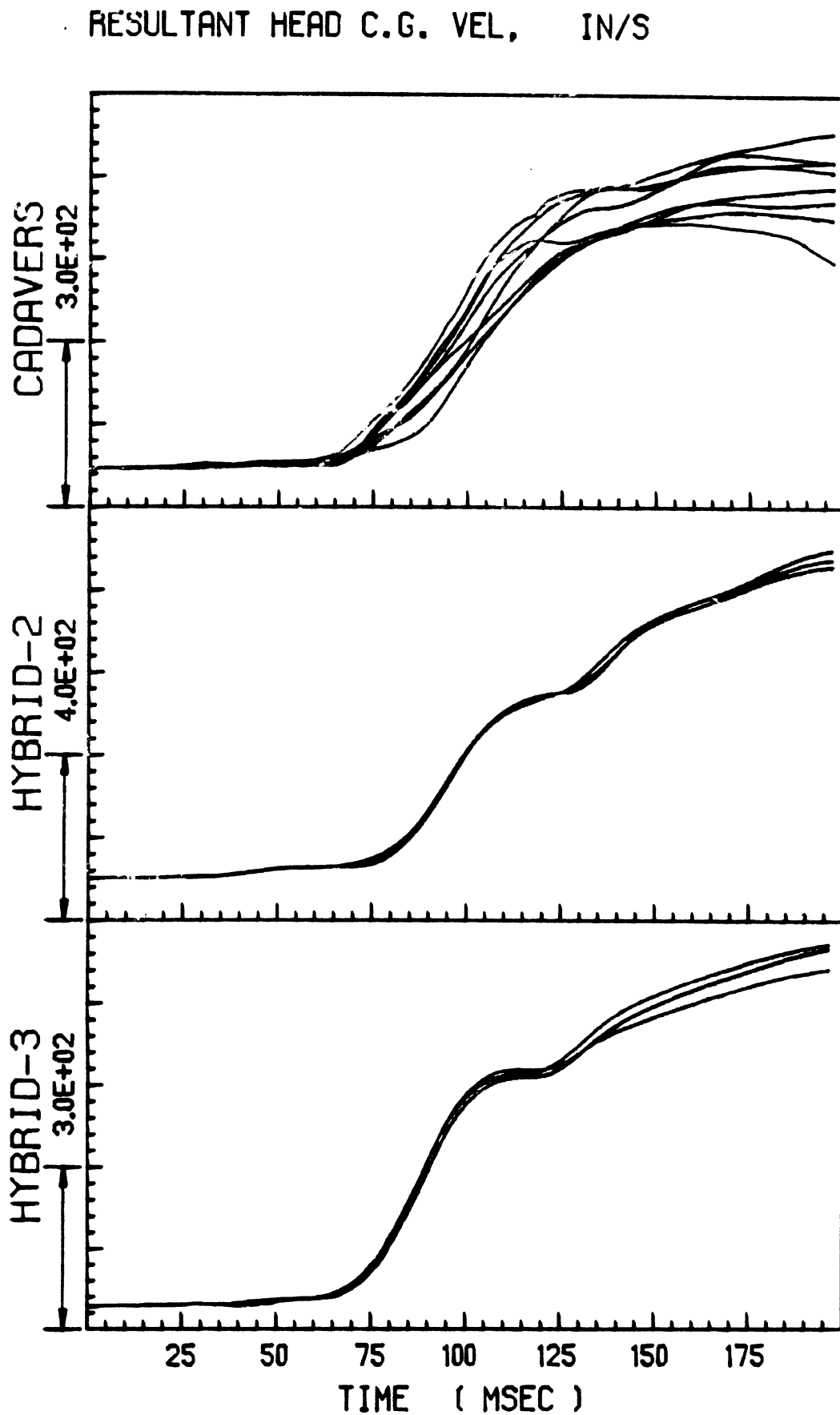


FIGURE 14. Resultant Head Center-of-Mass Velocity.
Mid-Severity Sled Runs -- A Composite Plot.

RESULTANT HEAD C.G. VEL, IN/S

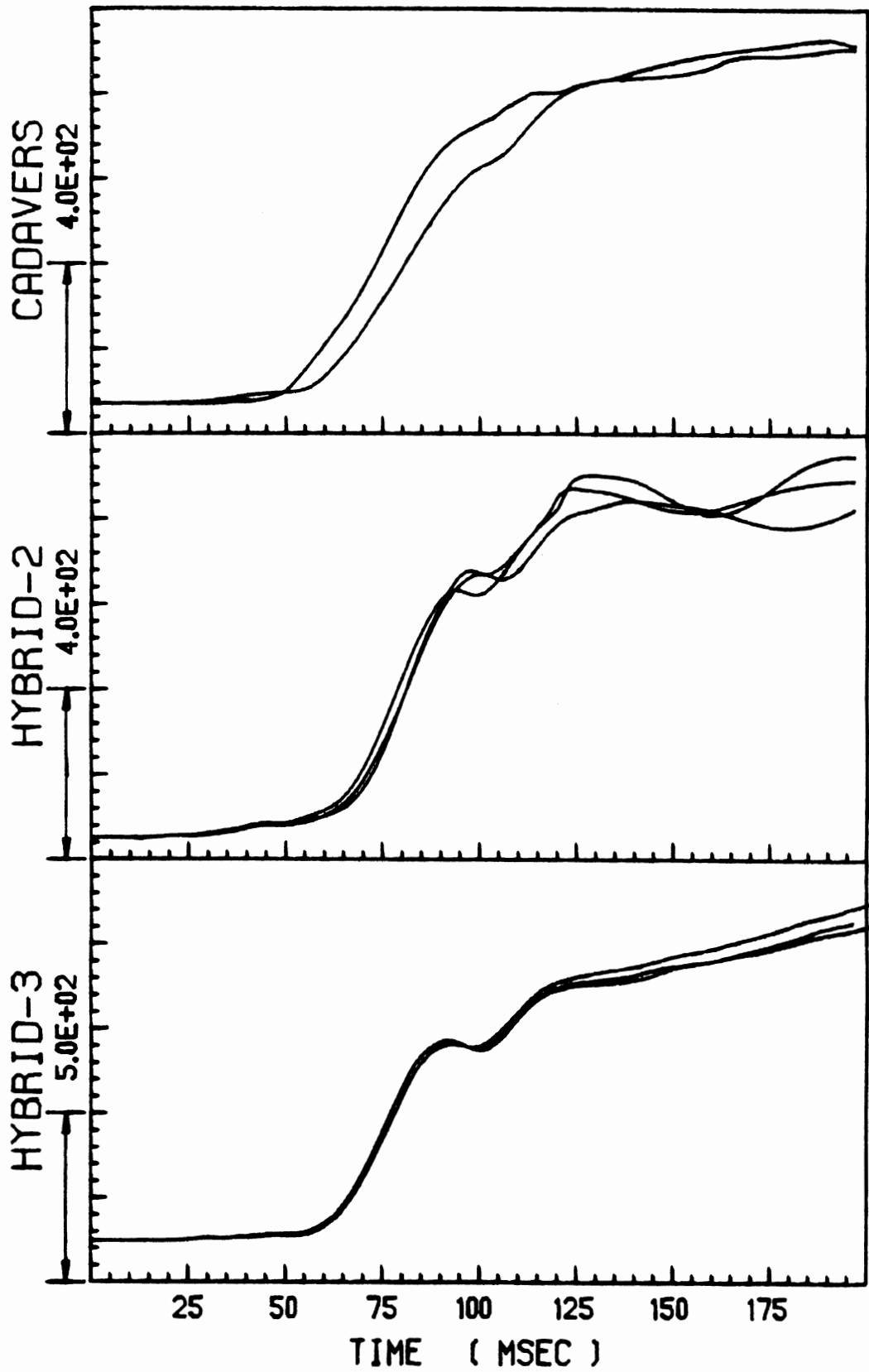


FIGURE 15. Resultant Head Center-of-Mass Velocity.
High-Severity Sled Runs -- A Composite Plot.

INTERNAL CHEST A-P ACC, G'S

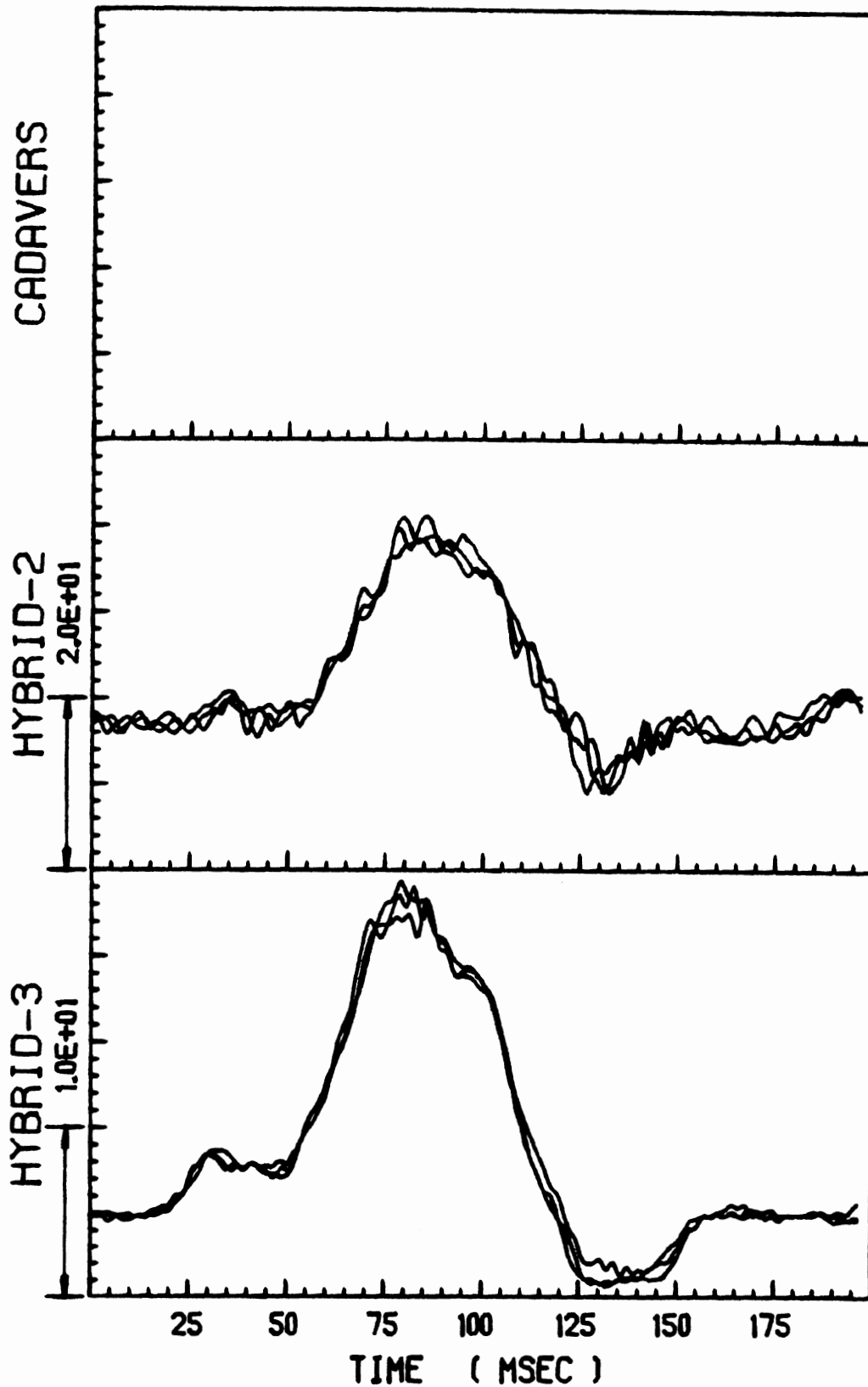


FIGURE 16. Internal Chest A-P Acceleration.
Low-Severity Sled Runs -- A Composite Plot.

INTERNAL CHEST A-P ACC, G'S

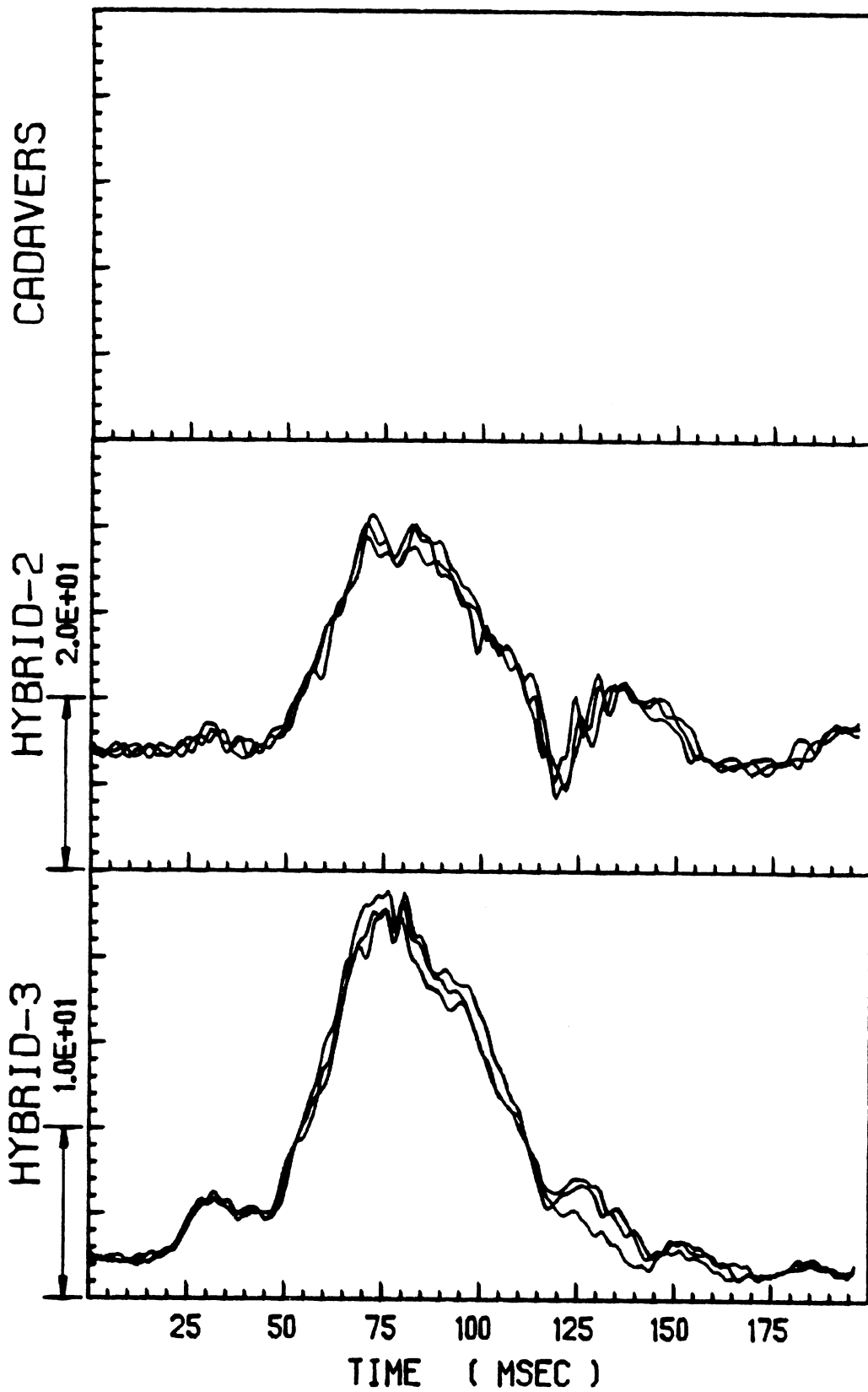


FIGURE 17. Internal Chest A-P Acceleration.
Mid-Severity Sled Runs -- A Composite Plot.

INTERNAL CHEST A-P ACC, G'S

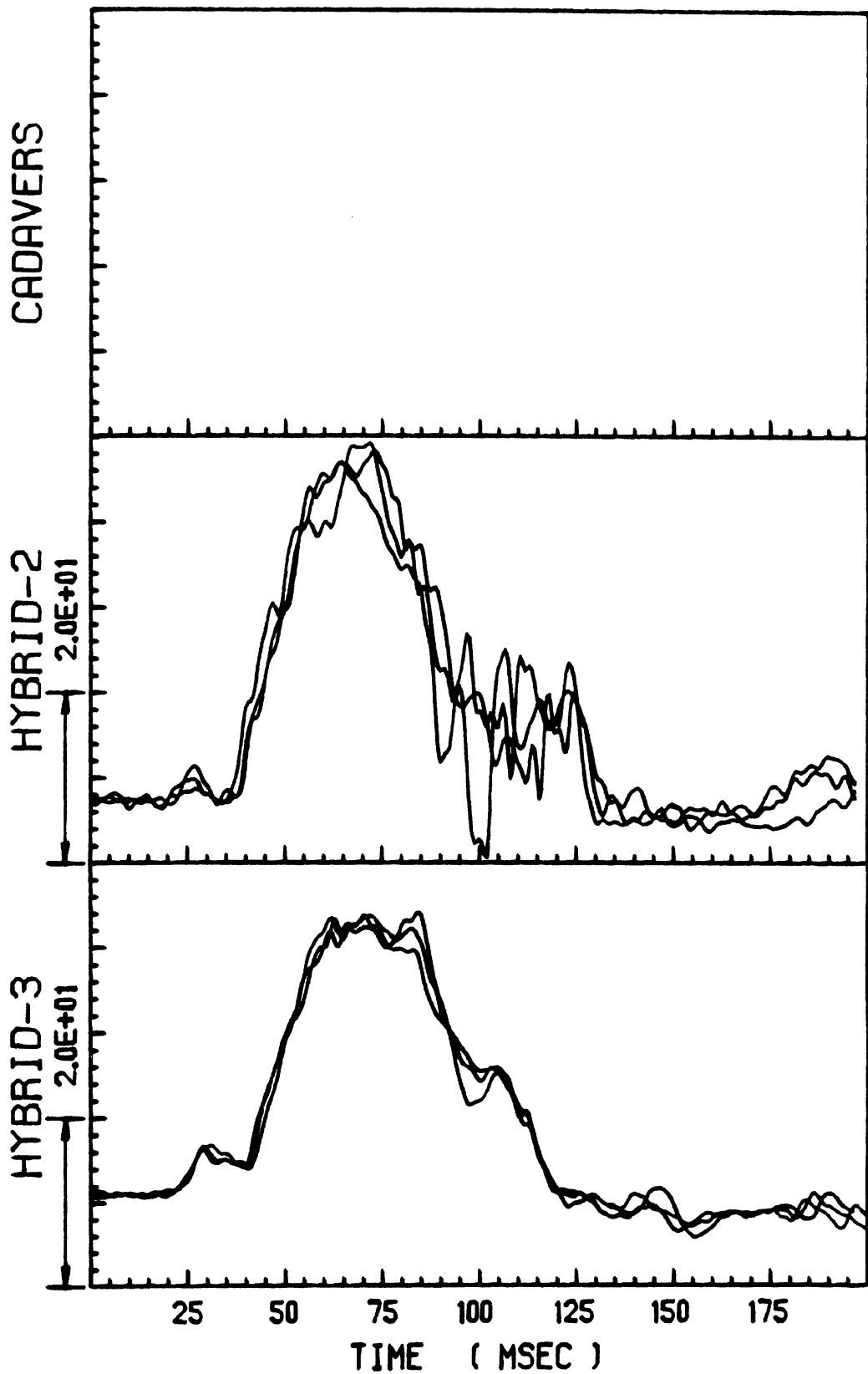


FIGURE 18. Internal Chest A-P Acceleration.
High-Severity Sled Runs -- A Composite Plot.

EXTERNAL CHEST A-P ACC, G'S

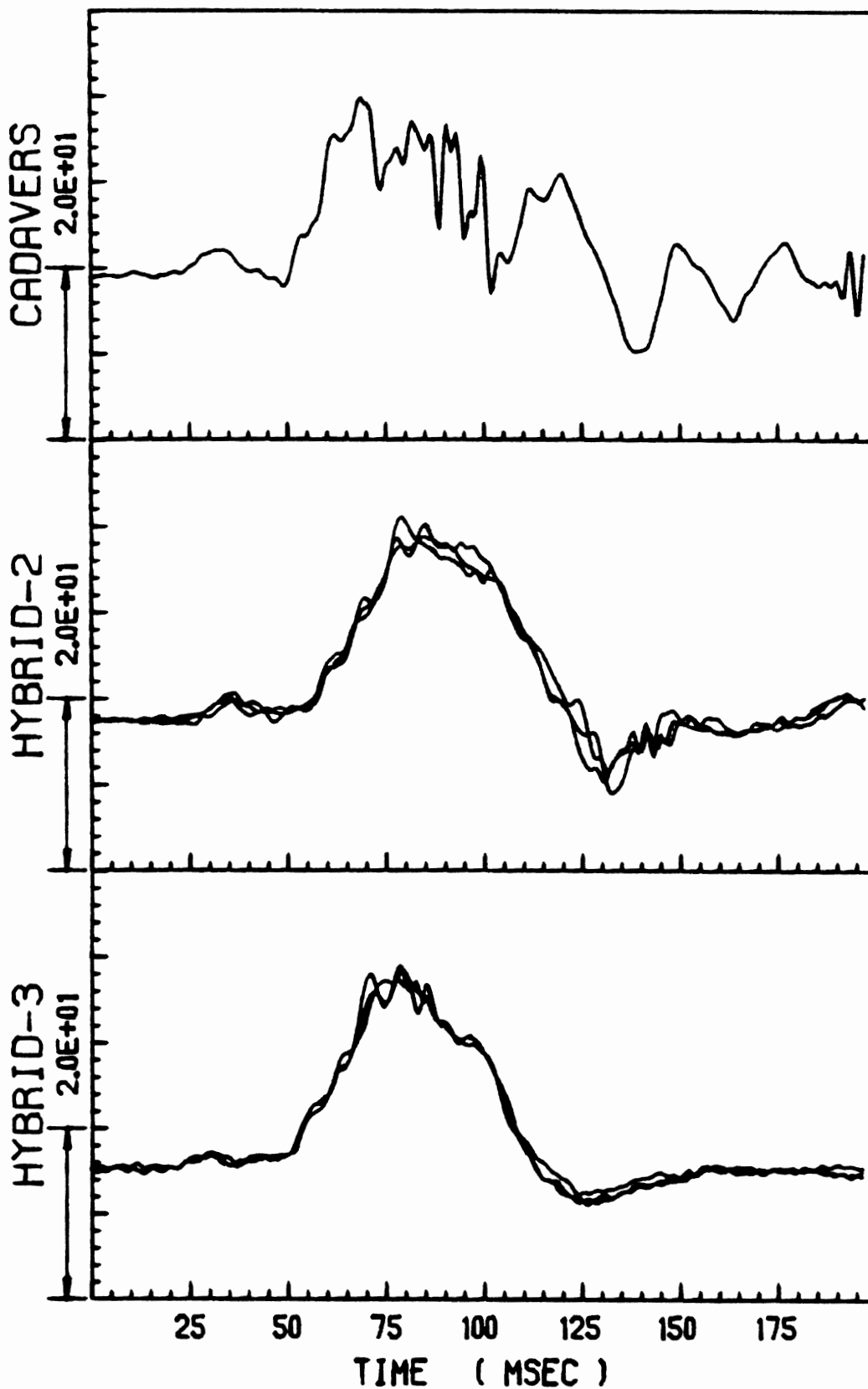


FIGURE 19. External Chest A-P Acceleration.
Low-Severity Sled Runs -- A Composite Plot.

EXTERNAL CHEST A-P ACC, G'S

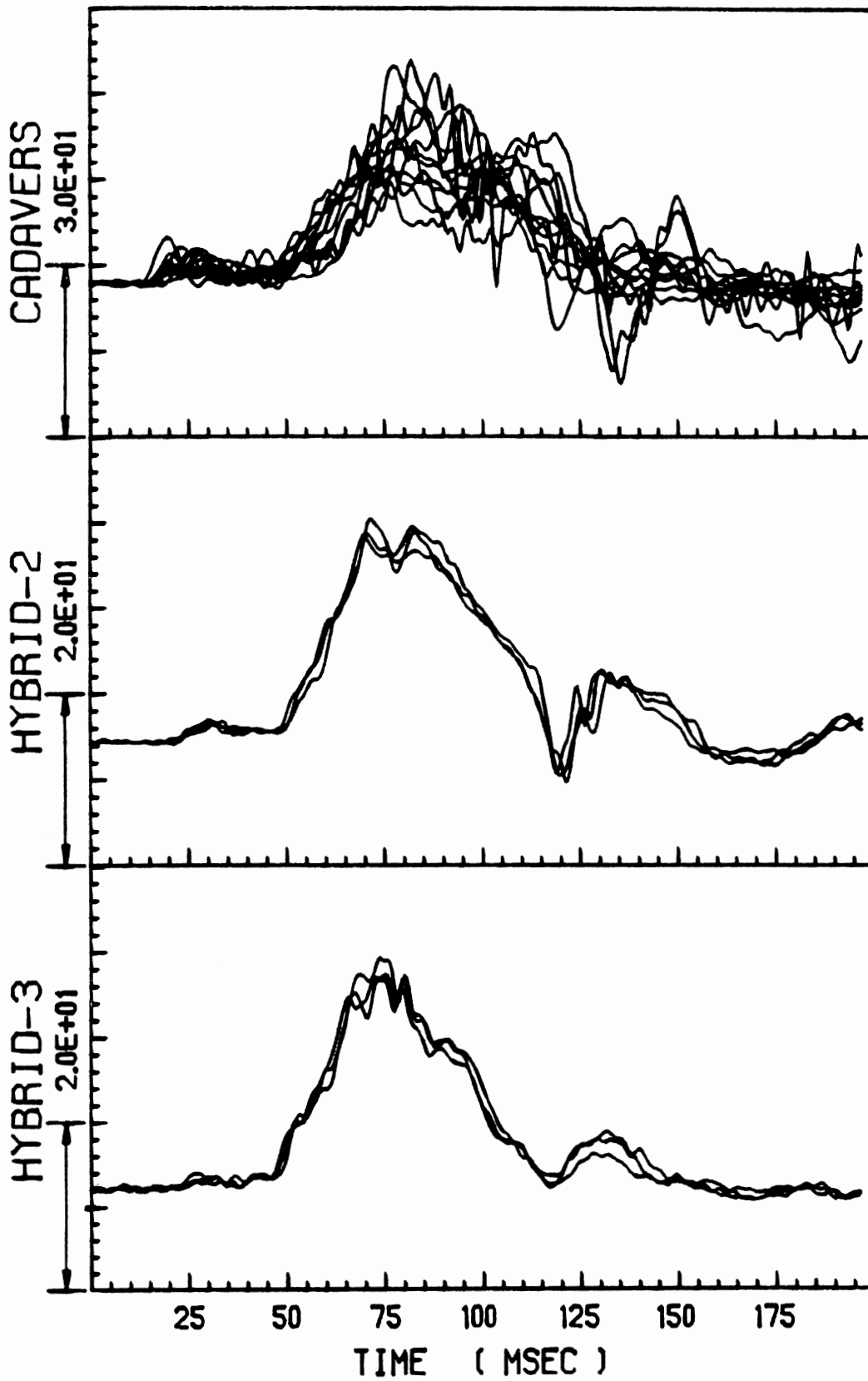


FIGURE 20. External Chest A-P Acceleration.
Mid-Severity Sled Runs -- A Composite Plot.

EXTERNAL CHEST A-P ACC, G'S

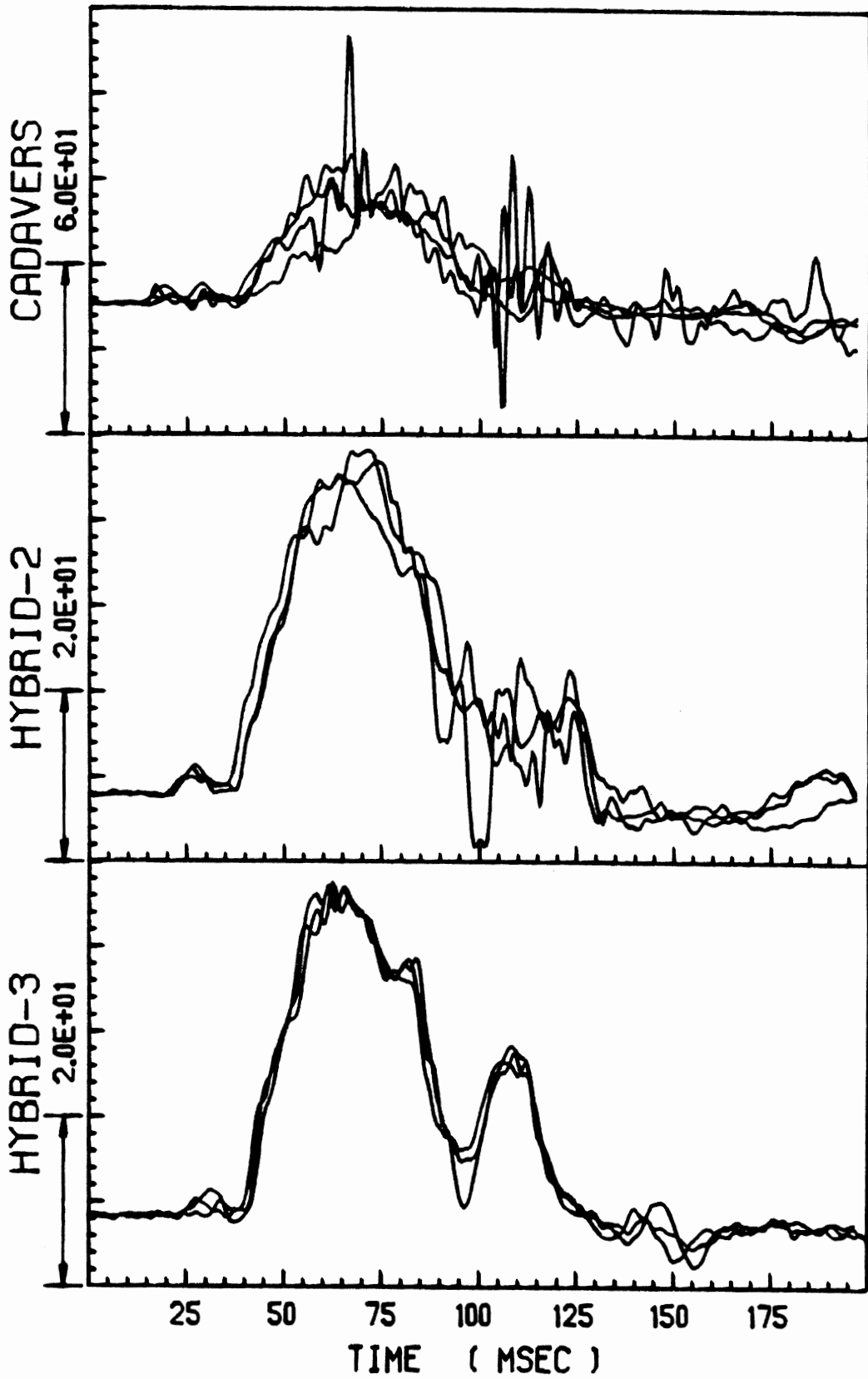


FIGURE 21. External Chest A-P Acceleration.
High-Severity Sled Runs -- A Composite Plot.

INTERNAL PELVIS A-P ACC, G'S

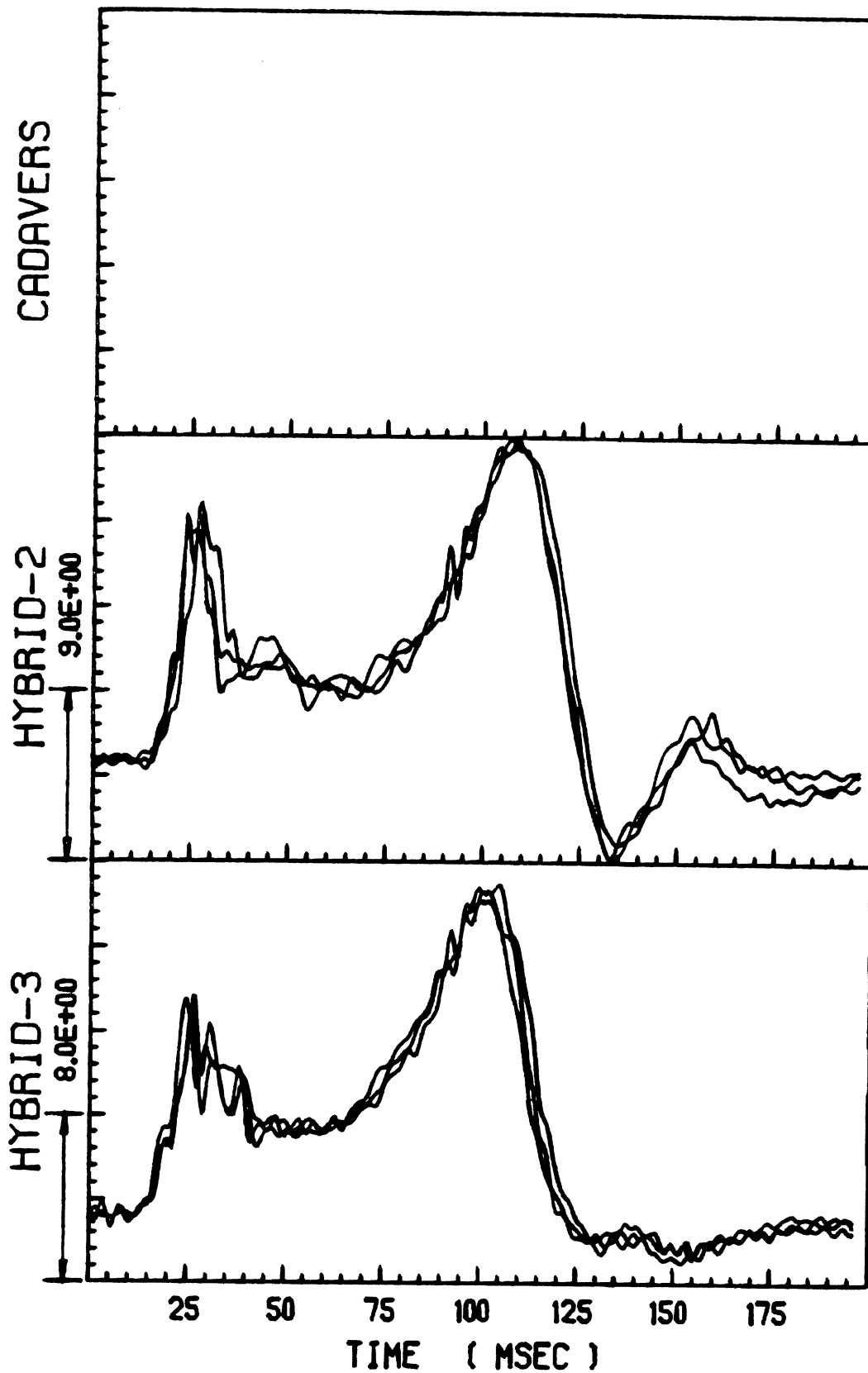


FIGURE 22. Internal Pelvis A-P Acceleration.
Low-Severity Sled Runs -- A Composite Plot.

INTERNAL PELVIS A-P ACC, G'S

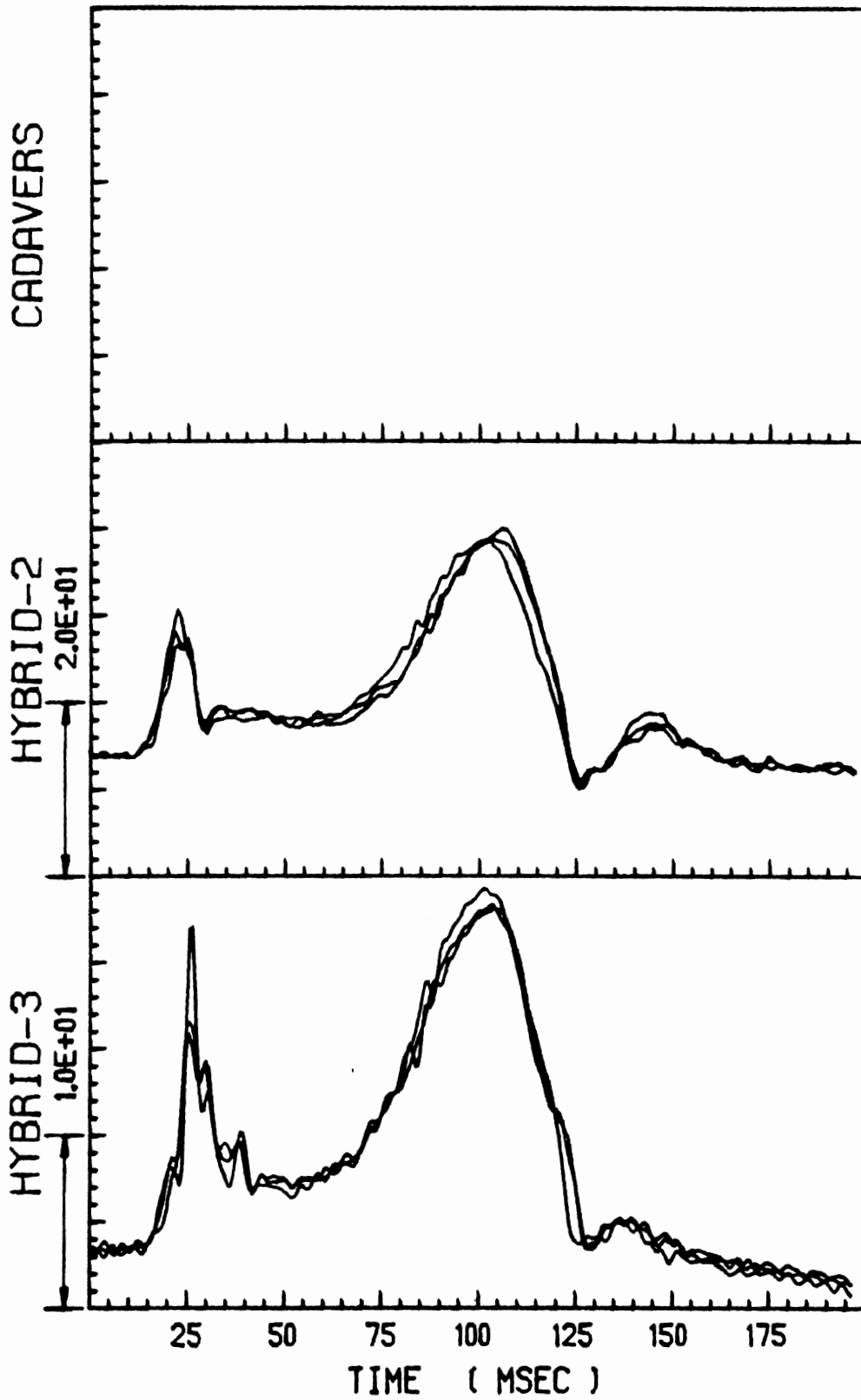


FIGURE 23. Internal Pelvis A-P Acceleration.
Mid-Severity Sled Runs -- A Composite Plot.

INTERNAL PELVIS A-P ACC, G'S

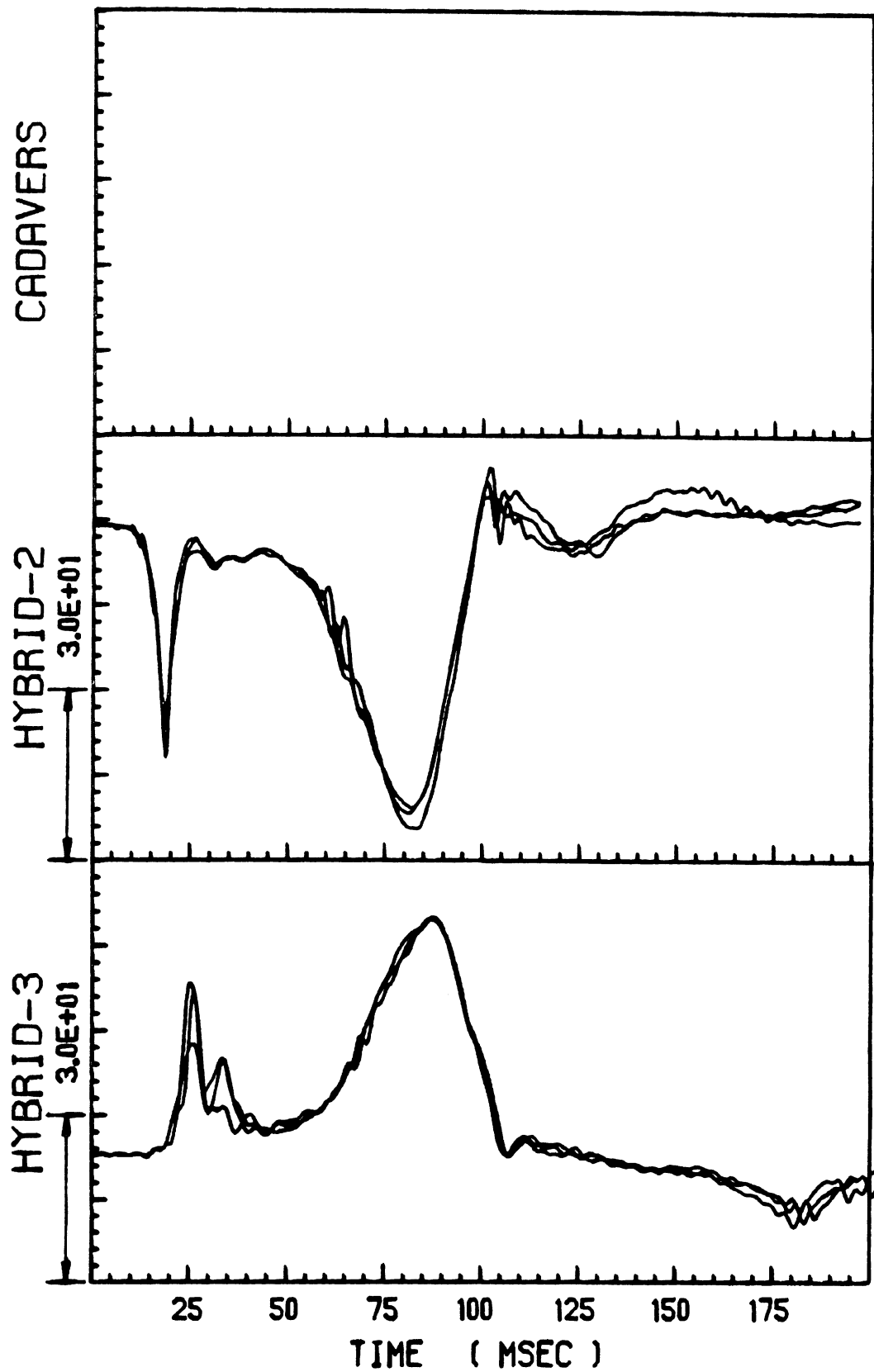


FIGURE 24. Internal Pelvis A-P Acceleration.
High-Severity Sled Runs -- A Composite Plot.

EXTERNAL PELVIS A-P ACC, G'S

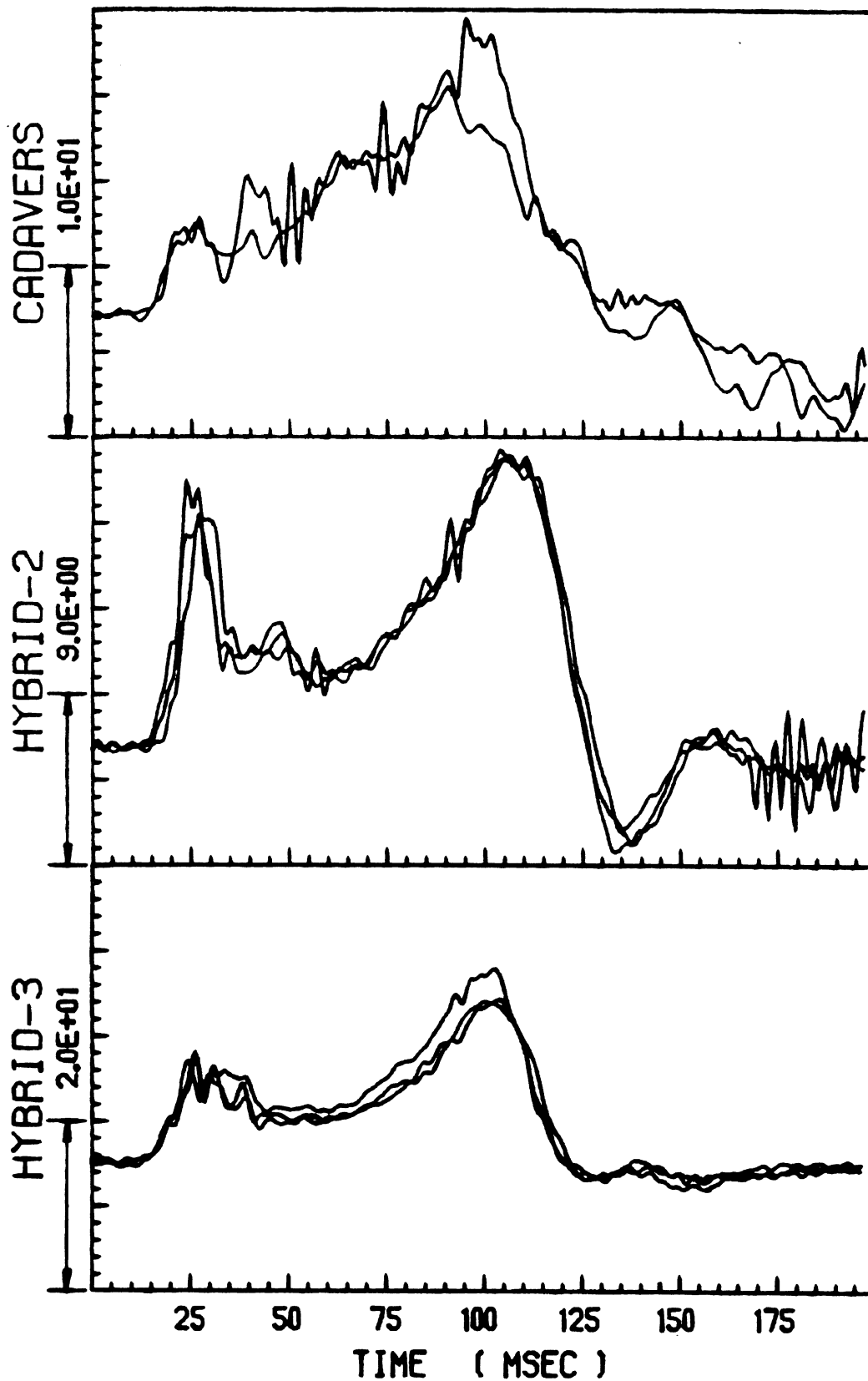


FIGURE 25. External Pelvis A-P Acceleration.
 Low-Severity Sled Runs -- A Composite Plot.

EXTERNAL PELVIS A-P ACC, G'S

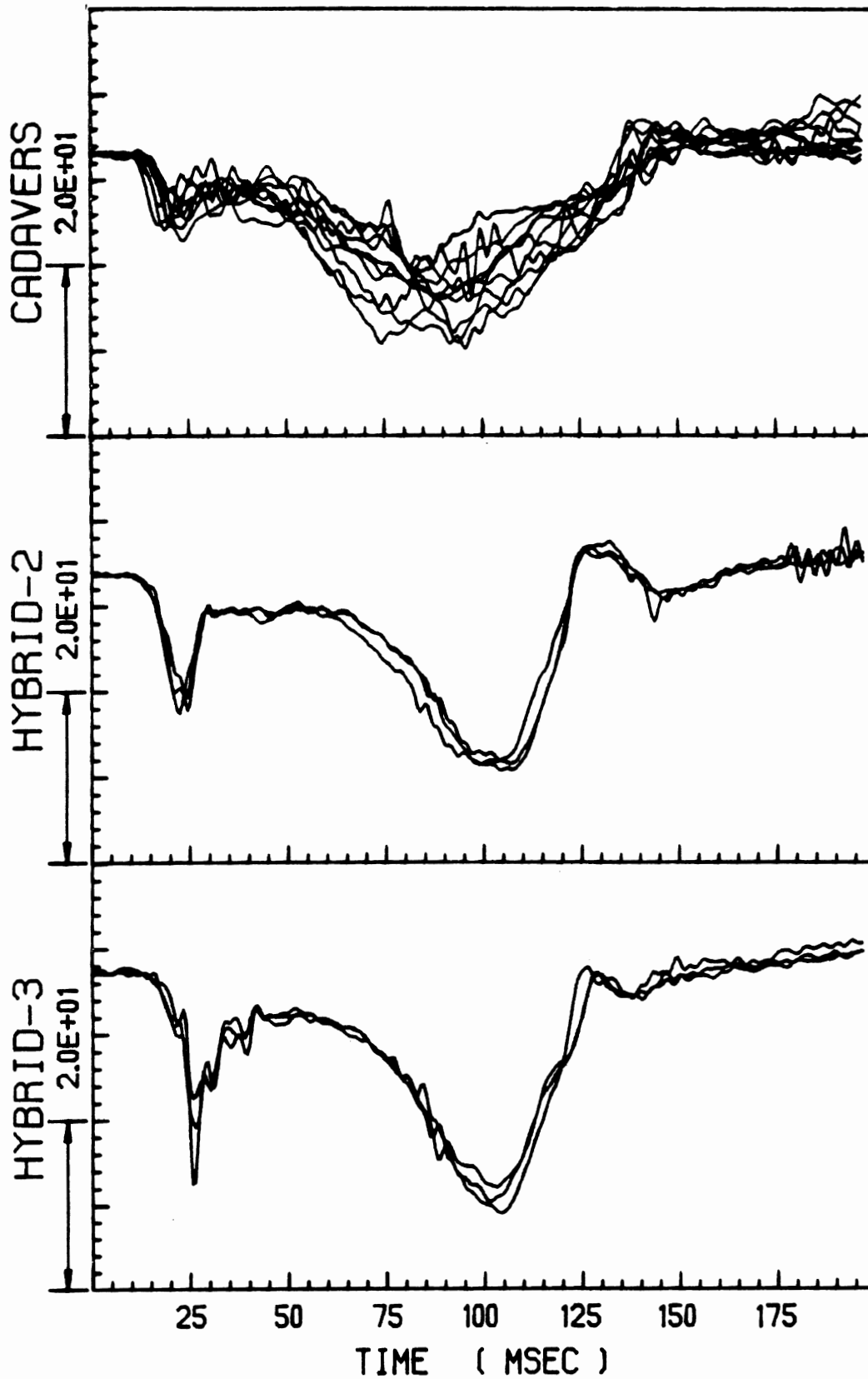


FIGURE 26. External Pelvis A-P Acceleration.
Mid-Severity Sled Runs -- A Composite Plot.

EXTERNAL PELVIS A-P ACC, G'S

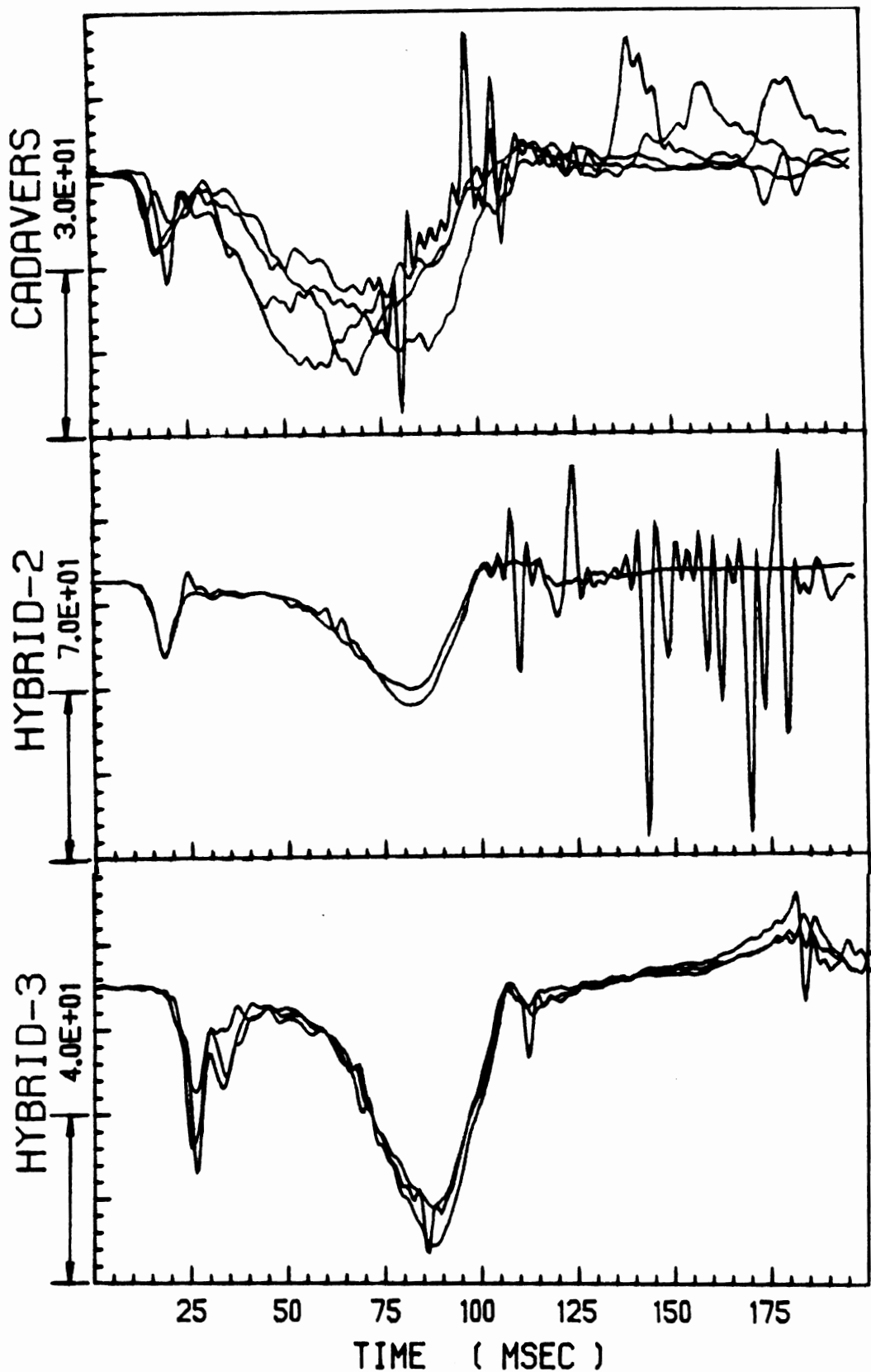


FIGURE 27. External Pelvis A-P Acceleration.
High-Severity Sled Runs -- A Composite Plot.

UPPER SHOULDER BELT FORCE, LBS

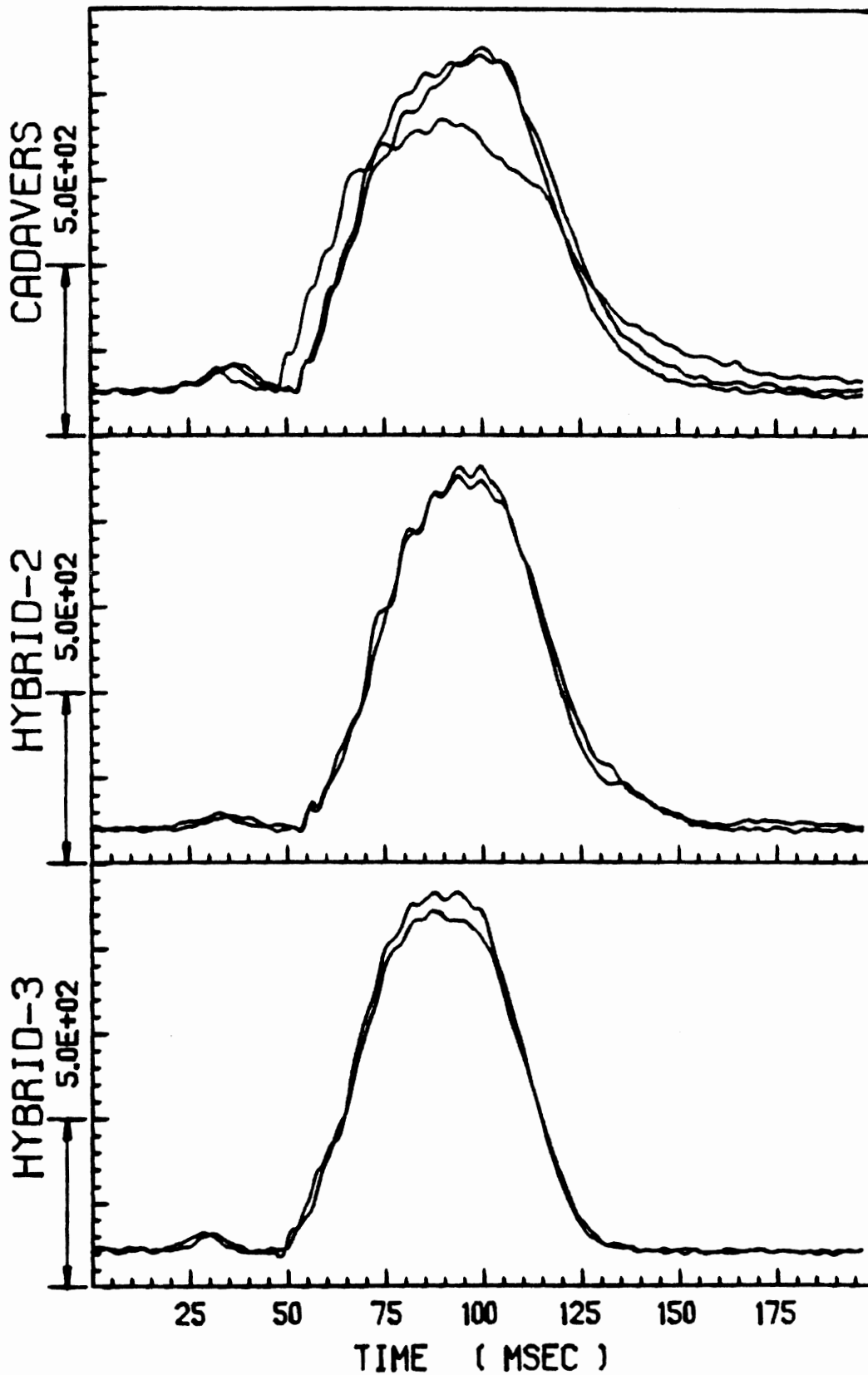


FIGURE 28. Upper Shoulder Harness Force.
Low-Severity Sled Runs -- A Composite Plot.

UPPER SHOULDER BELT FORCE, LBS

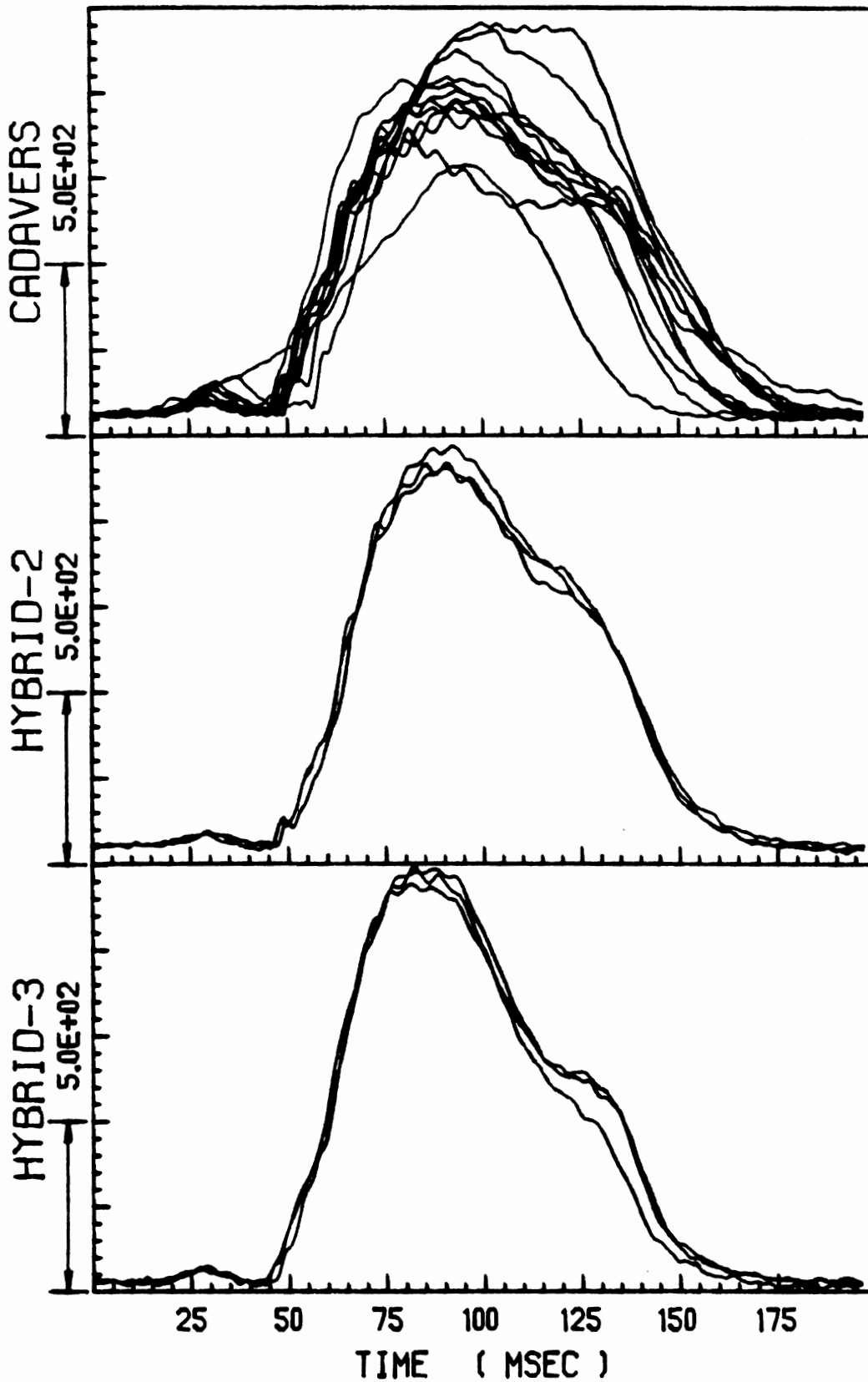


FIGURE 29. Upper Shoulder Harness Force.
Mid-Severity Sled Runs -- A Composite Plot.

UPPER SHOULDER BELT FORCE, LBS

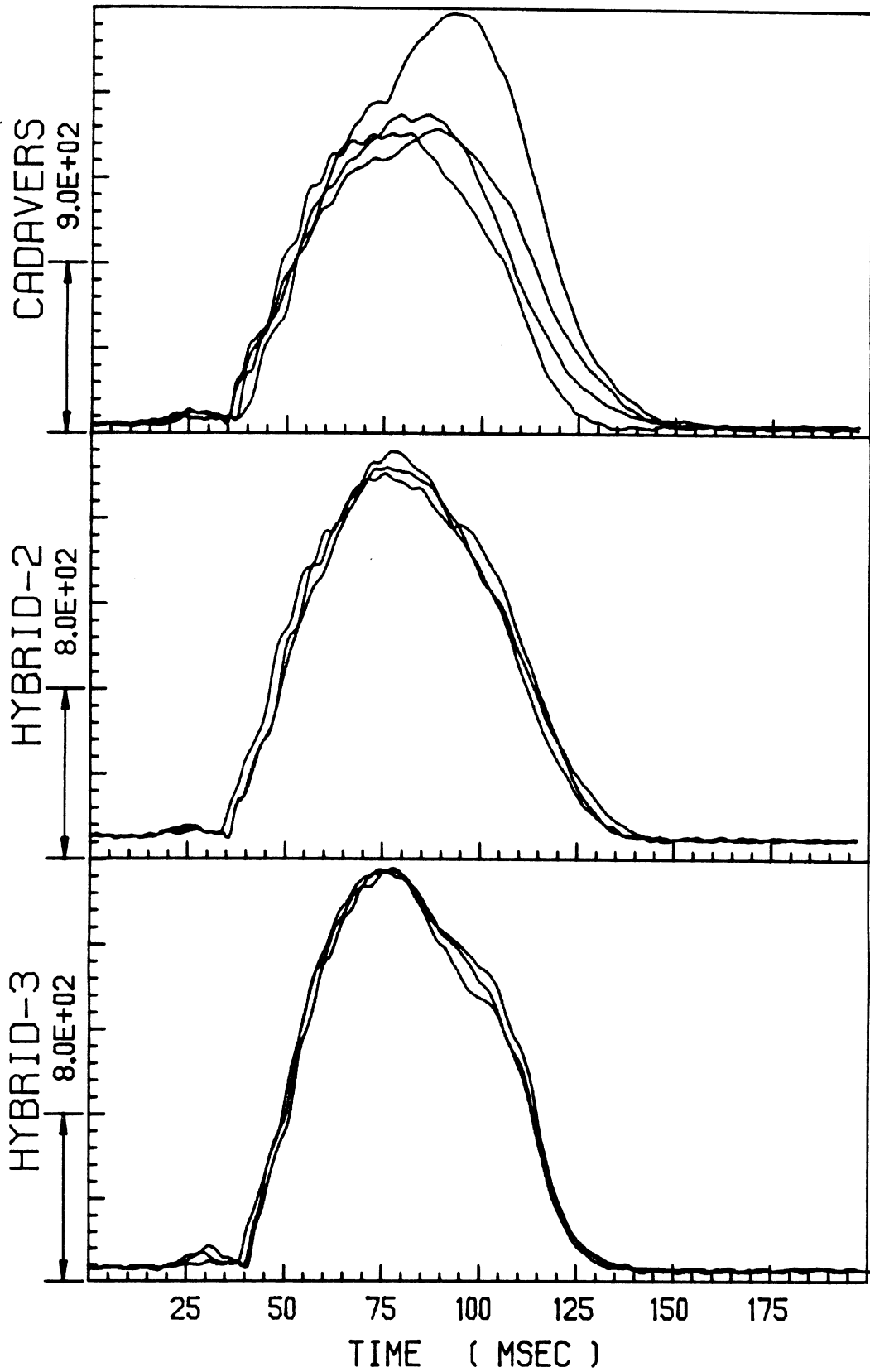


FIGURE 30. Upper Shoulder Harness Force.
High-Severity Sled Runs -- A Composite Plot.

LOWER SHOULDER BELT FORCE, LBS

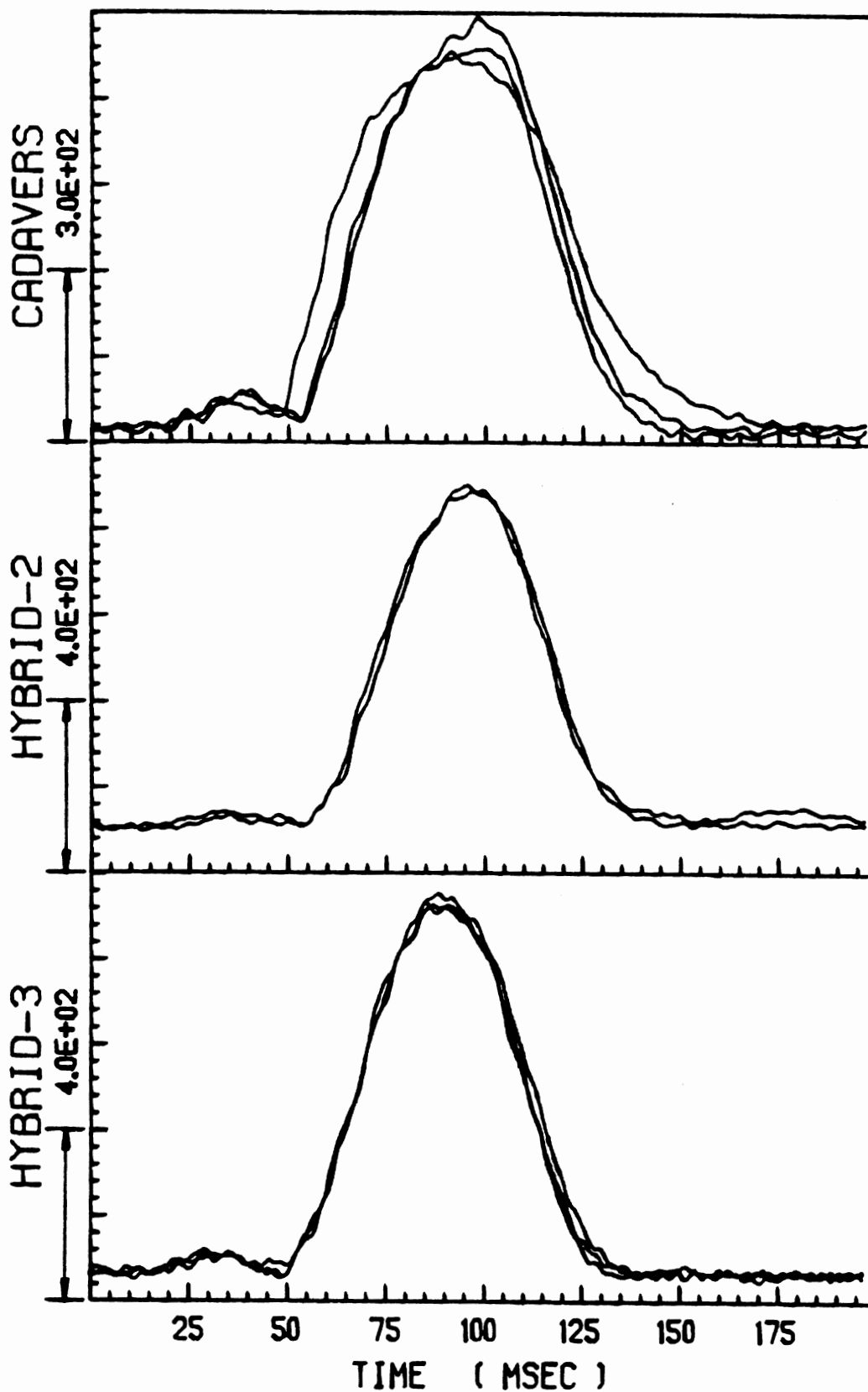


FIGURE 31. Lower Shoulder Harness Force.
Low-Severity Sled Runs -- A Composite Plot.

LOWER SHOULDER BELT FORCE, LBS

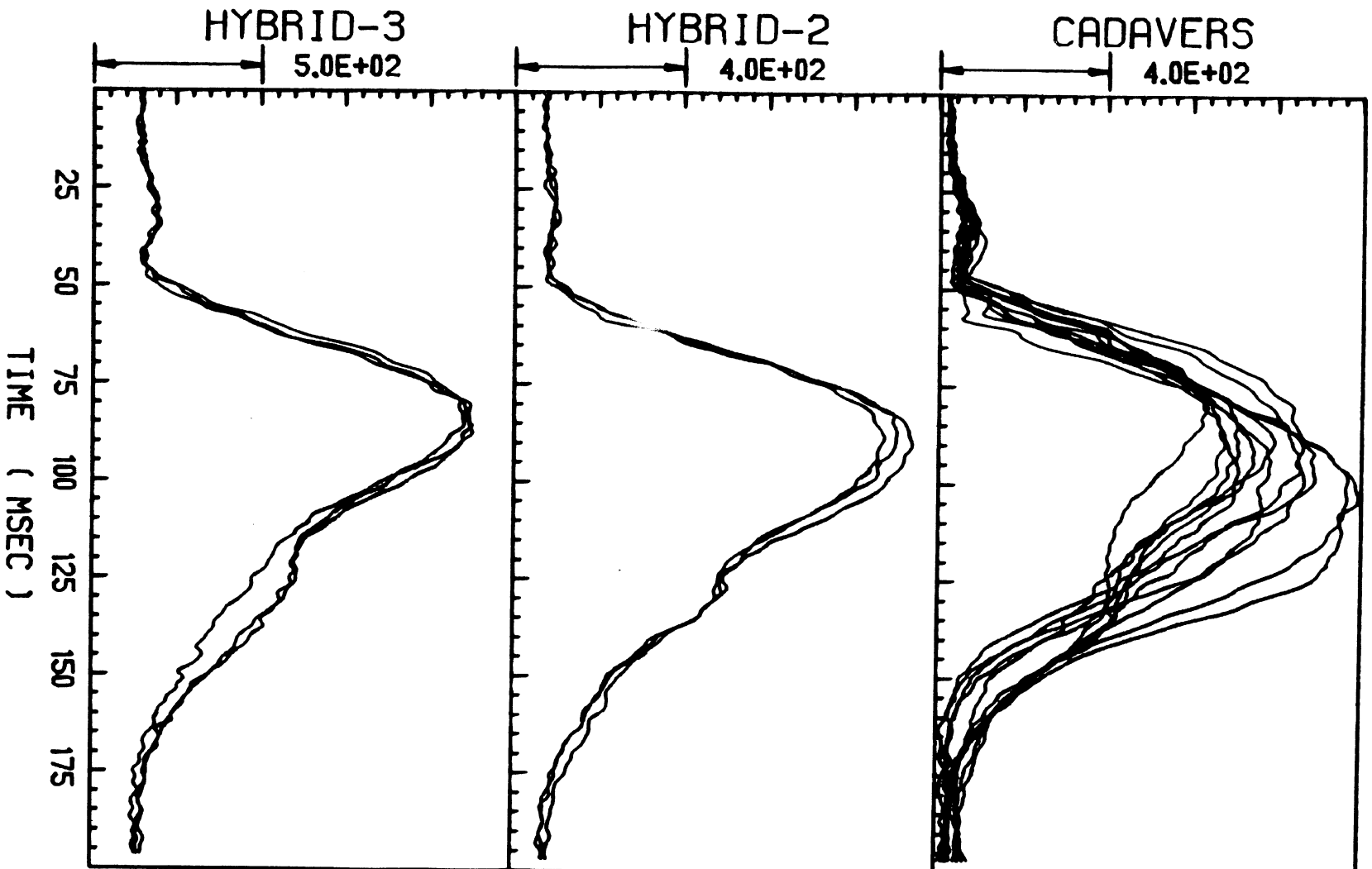


FIGURE 32. Lower Shoulder Harness Force.
Mid-Severity Sled Runs -- A Composite Plot.

LOWER SHOULDER BELT FORCE, LBS

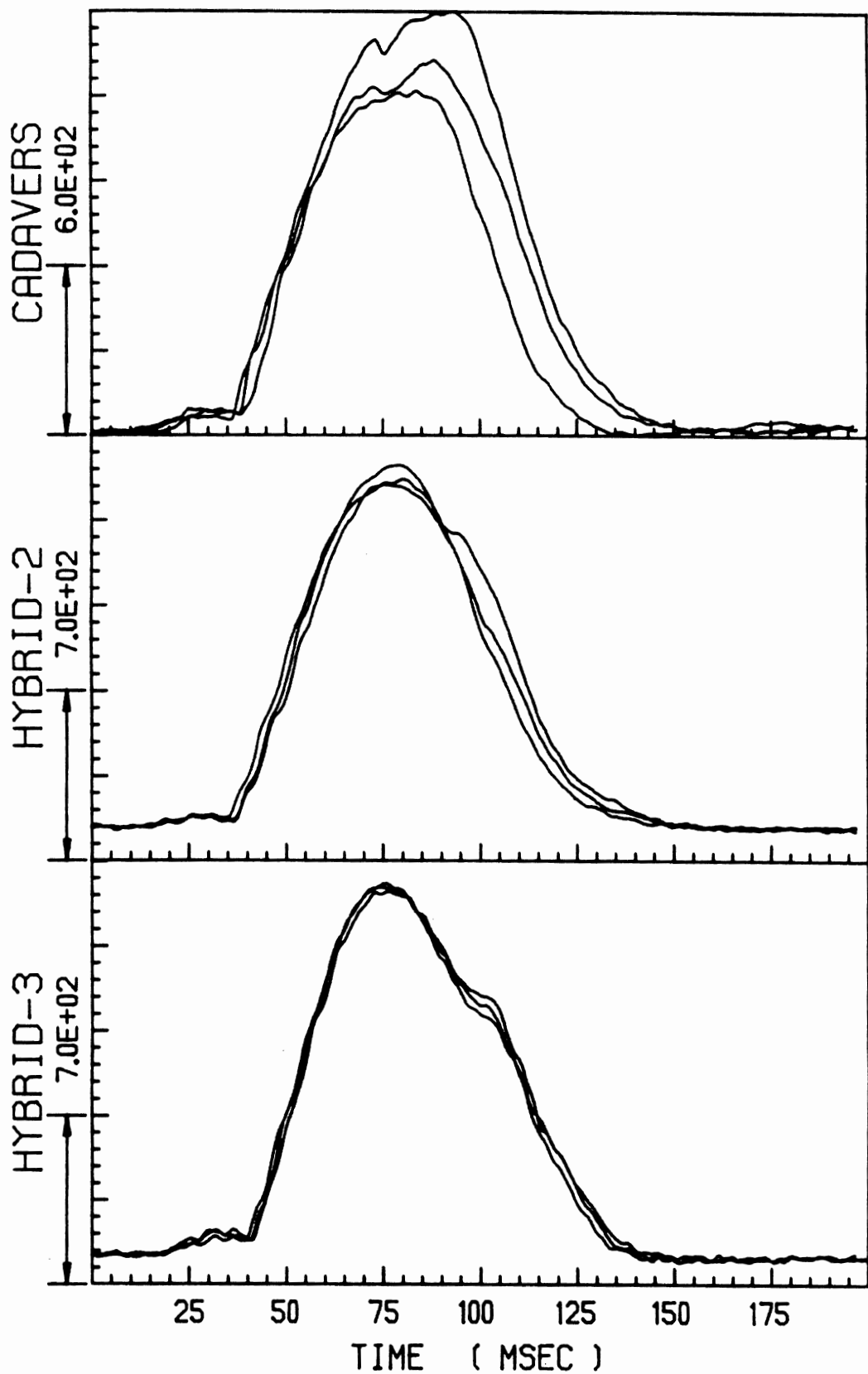


FIGURE 33. Lower Shoulder Harness Force.
High-Severity Sled Runs -- A Composite Plot.

LEFT LAP BELT FORCE, LBS

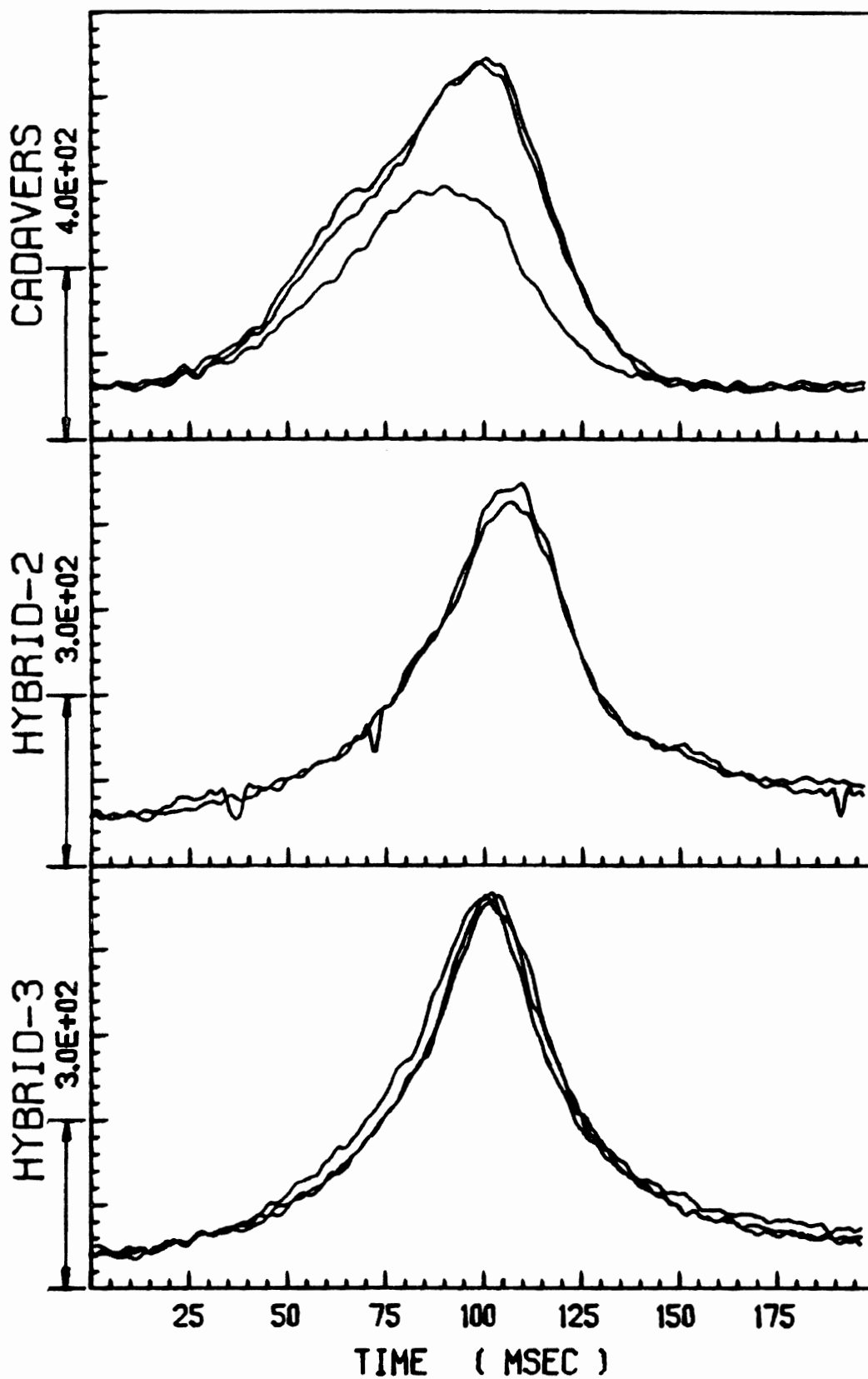


FIGURE 34. Left Lap Belt Load.
Low-Severity Sled Runs -- A Composite Plot.

LEFT LAP BELT FORCE, LBS

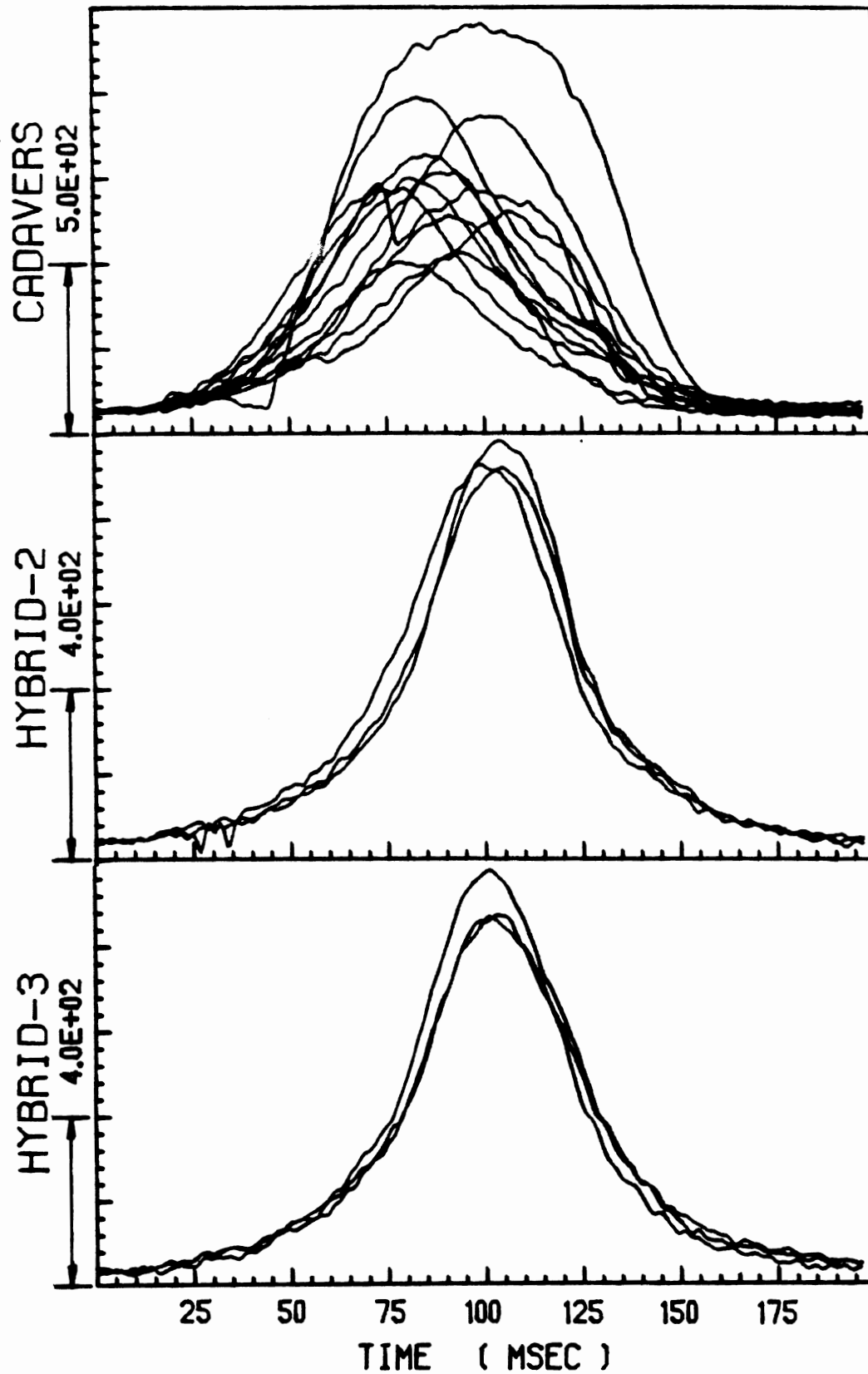


FIGURE 35. Left Lap Belt Load.
Mid-Severity Sled Runs -- A Composite Plot.

LEFT LAP BELT FORCE, LBS

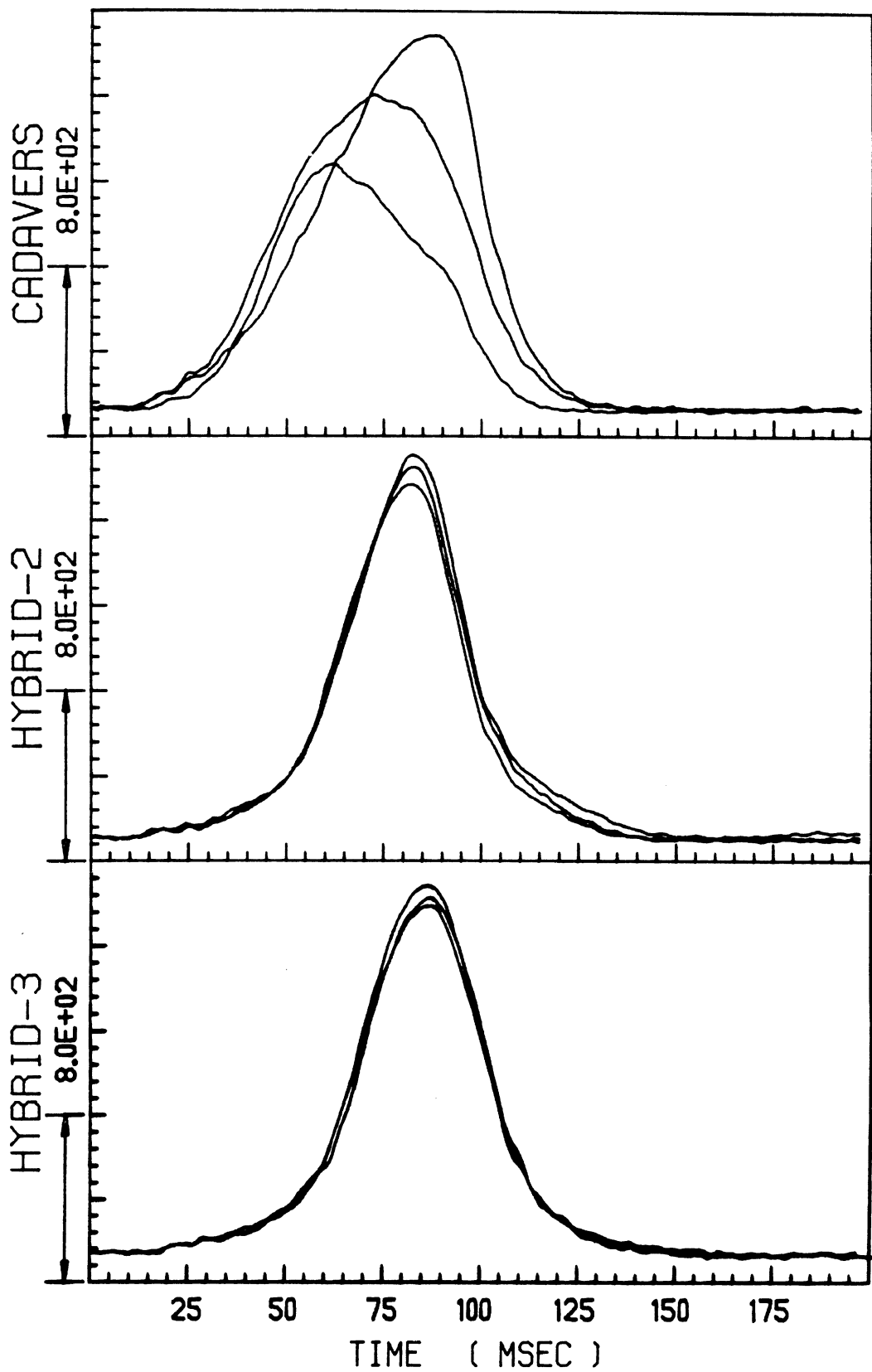


FIGURE 36. Left Lap Belt Load.
High-Severity Sled Runs -- A Composite Plot.

RIGHT LAP BELT FORCE, LBS

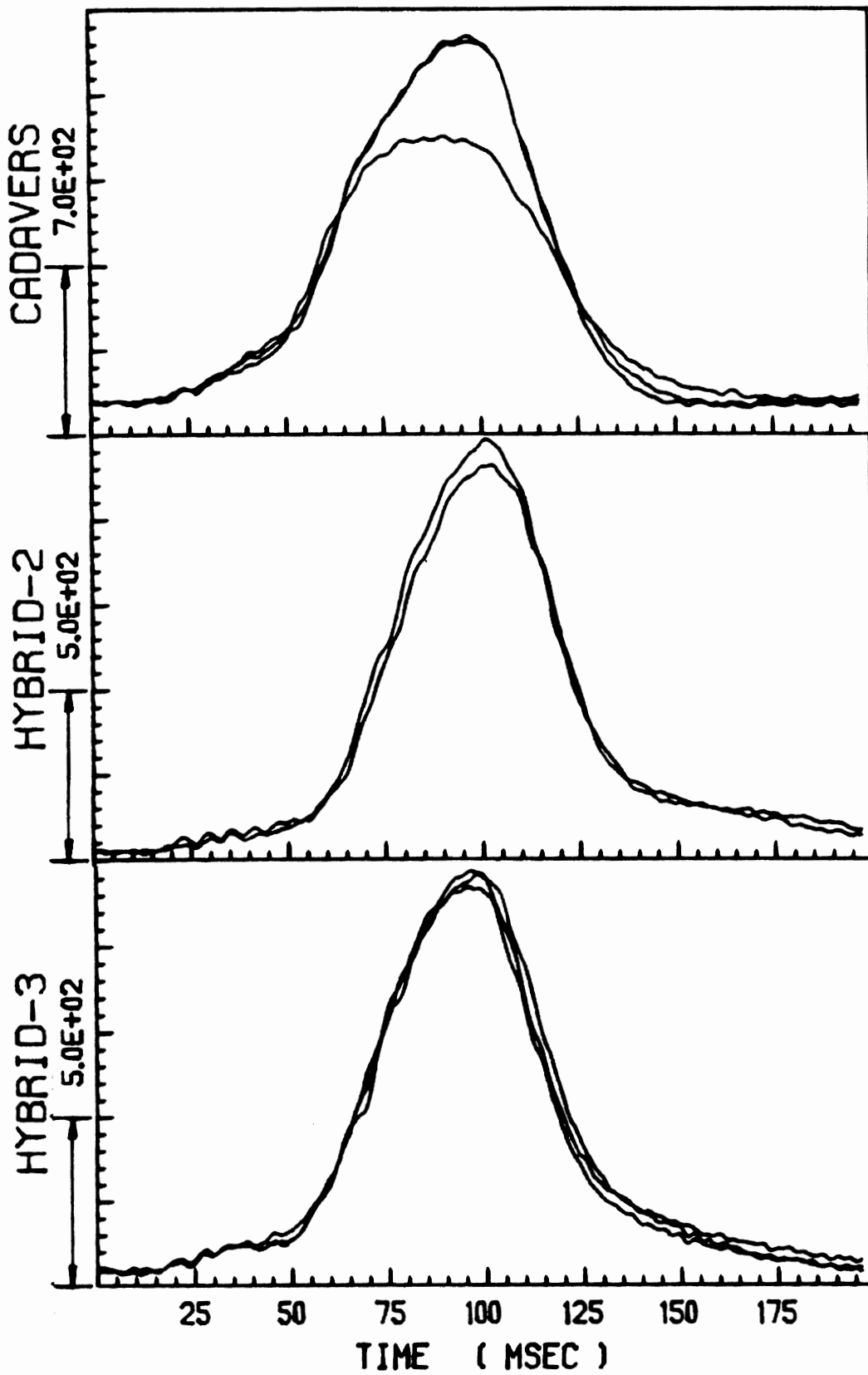


FIGURE 37. Right Lap Belt Load.
 Low-Severity Sled Runs -- A Composite Plot.

RIGHT LAP BELT FORCE, LBS

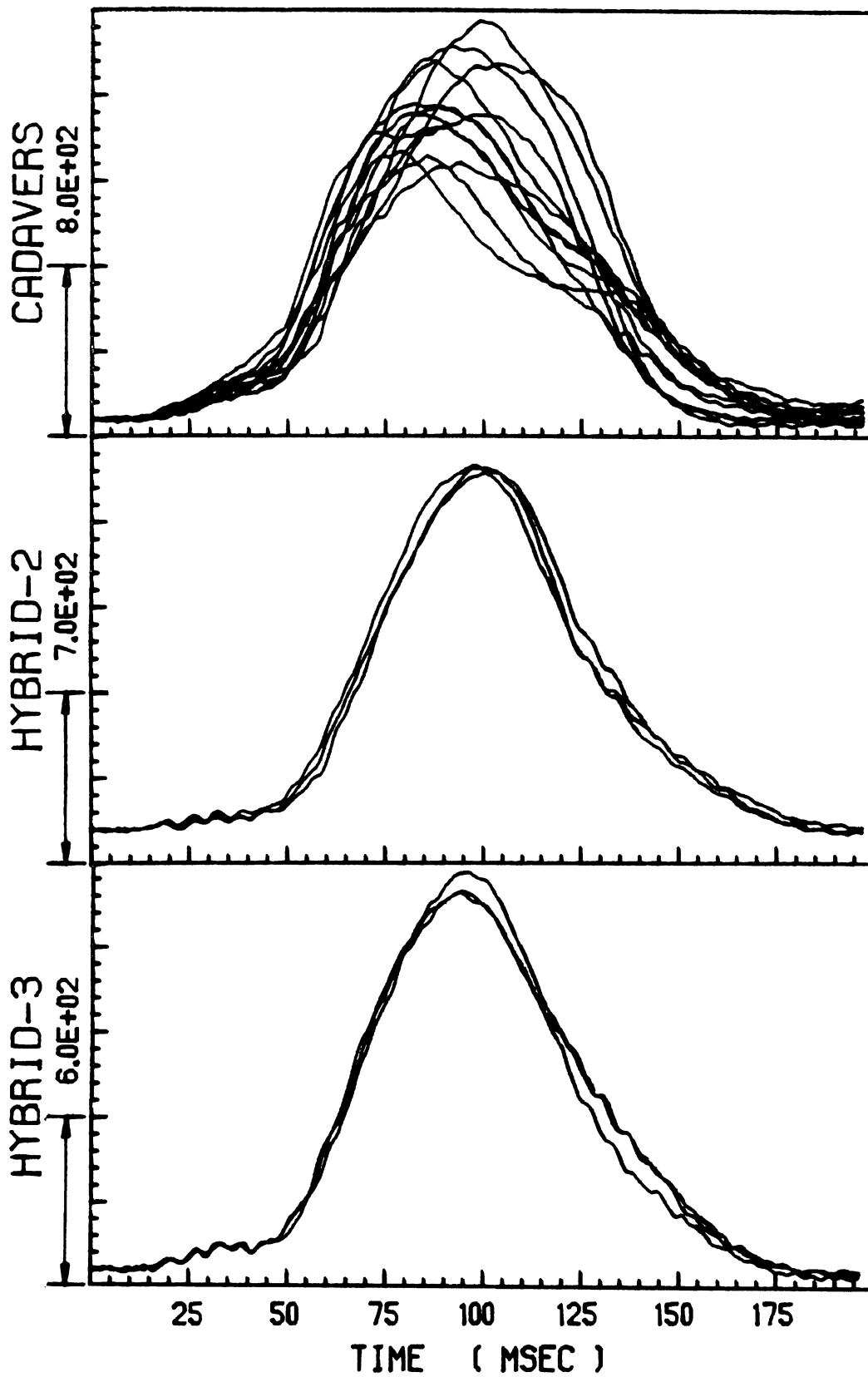


FIGURE 38. Right Lap Belt Load.
Mid-Severity Sled Runs -- A Composite Plot.

RIGHT LAP BELT FORCE, LBS

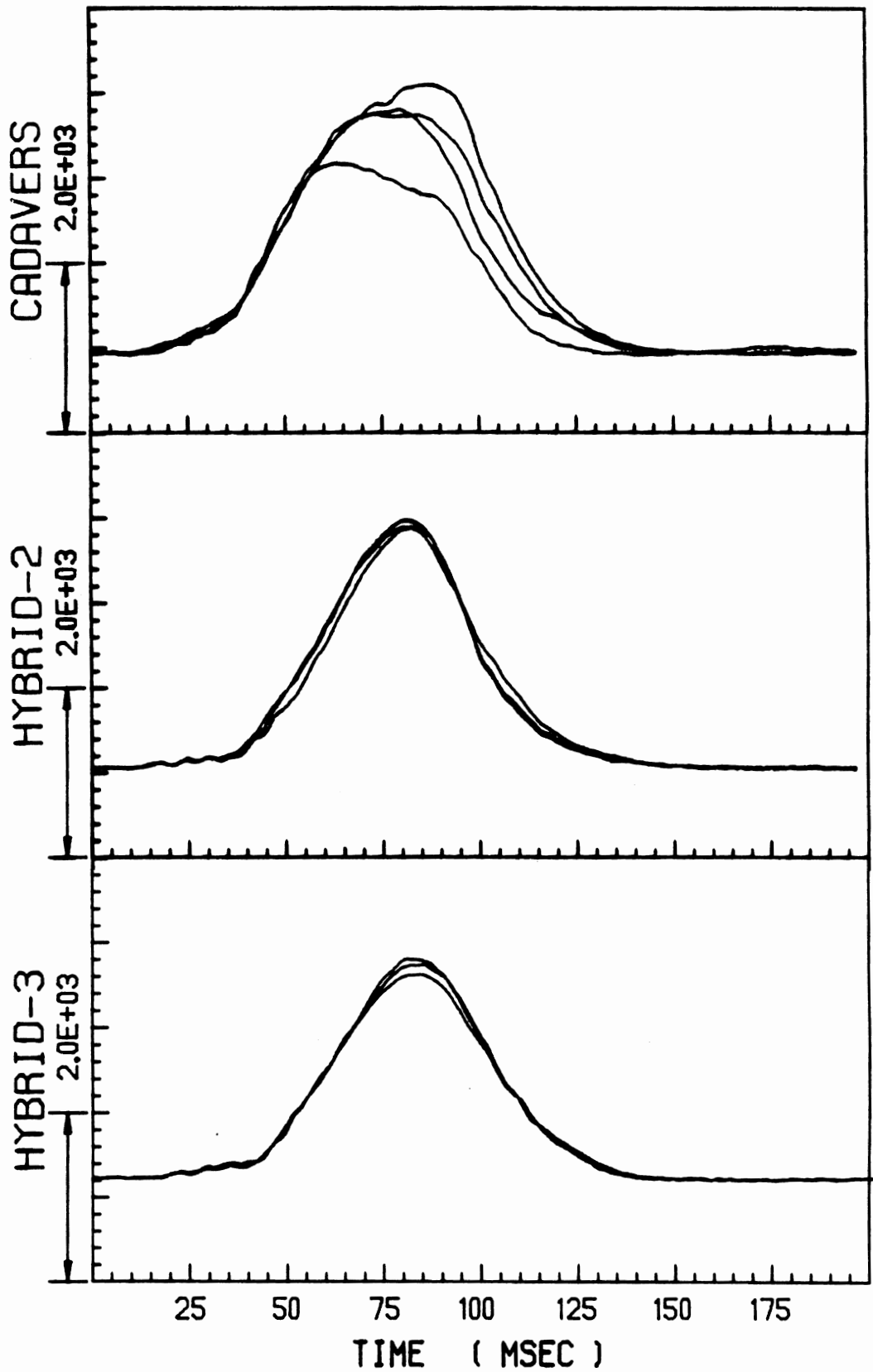


FIGURE 39. Right Lap Belt Load.
High-Severity Sled Runs -- A Composite Plot.

4. EXPERIMENTAL RESULTS

Chapter 5

C O M P U T E R S I M U L A T I O N S

The past several years have seen the development of sophisticated computer models for simulation of whole-body motions of an automobile occupant within a crash environment. In computer simulations, the mathematical model of the occupant may be viewed as a surrogate for the living human.

Use of whole-body motion models has both advantages and disadvantages in comparison with test programs using cadavers, anthropomorphic dummies, and sub-human primates. Primary advantages are facility and flexibility. A primary disadvantage is that good biomechanical data must be obtained if the simulation predictions are to be representative of human response.

Computer models have been developed for predicting dynamic responses in two and three dimensions. Two-dimensional models are useful, of course, only for simulation of events in which the primary motions are approximately planar. In this research program, kinematic responses to $-G_x$ decelerations of cadavers restrained by a three-point belt system have been found to be definitely three-dimensional. However, the magnitudes of responses in the X-Z plane are generally on the order of double the out-of-plane components, and the peaks for out-of-plane components generally occur later than peaks of in-plane components. It was therefore considered

reasonable to use the MVMA Two-Dimensional Crash Victim Simulator [12], probably the most advanced of currently available 2-D models, to simulate responses of cadavers in sled tests performed in this research program. In the context of this program, the computer model was thus used as an additional type of surrogate for cadavers.

5.1. Description of Simulations

The simulations conducted in this study may be described in terms of the surrogate, the restraint system, and the sled acceleration profiles. These test conditions are described below.

5.1.1. Cadaver Model. The data set developed for describing the cadaver for MVMA 2-D simulations does not represent any specific cadaver used in the sled tests. The simulated cadaver is 5 feet 8 inches and 140 pounds. This approximates the height and weight of several test cadavers.

Most of the anthropometric and biomechanical data used was taken from a study which investigated impact dynamics of free-fall victims [13,14]. Also used was a study which investigated the head-neck response of well-restrained human volunteers to -Gx sled decelerations [15,16]. In both of these studies, the MVMA 2-D model was used extensively. Sagittal-plane bending stiffness data for flexion and extension was derived from results reported by Mertz and Patrick [17] for adult male cadavers. Active muscle tension resistance to head-neck angulations was set to zero for the present study, as is appropriate for simulation of cadaver responses.

5. COMPUTER SIMULATIONS

5.1.2. Restraint System Model. The belt restraint system model in the MVMA 2-D Crash Victim Simulator is not capable of accurately representing the test restraint system in all respects. However, a reasonable approximation can be modeled. The primary problem is that the shoulder harness cannot be attached to the lap belt at a buckle. Since actual forward motion of the buckle is not large in comparison with the length of shoulder harness webbing between the buckle and the chest/shoulder area, the peak horizontal component of shoulder-harness force at the buckle can be expected to be small in comparison with that of the lap belt. For this reason, no large inaccuracies are introduced in the simulations by assuming the lower end of the shoulder harness to be fixed to an "anchor" on the sled at the initial position of the buckle.

The modeled belt restraint system included compensations for the dimensions of inextensible sections of the actual system, such as the buckle and anchor hardware. Also, out-of-plane webbing lengths were considered in the development of force-strain webbing characteristics supplied as input data to the computer model. The base stiffness was that of the webbing of the actual belt system. The loading curve was determined from a laboratory test to be nearly linear for loads less than about 800 lb and strains less than about 0.086; the constant stiffness determined was 9200 lbs/(in/in).

5.1.3. Initial Configuration. In the simulations, the cadaver was seated with approximate initial equilibrium between gravity and contact forces. The body link orientation was estimated to approxi-

mate the configuration of Cadaver WBR-4 in test A-869. In accordance with the setup conditions for all the sled tests, the initial upper leg angle was 5 degrees above the horizontal, the lower leg angle was 30 degrees above the horizontal, and the feet were fastened to a 45-degree toeboard. Examination of the film of test A-869 shows that the base of the neck (C7-T1) was initially about 16 degrees back from the vertical through the H-point. This condition was used as a constraint in estimating the initial torso link angles. The arms were positioned approximately as shown in the film. It was not possible to accurately define head and neck angles from the film. Initial values used were 3.6 degrees back from the vertical for the head and 20 degrees forward from the vertical for the neck. These are the values that were used in a previously mentioned study [15] for the living subjects and should be representative of setup conditions in the present study.

The seat modeled for the simulations was a good representation of the seat in the sled buck. The seatback was 25 degrees back from the vertical and was modeled with a hard foam surface. A composite of hard foam and soft foam was modeled for the head rest, and a hard seatboard was simulated.

5.1.4. Sled Accelerations. Computer simulations were made for three different severities of sled acceleration profiles. The low-severity profile was taken from test A-926; the medium- and high-severity profiles were from tests A-869 and A-866, respectively. The velocity changes and average accelerations for the profile

plateaus are summarized in Table 6.

TABLE 6. Velocity Changes and Average (Plateau) Accelerations of the Three Simulated Sled Profiles.

<u>TEST</u>	<u>SEVERITY</u>	<u>VELOCITY</u>	<u>ACCELER.</u>
A-926	low	16.7 mph	9.3 G's
A-869	medium	24.4 mph	9.8 G's
A-866	high	31.9 mph	19.8 G's

TABLE 7. Weights and Heights of Simulation "Cadaver" and the Cadavers of Three Simulated Tests.

<u>TEST</u>	<u>CADAVER</u>	<u>WEIGHT</u>	<u>HEIGHT</u>
Simulation "Cadaver"		140 lb	68 in.
A-926	WBR-7	171 lb	70 in.
A-869	WBR-4	135 lb	65 in.
A-866	WBR-3	126 lb	68 in.

5.2. Results of Simulations

The results reported here are for three simulations which differ only in the acceleration profiles of the sled. With respect to initial configuration, belt restraint system, and cadaver parameters, the data sets were identical. Each simulation predicts dynamic response of the 140-lb, 68-in cadaver previously described.

Because the model is capable of predicting only planar motions and because the cadavers used in the three actual sled tests are different in size from the simulation "cadaver," simulated responses are expected to correlate with test responses in varying degrees. Cadaver anthropometry is summarized in Table 7. Since the height and weight of cadavers WBR-3 and WBR-4 are in best agreement with the simulation cadaver values, experimental responses for tests A-866 and A-869 are expected to be in best agreement with simulation results. These are the high- and medium-severity acceleration profile tests.

5.2.1. Printer-Plot Sequence. Figures 40 through 42 illustrate simulated occupant motion. These are selected "frames" from a time sequence of printer-plots generated by the MVMA 2-D model for test A-869. With the exception of arm motion, the kinematics illustrated are found to be very similar to motions observed on the test film. Simulated arm motions are somewhat greater than in the tests, in which the arms do not go far above the horizontal as they swing forward. The reason for this difference is made obvious by viewing the film. The simulated shoulder articulations are strictly in the plane of simulation, while in the tests there is a significant component of upper arm abduction.

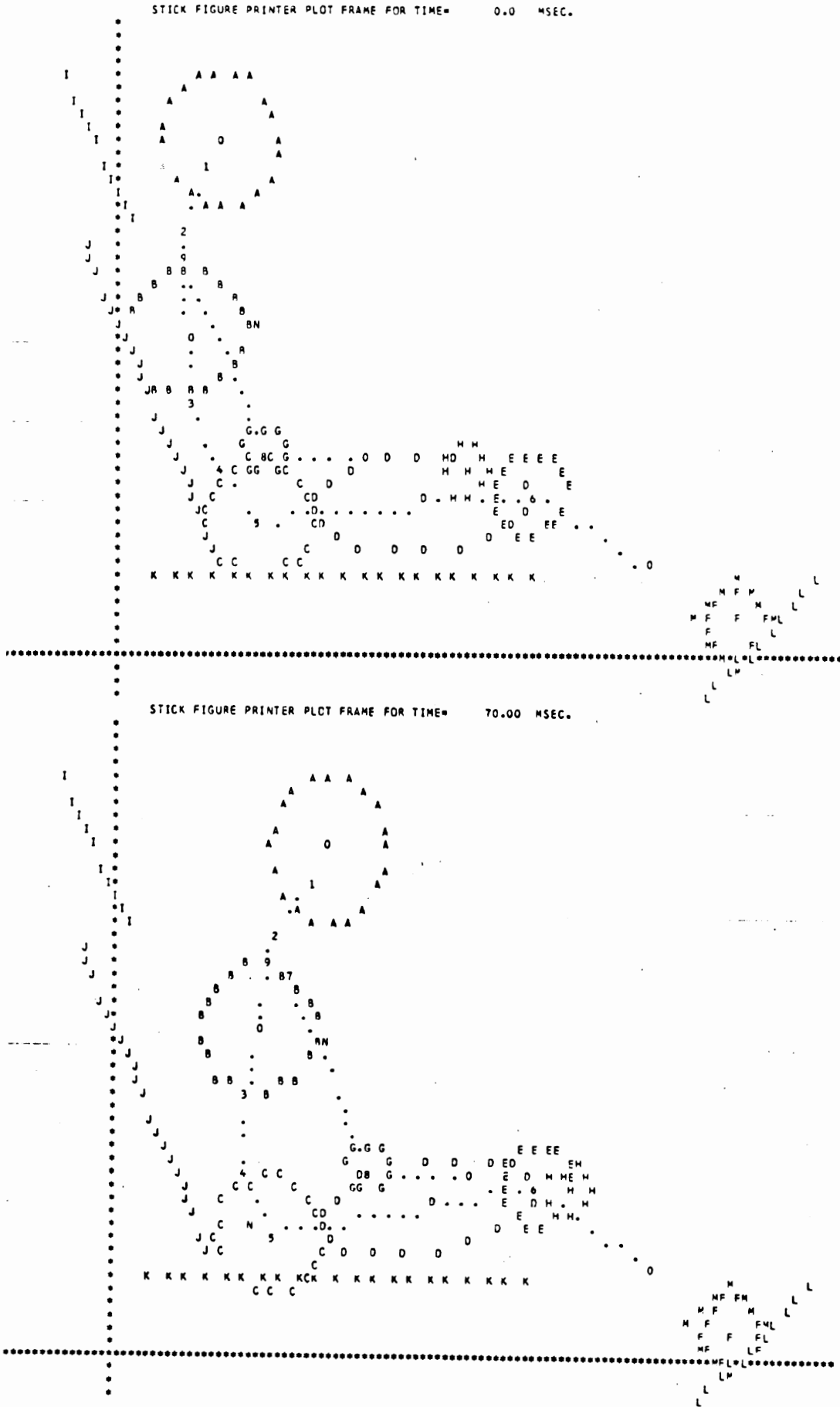


FIGURE 40. Printer-Plot Time Sequence from Simulation of Test A-869 (t=0 and t=70 ms).

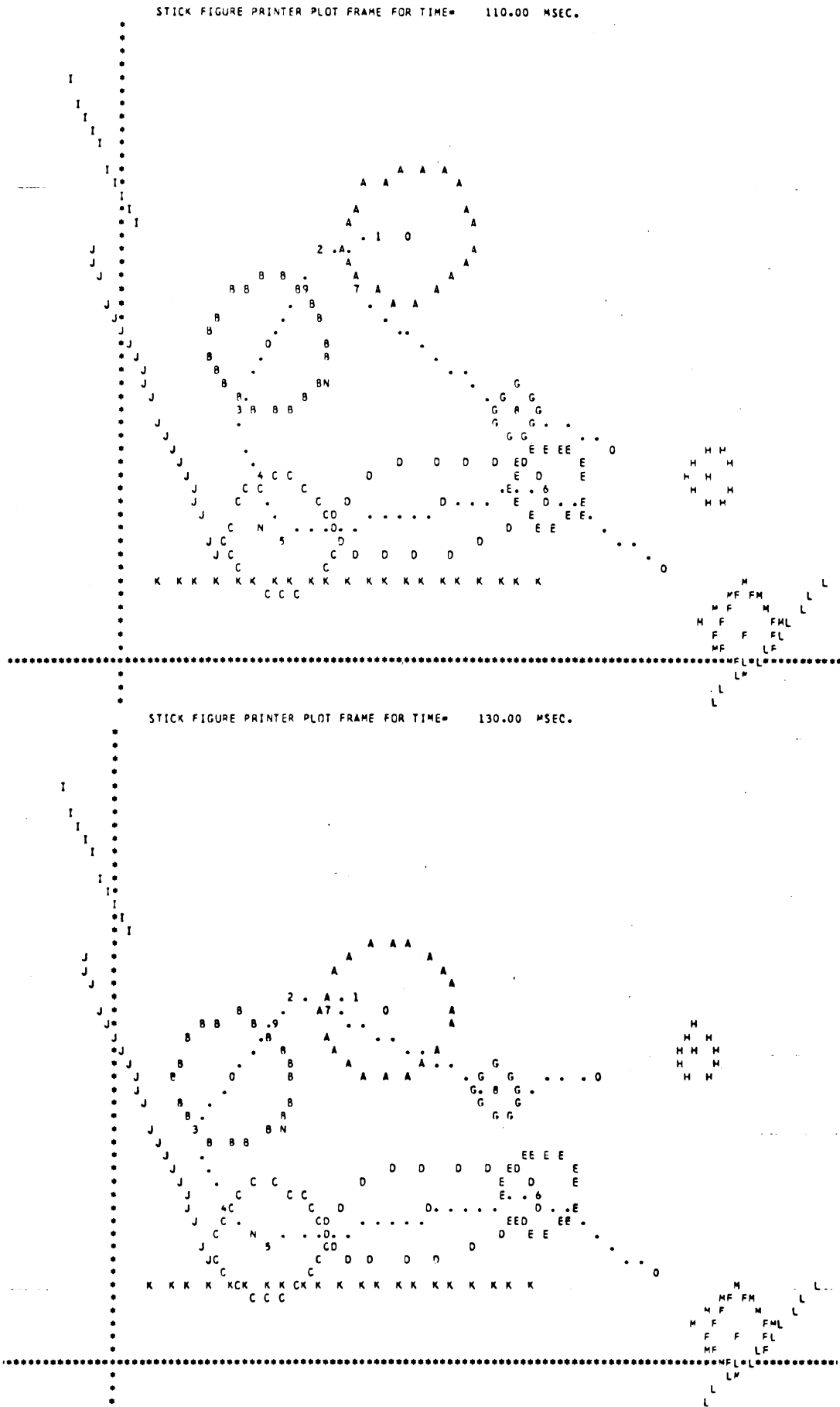


FIGURE 41. Printer-Plot Time Sequence from Simulation of Test A-869 (t=110 and t=130 ms).

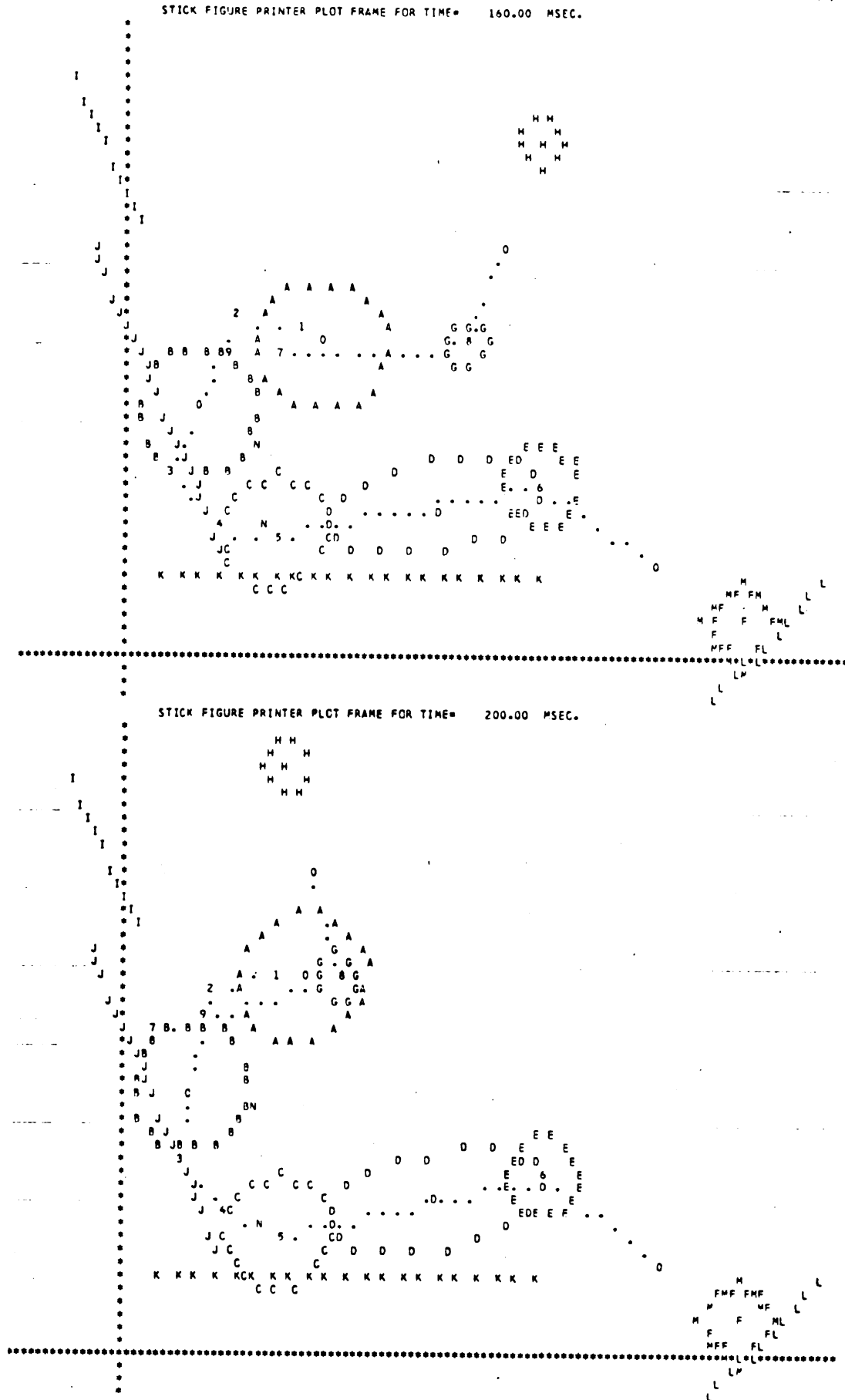


FIGURE 42. Printer-Plot Time Sequence from Simulation of Test A-869 (t=160 and t=200 ms).

5.2.2. Low-Severity Results. Figures 43 through 45 show graphical results for simulation and test dynamics for the low-severity test (test A-926, 171-lb, 70-in cadaver WBR-7).

Head responses were selected as the primary descriptors of subject response in the sled test program and also as the primary indicators of correlation between computer simulation and actual test dynamics. The graphs in this section and in the next two show head pitch velocity, head pitch acceleration, the A-P and S-I components of head center-of-mass acceleration, and the belt loads. The head angular motions plotted for the tests are for the angular velocity vector component along the lateral head axis. Best agreement with simulated in-plane pitching can be expected before out-of-plane motions in the tests become significant.

5.2.3. Medium-Severity Results. The parameter values for the simulation cadaver better approximate the test cadaver for test A-869 than the cadaver used in either of the other tests simulated. The simulation cadaver weight and height are 140 lb and 68 inches; cadaver WBR-4 of test A-869 is 135 lb and 65 inches. Graphical results for this test are shown in Figures 46 through 48.

5.2.4. High-Severity Results. The weight and height of cadaver WBR-3, which was used in test A-866, are 126 lb and 68 inches. Simulation and test dynamics for A-866 are shown in Figures 49 through 51.

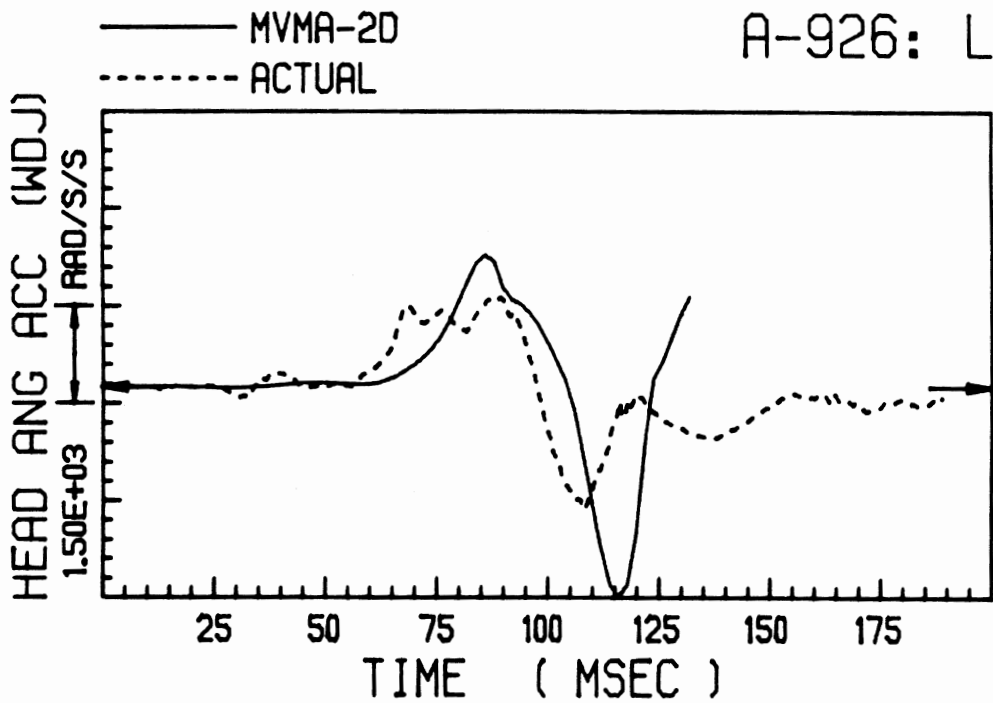
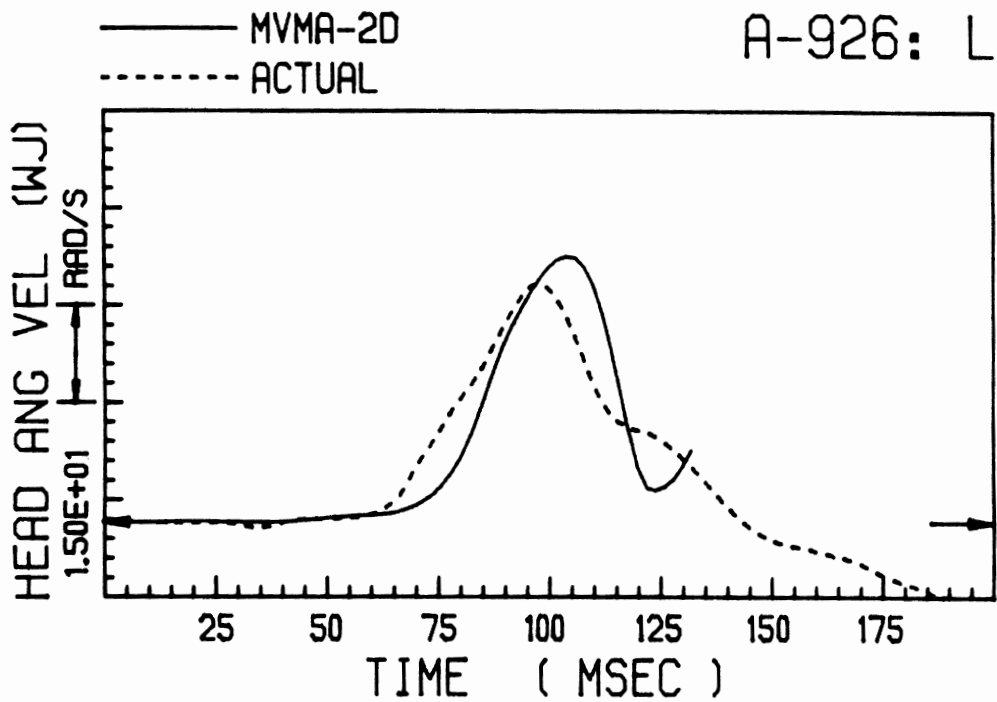


FIGURE 43. Head Pitch Velocities and Accelerations for Low-Severity Test, A-926.

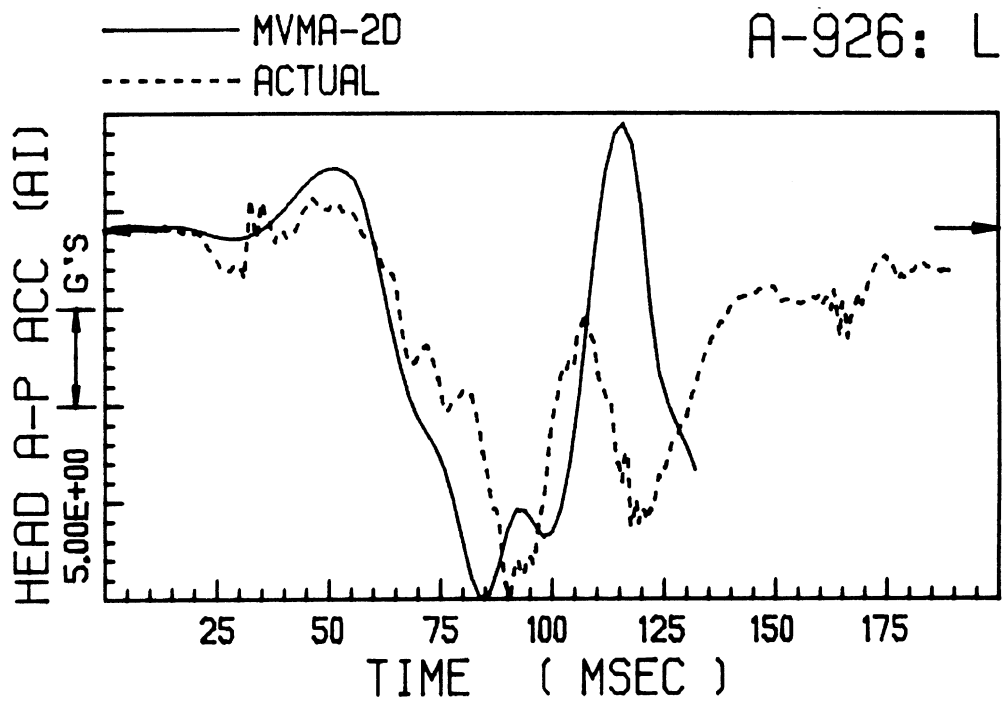
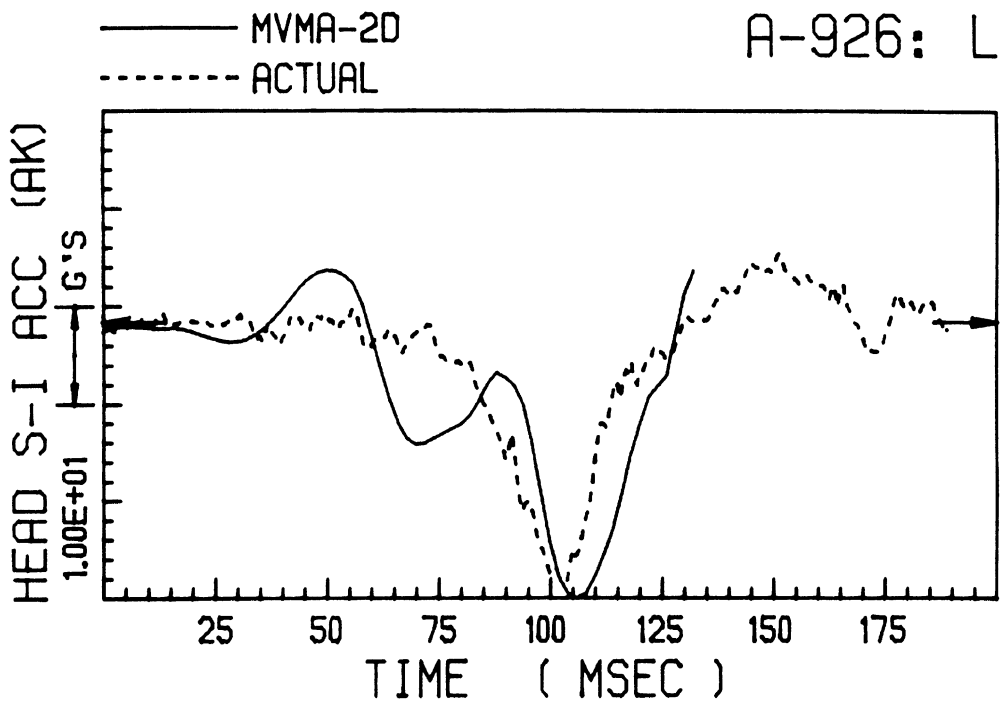


FIGURE 44. Anatomical Components of Head Center-of-Mass Acceleration for Low-Severity Test, A-926.

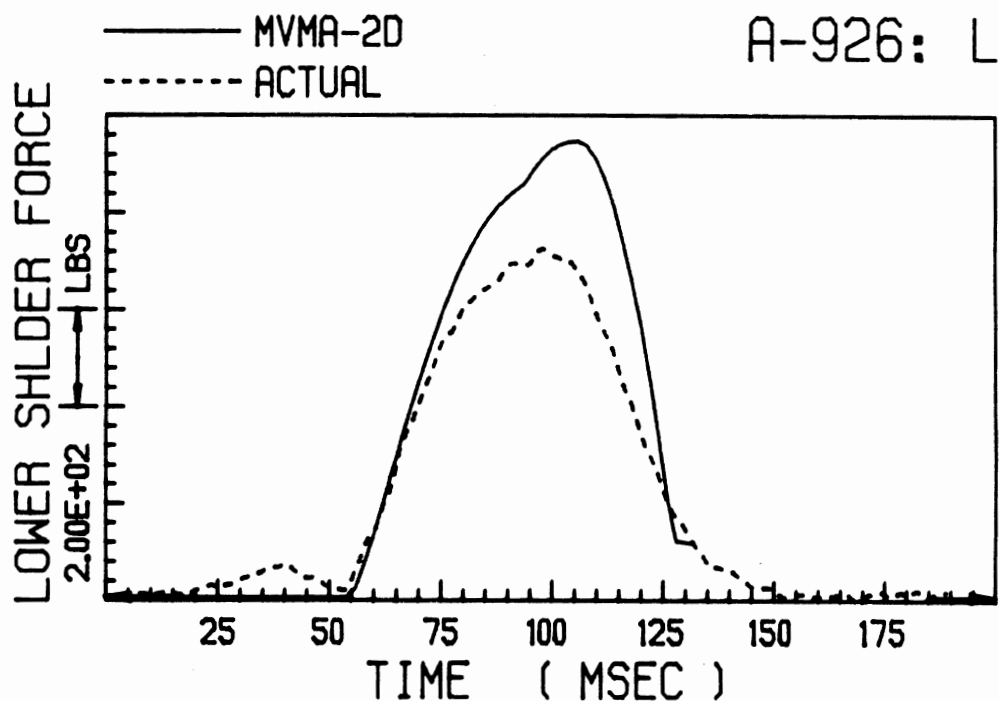
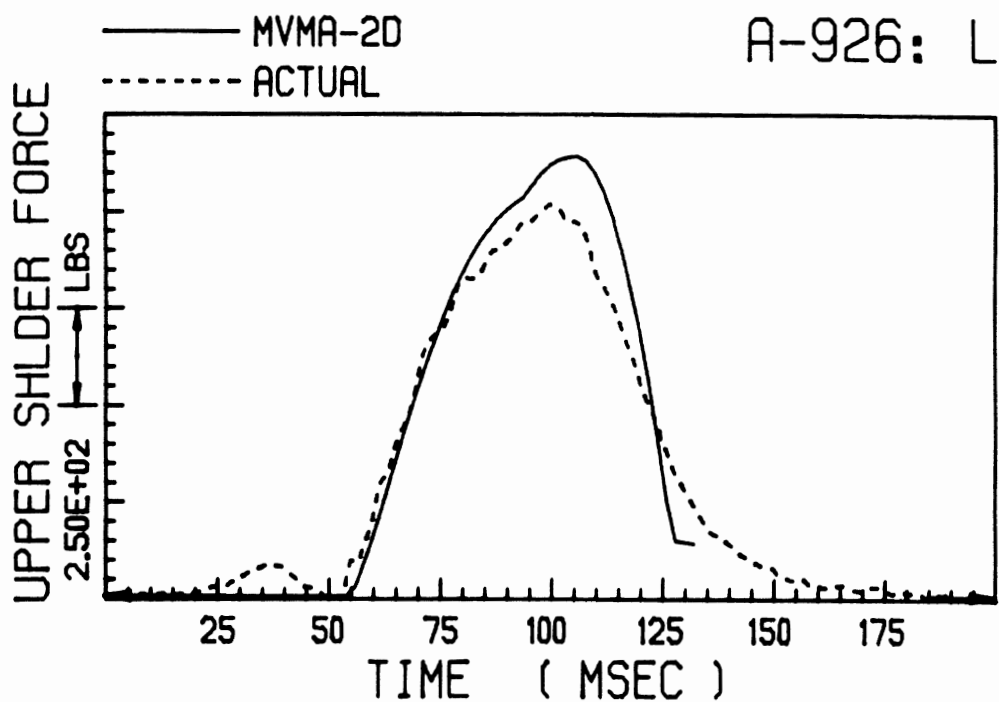


FIGURE 45. Simulation and Actual Torso Belt Loads for Low-Severity Test, A-926.

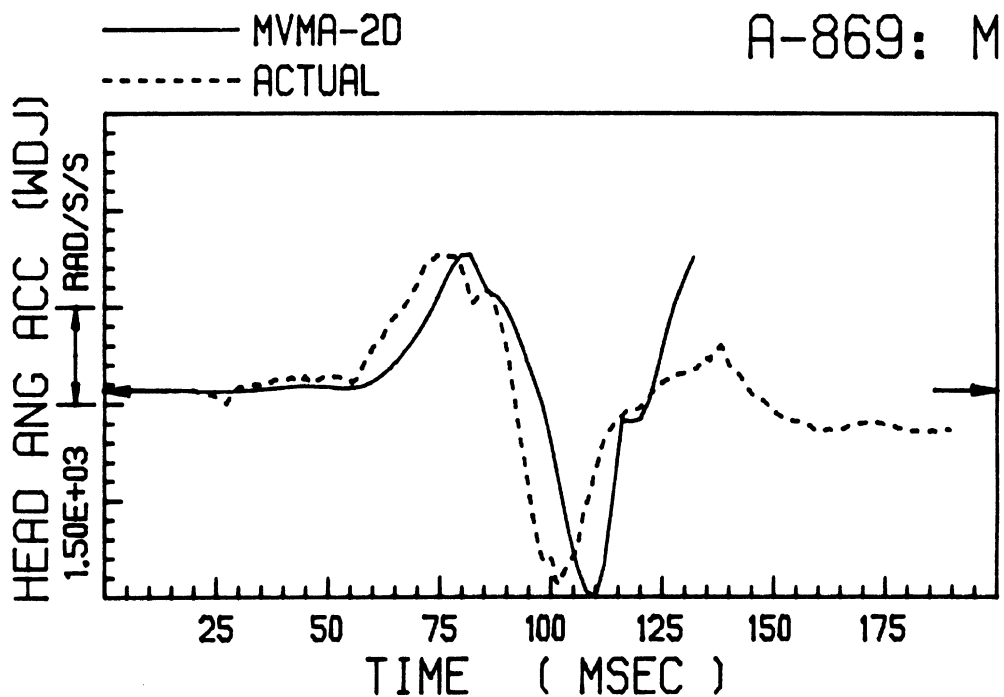
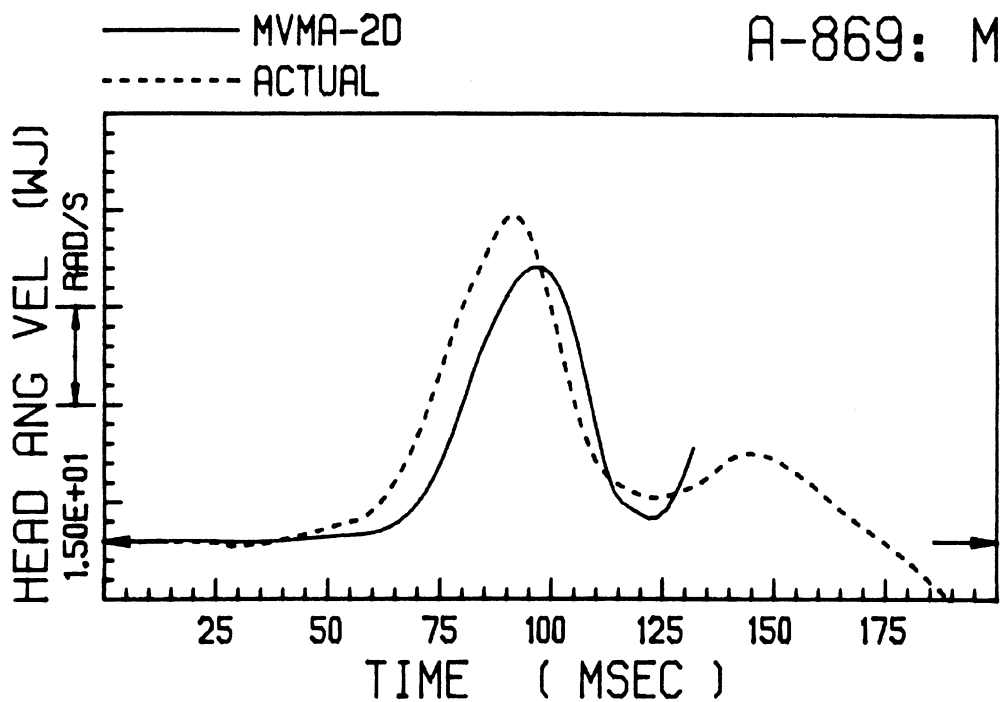


FIGURE 46. Head Pitch Velocities and Accelerations for Mid-Severity Test, A-869.

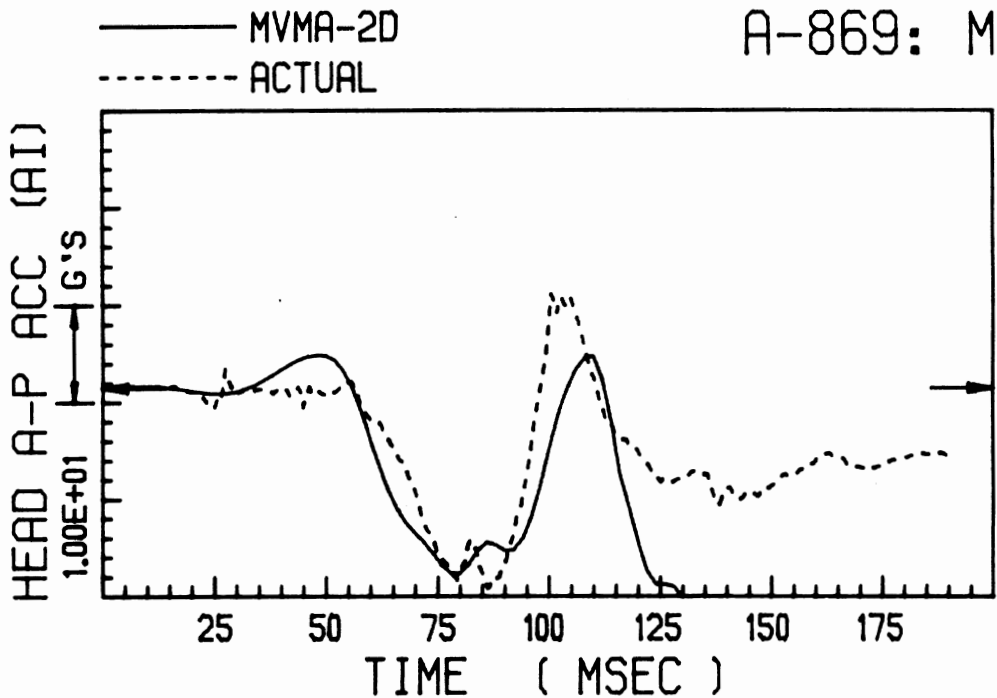
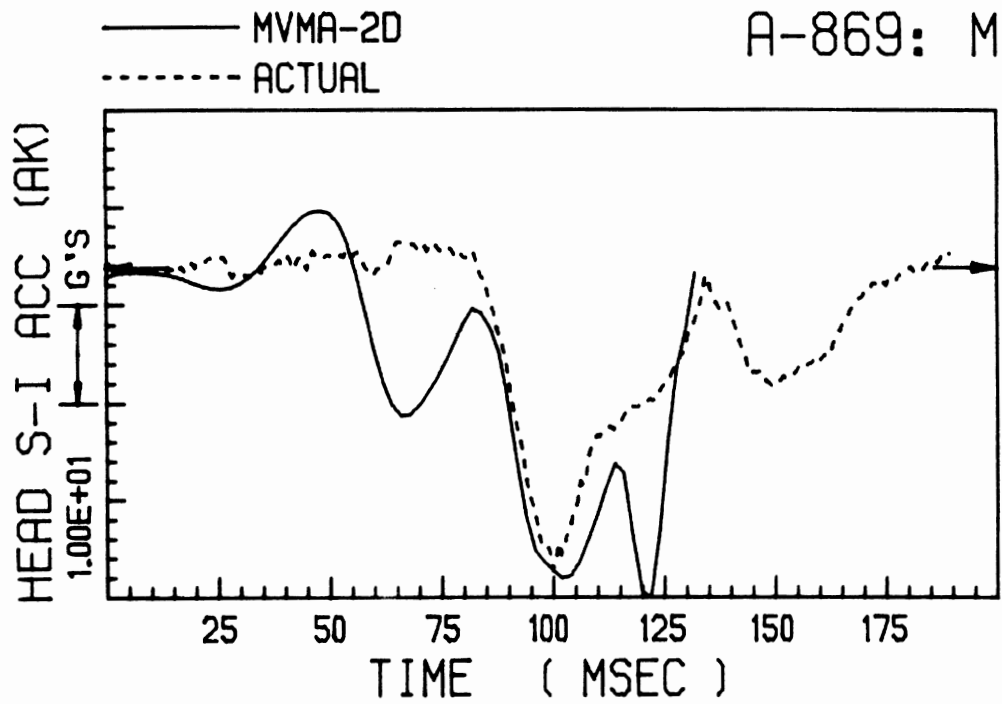


FIGURE 47. Anatomical Components of Head Center-of-Mass Acceleration for Mid-Severity Test, A-869.

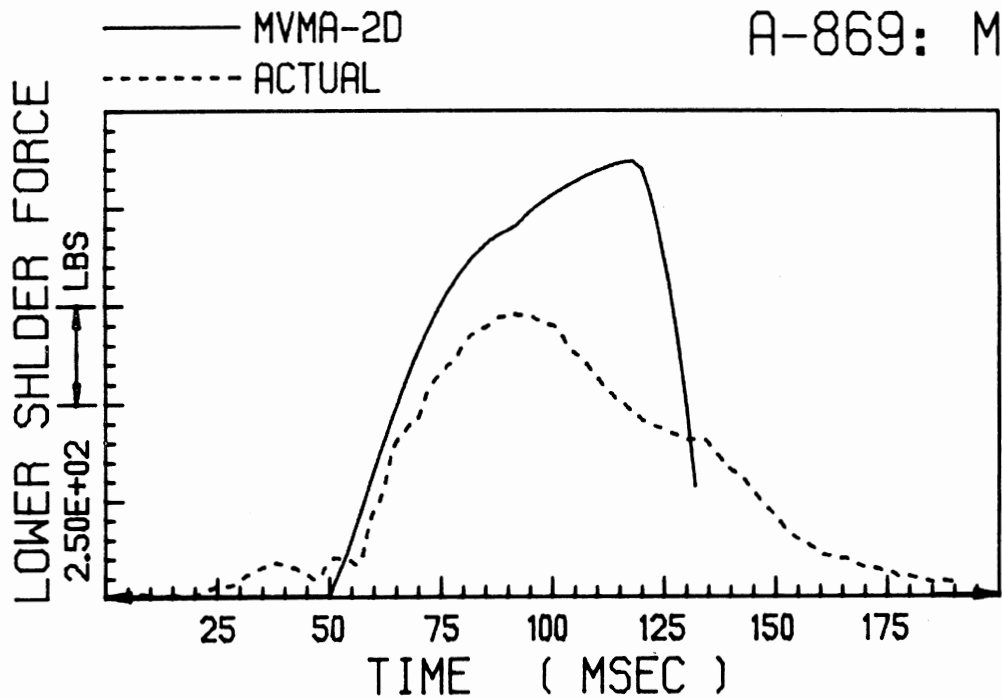
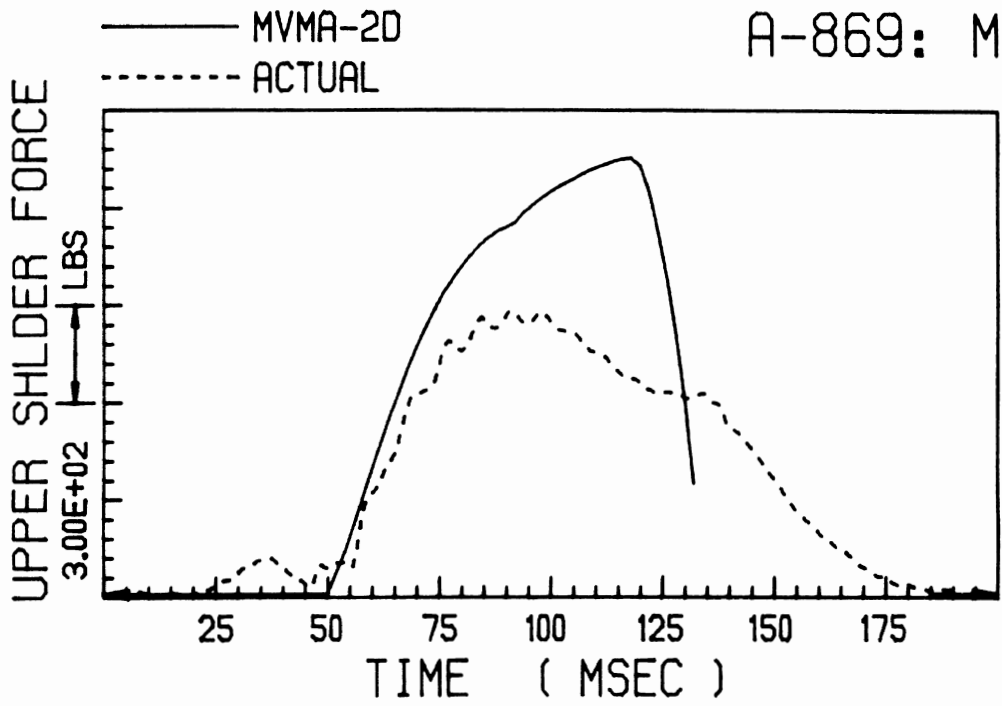


FIGURE 48. Simulation and Actual Torso Belt Loads for Mid-Severity Test, A-869.

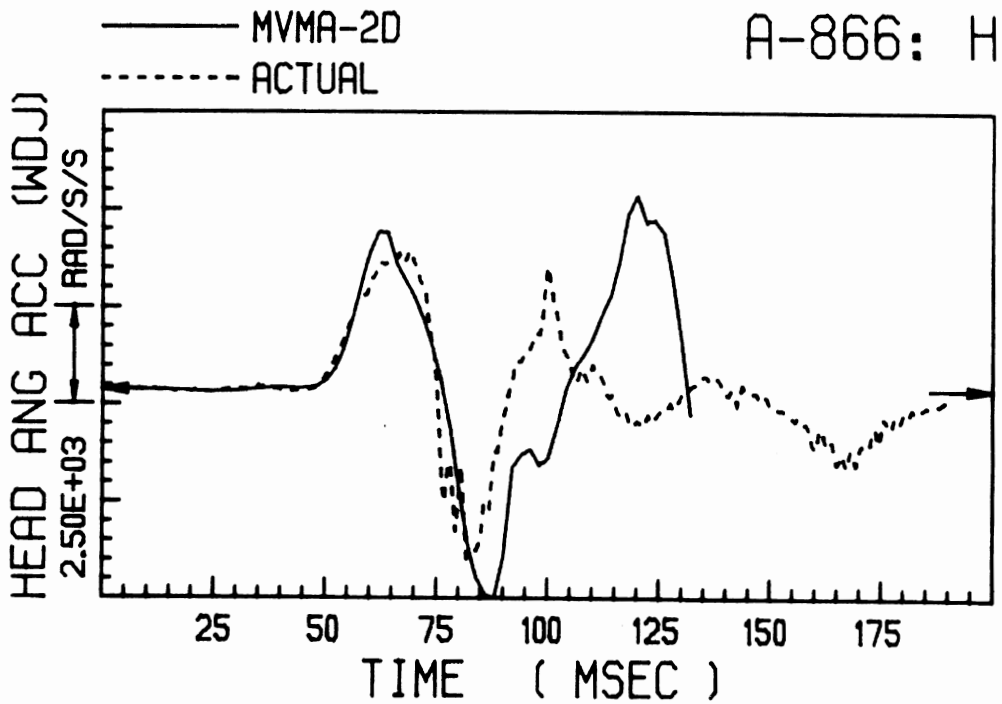
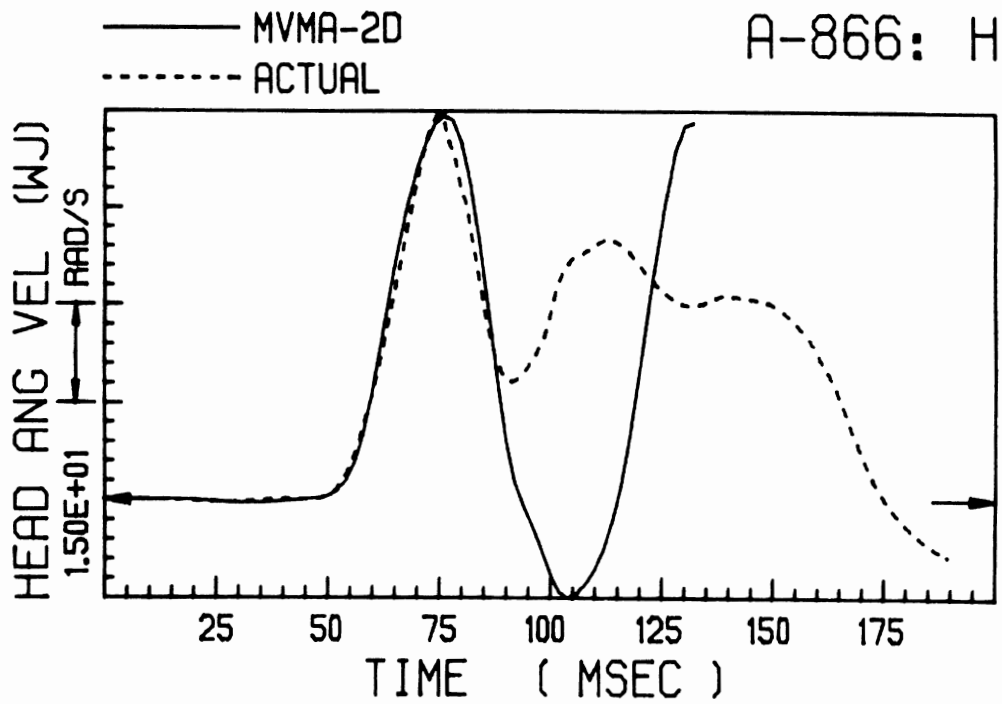


FIGURE 49. Head Pitch Velocities and Accelerations for High-Severity Test, A-866.

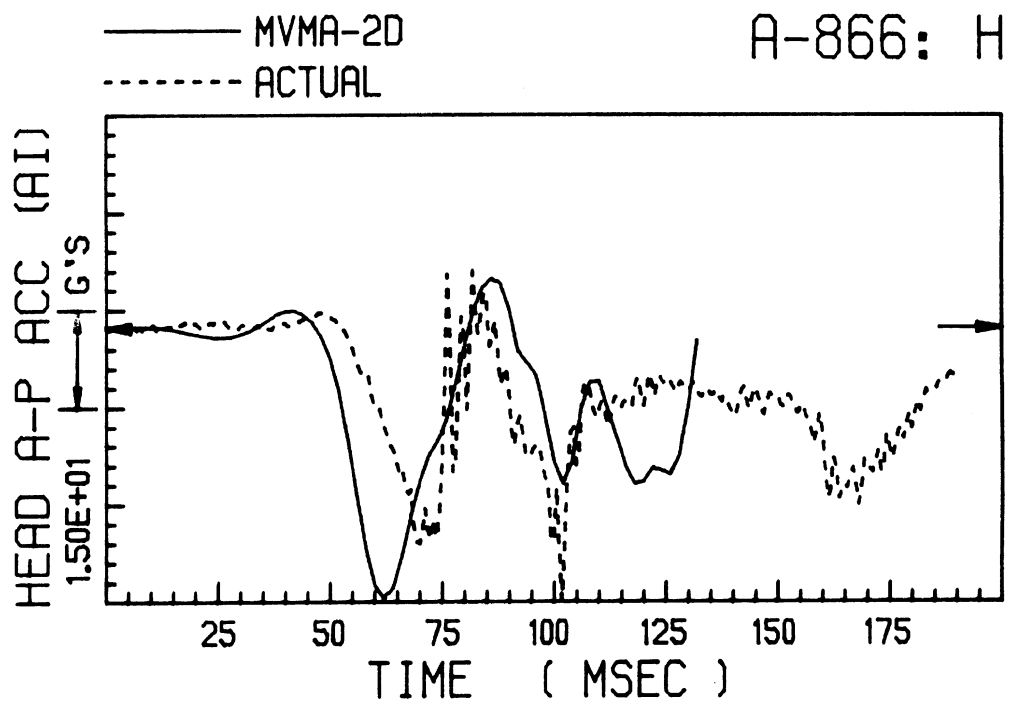
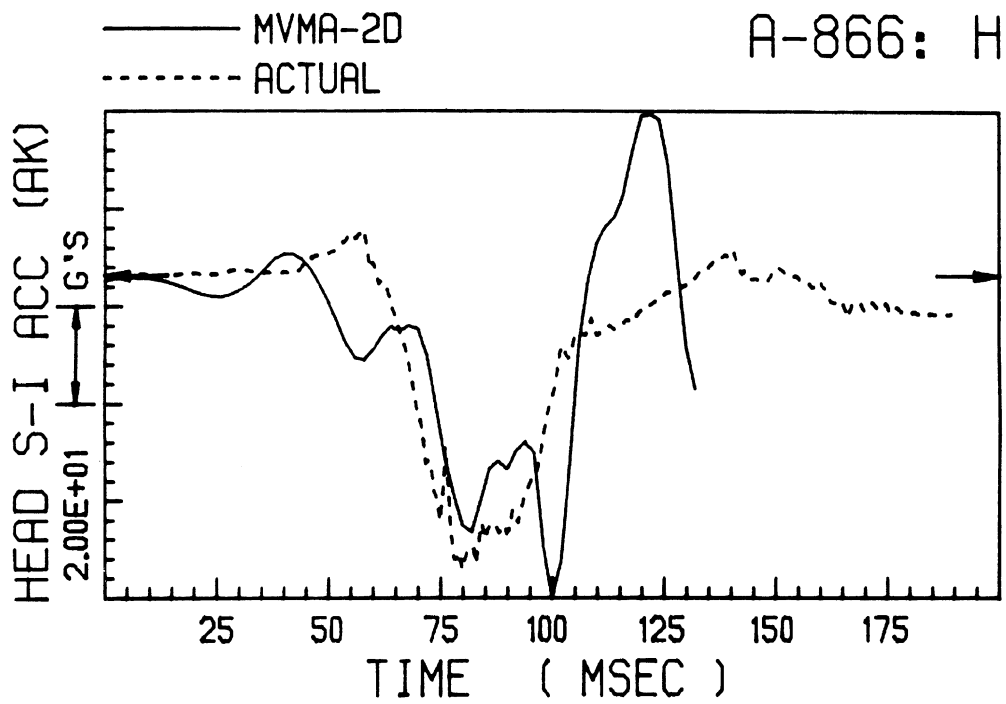


FIGURE 50. Anatomical Components of Head Center-of-Mass Acceleration for High-Severity Test, A-866.

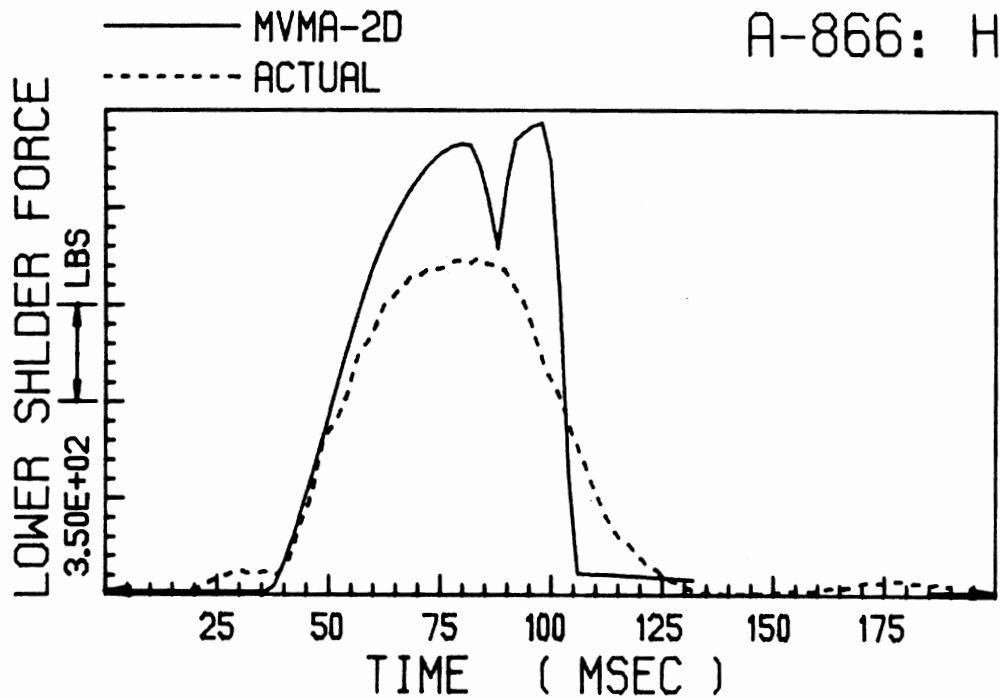
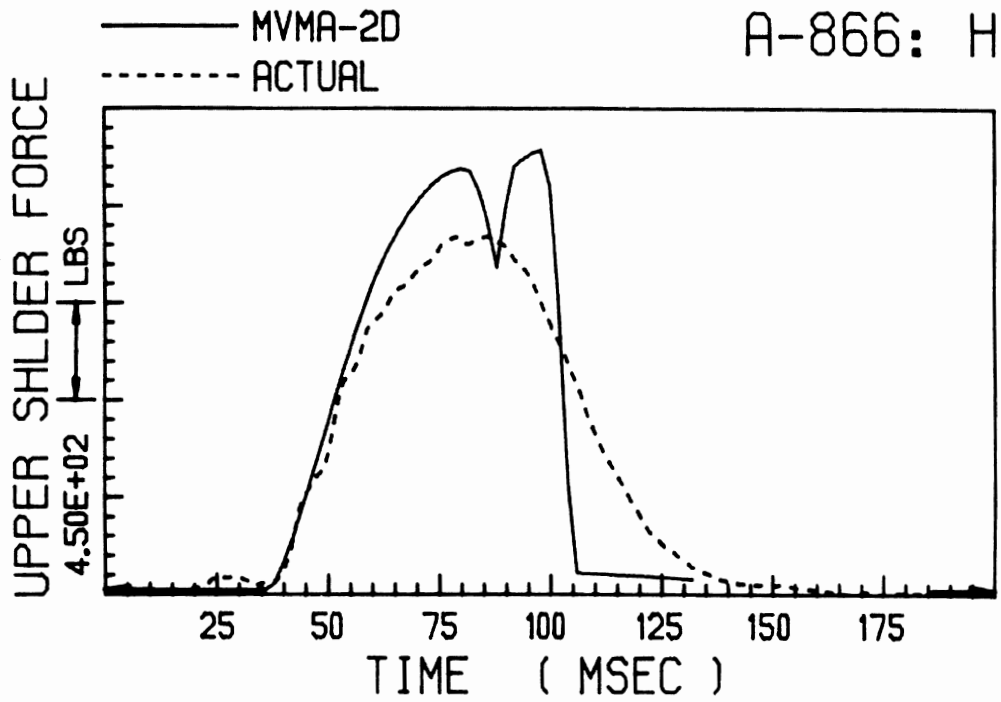


FIGURE 51. Simulation and Actual Torso Belt Loads for High-Severity Test, A-866.

5.3. Discussion of Simulations

Discussion of simulation results should be prefaced by emphasis of a primary feature of the simulations, namely, that a single "simulation cadaver" was used for all three simulations, while three different cadavers of various heights and weights were used in the corresponding sled tests (see Table 7). Consequently, simulation and test responses are not expected to be in exact agreement. The results demonstrate that it is possible to accurately predict all the basic characteristics of the dynamic responses with respect to peak magnitudes, phases and curve waveform and that these characteristics are seemingly much more sensitive to deceleration conditions than to moderate variations of subject anthropometry.

Magnitudes and phase for predicted pitch velocities, pitch accelerations, and anatomical components of linear head accelerations are seen to be in good agreement with test results through the second peak (positive or negative) in each response history. Predicted peak belt loads range from 13 to 54 percent higher than test results for the upper and lower segments of the shoulder harness. Predicted peak lap belt loads are generally low and differ from test peaks by an average of 16 percent. Predicted peaks for translational accelerations of the head, thorax and pelvis are in reasonably good agreement with test results, differing by an average of 13 percent. Peak acceleration responses and belt loads are summarized in Table 8.

Modifying the action of the lap belt would not significantly alter head-neck response since the pelvis is well-restrained in both

TABLE 8. Peak Values for Accelerations Responses and Belt Loads.

	<u>LOW-SEVERITY</u> <u>(A-926)</u>		<u>MID-SEVERITY</u> <u>(A-869)</u>		<u>HI-SEVERITY</u> <u>(A-866)</u>	
	<u>TEST</u>	<u>SIMUL</u>	<u>TEST</u>	<u>SIMUL</u>	<u>TEST</u>	<u>SIMUL</u>
Left Lap Belt Load (lb)	756	546	569	619	1148	1042
Right Lap Belt Load (lb)	1509	1095	1375	1205	2232	2048
Upper Shoulder Belt Load (lb) ...	1007	1134	871	1343	1636	2037
Head Transl. Accel. (G's)	28	30	34	39	63	70
Internal Thorax Accel. (G's)	(26)' (20)"	24	(25)' (22)"	25	(59)' (34)"	52
Internal Pelvis Accel. (G's)	(23)' (16)"	16	(25)' (24)"	18	(41)' (48)"	35

 ()' and ()" are Hybrid-II and Hybrid-III responses, respectively.
 (No internal instrumentation in cadavers.)

test and simulation and the neck is remote from the pelvis. Somewhat more effect might be expected from modifying shoulder harness action, but no effort was made to improve the modeling of any portion of the restraint system. Shoulder harness loads may be high because belt loading was represented as strictly linear while, in fact, the webbing softens for strains greater than 0.086 and loads greater than 800 lbs.

Although there is considerable similarity between simulation and test results for head responses through the second peak of each response history, there is considerable disagreement, of an oscillatory nature, after the second peak. (Simulation results are not shown beyond 130 ms.) This is explained partly by the fact that out-of-plane motions in the tests begin to become significant, but the differences are caused mostly by a model shortcoming. In this domain of the responses, the oscillations correlate exactly with peak "joint-stop" torques at the upper- and lower-neck articulations of the two-joint, MVMA 2-D neck. Joint-stop activity is more severe than reasonable because: 1) nonlinear joint stiffness are unreasonably large except for small and moderate angulations, and 2) too little viscous damping is modeled. Without modifications to the analytical model and the computer code for the MVMA 2-D Crash Victim Simulator, it is not possible to both more accurately represent the neck with regard to nonlinear static loading characteristics and velocity-dependant energy loss and also guarantee proper hysteretic energy loss upon unloading.

In short, the opportunity offered by this study to compare model predictions with cadaver response has pointed out the need for an improved, more general joint model. In particular, it is clear that minimum improvements would include: 1) the addition of a linear term to the quadratic and cubic joint-stop torques of the current model (April 1978), and 2) a modification to make viscous damping coefficients dependent on angulation (at least, zero and non-zero in different parts of the range). Ideally, provision should be made

for tabular specification of joint torque loading curves.

With the model improvements just outlined and appropriate specification of associated biomechanical data, the improper oscillations seen after the first two peaks in head responses should be absent because of softer loading and dissipation of kinetic energy. While it is desirable to eliminate the aforementioned inaccuracies in predicted responses, it should be noted that the usefulness of results obtained and illustrated in Figures 46 through 54 is uncompromised. Since maximum values for the response parameters always occur as one of the first two peaks in test results, the domain after the first two peaks of the predicted responses may simply be neglected as long as the peak values of responses are of primary interest. Agreement between predicted and test responses is excellent through the first two peaks, particularly for the cadavers of tests A-866 and A-869, which are both near to the simulation cadaver in height and weight. Table 9 summarizes the phase and peak responses for the three tests and simulations.

TABLE 9. Magnitudes and Phases of Head Responses.
(Primed peak numbers indicate "plateau" peaks.)

HEAD RESPONSE	PEAK NO.	LOW-SEVERITY (A-926)		MID-SEVERITY (A-869)		HI-SEVERITY (A-866)	
		TEST	SIMUL	TEST	SIMUL	TEST	SIMUL
Pitch Vel. (rad/s @ ms)	1	36.7 @ 98	40.9 @ 104	50.2 @ 92	42.3 @ 97	59.4 @ 75	59.2 @ 76
	2		5.0 @ 124	6.8 @ 123	3.5 @ 122	18.1 @ 91	-15.1 @ 104
Pitch Acc. (r/s/s @ ms)	1	1247 @ 69	2031 @ 86	2115 @ 76	2105 @ 82	3545 @ 69	4034 @ 62
	1"	1342 @ 87					
A-P Acc. (G's @ ms)	2	-1895 @ 108	-3254 @ 116	-3008 @ 102	-3203 @ 110	-4468 @ 82	-5366 @ 88
	1	19.0 @ 91	19.1 @ 84	19.1 @ 79	19.1 @ 80	33.3 @ 70	41.7 @ 62
S-I Acc. (G's @ ms)	1"			20.6 @ 86		32.3 @ 74	
	2	4.3 @ 108	-5.4 @ 116	-9.6 @ 101	-3.3 @ 110	-8.7 @ 82	-7.4 @ 86
S-I Acc. (G's @ ms)	2"			-9.3 @ 104			
	1	26.5 @ 103	28.4 @ 106	31.1 @ 100	31.9 @ 102	60.6 @ 80	52.8 @ 82
S-I Acc. (G's @ ms)	1"				33.8 @ 122		66.2 @ 100
	2	-0.1 @ 132	-5.2 @ 132	0.9 @ 134	-6.2 @ 136		-33.1 @ 122
S-I Acc. (G's @ ms)	2"	-7.0 @ 151					

Chapter 6

DISCUSSION OF RESULTS

This program has generated a great deal of detailed data and analyses of such data depend to a great extent upon the specific interests or viewpoints of the reader. This chapter of the report will present discussions of some areas of the test results which are felt to be of general interest to researchers in biomechanics. More specific analyses are left to the reader through the use of the detailed data appendices of this report.

The following sections discuss specific features of the experimental program and comparisons of the responses obtained with the three human surrogates tested in this program, namely, cadavers, Part 572 (Hybrid II) ATD and Hybrid III ATD.

6.1. Factors Influencing the Experimental Results

In this section, the effects of repeated tests upon cadaver responses and the effects of embalming are discussed.

6.1.1. Effects of Repeated Tests. Many of the cadavers were tested more than once in the earlier stages of the program. This procedure was later abandoned and subsequently only single tests were conducted on each cadaver. The reason for this was primarily a concern over the effects of structural damage of the thorax on the

response measures. A secondary concern relates to the possible general loosening or modification of structural linkages and resistance to motion that might occur in the skeletal system during the first test. Examination of the test results of those cadavers that were tested only once and comparison of the results with those obtained by repeated tests, with all tests at the same severity level, allows the assessment of such effects. The mid-severity tests provide the bulk of such data.

TABLE 10. Comparison of Mid-Severity Chest Acceleration Peak Data.

TEST SERIES NUMBER	SLED TEST NUMBER		PEAK RESULTANT CHEST ACCEL., g		NUMBER OF FRACTURES		
	1st Run	2nd Run	1st Run	2nd Run	Right	Left	Strnm.
WBR-4	A-869	A-870	36	39	3	5	1
WBR-5	A-874	A-875	32	33	4	2	1
WBR-8	A-934	A-935	24	28	7	4	1
WBR-9	A-938	---	30	--	2	3	0
WBR-11	76B002	---	24	--	5	2	0
WBR-12	76B003	---	30	--	2	0	3
WBR-14	76B005	---	24	--	5	3	1

The results of the single run tests (WBR-9, 11, 12 and 14) indicate that significant numbers of rib fractures occur during the first mid-severity run. Thus, it can be assumed that in all mid-

severity tests the first run produced some degree of structural disruption in the thorax. These results are summarized in Table 10, along with the peak resultant chest acceleration values for the pertinent mid-severity tests.

Comparison of the first and second run peak resultant chest acceleration values shows that the second run values are slightly higher. Similarly, an examination of the acceleration time-histories (Appendix C) reveals that the waveforms are generally the same for repeated runs with the second run peak having a slightly longer duration than the first run peak. In general, the repeated tests did not appreciably change the thoracic response, as measured by the thoracic spine accelerometers, which may be indicative of the relative insensitivity of the thoracic spine acceleration to deformation of the rib cage from frontal loading due to shoulder harnesses.

The cervical spine (neck) is another region of the skeletal structure of the body that could be effected by repeated tests. The cervical spine linkage and its resistance to motion exert a strong influence on the dynamic response of the head in the type of impact tests conducted in this program. Review of the rotational and translational head acceleration time-histories for the repeated runs of cadavers WBR-4, 5 and 7 shows that the repetition of runs on the same cadaver produce very similar head acceleration profiles both in magnitude and in waveform.

Thus, it appears that the repeated run technique used early in the program did not invalidate the data produced on head and chest acceleration response during the second test.

6.1.2. Effects of Embalming. Two embalmed cadavers were tested in the WBR program. The main purpose for using embalmed cadavers was to determine if the embalming process, which stiffens soft tissue structures, could minimize the rib fractures that were found to be occurring with the unembalmed cadaver tests. The embalmed cadavers were prepared for testing by limbering the knee, hip, elbow and shoulder joints until they were flexible and easily moved.

The embalmed cadaver test series consisted of two mid-severity followed by a single high-severity runs on one of the two cadavers, and of a high-severity run conducted on the second cadaver, for a total of four embalmed cadaver tests. In this series of tests, significant numbers of rib fractures were still produced. From these tests, it was not apparent that stiffening of the soft tissues of the thoracic organs and intercostal tissues had a marked effect on the number or distribution of rib fractures. The age and medical history of the cadaver are more likely to be the major factors that influence rib fractures.

The response measures did not appear to be significantly effected by embalming. The chest acceleration time-histories were comparable in magnitudes and waveforms to similar tests with unembalmed cadavers. With the head response, there did appear to be a tendency for the embalmed cadaver to produce less-sharp peaks in head acceleration but the magnitude was not conclusively modified (compare WBR-3, 10 and 15). This effect could be attributed to greater resistance to motion on the cervical spine of the embalmed cadaver.

6. DISCUSSION OF RESULTS

6.2. Comparison of Human Surrogate Test Results

Three human surrogates were used in the experimental phase of the WBR program: cadavers, Part 572 ATD or Hybrid II and Hybrid III ATD. In this section, results from testing these surrogates are compared.

6.2.1. Head-Neck Response. The dynamic response of the head, as indicated by head acceleration measurements, is controlled primarily by the neck linkage and its resistance to motion. Comparisons of the head responses of the three surrogates is thus a comparison of the neck characteristics. In the case of cadavers, the neck linkage is an accurate representation of the living human neck but the resistance to motion (muscle tone) is lacking. The Hybrid II dummy neck is monolithic rubber structure that has been noted to be relatively stiff in comparison to the human neck, while the Hybrid III neck design represents an intermediate area between the two extremes. It has a segmented structure that is not as complex as that of the human neck with motion resisting elements that are not as stiff as the Hybrid II neck. These general characteristics are evident when comparing the head motion responses of the three surrogates. The most direct measure of neck response is the angular acceleration of the head. Figures 4, 5 and 6 show the comparisons of the resultant head angular accelerations for the three surrogates at the three test severities. Note that the first major peak, which is related to the motion resistance level of the neck, is lowest in magnitude for the Hybrid II data. This is

consistent with the stiff nature of the Hybrid II neck. The second major peak, which is related to the stopping of the head motion, occurs later with the Hybrid II in comparison with the cadavers and Hybrid III. The Hybrid III waveforms tend to be more like the cadaver responses than those of the Hybrid II. The cadavers exhibit much greater variability in their response than the dummies do and the Hybrid III produced the most consistent response of all. The similarity of the Hybrid III head angular acceleration response to that of the cadavers is shown also in the head angular velocity comparisons of Figures 7, 8 and 9. The head angular velocity traces for the Hybrid II tests exhibit a characteristic sustained rebound velocity that is not as pronounced with either the cadavers or the Hybrid III responses. This again is a manifestation of the neck construction of the Hybrid II.

The translational acceleration responses (Figures 10, 11 and 12) and translational velocity responses (Figures 13, 14 and 15) of the head exhibit less pronounced differences between the surrogates than the head rotational motion responses.

An additional aspect of the head motion which is not apparent from the summary plots of the resultant accelerations and velocities is the differences in the three-dimensional nature of the motion of the head for each of the surrogates. In order to investigate the nature of any such differences, it is necessary to look at the individual components of the translational and rotational motion since the resultant is a root-mean-square blending of those components. This requires examination of the results in Appendix C and in

Reference [3] (for the Hybrid III results). As with the resultant data, the translational component responses are generally similar. The rotational data does show some differences, however. In particular, the Hybrid III head motions displayed lower angular accelerations about the S-I axis (yaw) and consequently lower angular velocities about that axis. Both cadavers and the Hybrid II tests produced higher values about that axis.

An example of the differences between the three surrogates in terms of three-dimensional angular motion can be seen by considering the angular acceleration peak values associated with the stopping of head motion during maximum forward excursion of the surrogate. This motion represents a highly complex three-dimensional motion as the surrogate interacts with the shoulder harness. The medium severity runs were analyzed for the peak values of all three components of angular acceleration and it was found that the mean peak values for the cadavers were the largest in all three directions. The component about the L-R axis (pitch) was the major value with the Hybrid III mean value being 93% of the mean cadaver value, while the Hybrid II was 52%. The components about the A-P(roll) and S-I(yaw) axes were much smaller than the pitch value about the L-R axis (30-40%) but there were interesting variations in the relative magnitudes between the surrogates. For mean peak angular acceleration about the S-I axis, the Hybrid II produced a value that was 79% as great as the cadaver value, while the Hybrid III produced only 35%. For values about the A-P axis the Hybrid II produced 22% and the Hybrid III produced 64% of the value produced by the cadavers. This

indicates that, with respect to the motion resistance of the neck, the stopping motion of the dummies is more restricted in certain directions than it is in the cadavers. It would appear that for motion about the S-I axis the Hybrid III neck is the stiffest while for motion about the A-P axis the Hybrid II neck is the stiffest. These observations are consistent with the construction features of these necks.

6.2.2. Chest Response. It is not possible to mount accelerometers internal to the chest in cadavers. In this test program, the chest accelerometers were mounted externally on both the cadavers and the dummies at levels which were comparable in S-I location to the plane of internally mounted accelerometers in the dummies. Plots of the A-P axis accelerometer data of the dummies (internal and external) and the cadavers (external) are given in Figures 16 through 21 for various test severities. Only the A-P axis data were chosen for comparison because of the different spatial location of the internal and external accelerometers. In the Hybrid II data, the A-P accelerations for both internal and external mounting points are very similar in magnitude and waveform whereas for the Hybrid III, the external data are consistently higher in magnitude (16-29%) and exhibited differences in waveform, particularly during the rebound or unloading phase of the traces.

Comparison of the external A-P accelerometer data from all three surrogates (Figures 19, 20 and 21) shows that the magnitudes and waveforms of the two dummies are generally comparable to those

obtained with the cadavers. The cadaver responses were more variable and of a more oscillatory nature which may be due to rib fracture effects and vertebral body motions not present with the dummies.

6.2.3. Pelvis Response. As with the chest accelerometers, it was not possible to mount the pelvis accelerometers internally in the cadavers. Figures 22, 23 and 24 present the A-P acceleration traces for the internally mounted dummy accelerometers while Figures 25, 26 and 27 present the comparable externally mounted data for the cadavers and dummies. The Hybrid III external peak values tended to be consistently higher (approximately 30%) than the internal values while the Hybrid II external values were consistently lower than the internal values.

The cadaver data exhibited broader waveforms with lower peak values than the comparable dummy data. The dummy responses also featured an initial acceleration spike which was much more pronounced than that which occurred with the cadavers. These differences in response may be related to differences in pelvic mass distribution and chest-pelvis linkages.

6.2.4. Restraint System Loads. The restraint system load data are presented in Figures 28, 29 and 30 (upper shoulder belt loads), Figures 31, 32 and 33 (lower shoulder belt loads), Figures 34, 35 and 36 (left lap belt loads) and Figures 37, 38 and 39 (right lap belt loads). The upper shoulder belt data for the three surrogates

were generally comparable in magnitude (although the variations in cadaver subject weight caused some individual traces to vary greatly from the mean data) but the cadaver responses exhibited longer duration waveforms than those for the dummies. Some differences were evident in the lap belt magnitudes, particularly the right lap belt values (which include the shoulder harness loads). These discrepancies may reflect differences in the structural linkages between the torso and the lower body as well as mass distribution differences between the surrogates.

Chapter 7

C O N C L U S I O N S

The general objective of the WBR program was to generate data on the kinematic response of human surrogates, restrained by a three-point belt system and subjected to a realistic automotive impact environment. The immediate objectives were to develop, demonstrate and employ the techniques necessary for measurement of the kinematic response.

Evaluation of this research effort should be based on the success in achieving the goals defined at the onset of the program and modified during its course. Consideration should also be given to the indirect benefits gained from the experimental and analytical techniques developed for use in this program but are of general applicability in other research programs. Finally, the overall merits of this program cannot be completely assessed until the generated data is put to actual use for improvement of the anthropometric test devices and mathematical models.

7.1. Experimental Methods

Procedures for handling and preparing cadavers for a sled test were developed. These include a step-by-step protocol for moving, storing and placing the cadaver for surgery, x-raying and for testing. Instrumentation mounting techniques were also developed to

allow effective and reliable monitoring of various transducer signals. Thus, transducers were mounted on the skull for measurement of the head motion and on the thoracic spine and pelvic complex to measure the chest and pelvis accelerations.

7.2. Analytical Methods

Several new analytical techniques were developed, validated and applied during this program. Some were initiated, but were not completely ready for application until the final year.

The new analytical procedures that were developed, in part for this program, include a general-purpose digital filtering technique, a three-dimensional motion analysis program to measure the motion of the head or any other rigid body, a three-dimensional x-ray technique to locate implanted instrumentation and, finally, an improved Head Injury Criterion (HIC) computation algorithm. All these are described in detail in Appendix A.

7.3. Computer Simulations

The computer simulations carried out for this program produced four major accomplishments. First, it has demonstrated that a two-dimensional whole-body motion model can be used effectively for simulating important events of a crash history which include large motions in three dimensions. Second, the study has demonstrated that anthropometric and biomechanical data developed for the head and neck of the MVMA 2-D model are reasonable, while at the same time suggesting significant improvements that might be made in the

7. CONCLUSIONS

joint model. Third, this study has provided an additional degree of validation of a crash victim simulator which is finding more and more use as a research tool. Finally, the degree of agreement between predicted and experimental head and neck responses suggests that research programs combining computer simulations with instrumented tests might be particularly productive.

7.4. Some Aspects of the Results

The discussion of experimental results (Chapter 6) emphasized the differences between the responses of various surrogates. In particular, the discussion pointed out some of the factors influencing the experimental results and concluded that repeated runs on the same cadaver did not invalidate the results of the second run, and that embalming did not significantly affect the response measures.

The discussion of Chapter 6 included a comparison of responses of the various tested human surrogates. Specifically, it was concluded that the head-neck response is consistent with the physical construction of the various necks. It was also concluded that the chest response of both Hybrids II and III, as measured by spinal accelerometers, is in general agreement with that of the cadavers, although the cadaver chest response were more variable and oscillatory, which may be attributed to rib fracture effects and vertebral body motions not present in either dummy. The pelvic response of cadavers had a broader waveform than that of the dummies, but all were in general agreement. Any discrepancies may

be due to differences in the pelvic mass distribution and chest-pelvis linkages. Similar observations may be made about the restraint system loads.

A great deal of kinematic response data has been generated by the WBR program. Analyses of this data depend to a great extent upon the specific objective of the investigator. Through detailed examinations, of the type presented in Chapter 6, it is possible to attain the ultimate objectives of this program, namely, to identify similarities and differences in kinematic response of the various types of surrogates, and to point out areas that need improvement in anthropomorphic test devices and in development of mathematical models.

<

Chapter 8

R E F E R E N C E S

1. J.W. Melvin, N.M. Alem, and J.B. Benson, Whole-Body Response Research Program. First Year Final Report, HSRI, March 11, 1975, 84 p., Report No. UM-HSRI-BI-75-1. Sponsored by GMRL, Biomedical Science Division.
2. N.M. Alem, J.B. Benson, and J.W. Melvin, Whole-Body Response Research Program. Second Year Final Report, HSRI, January, 1976, 473 p., Report No. UM-HSRI-76-3. Sponsored by GMRL, Biomedical Science Division.
3. N.M. Alem, J.B. Benson, and J.W. Melvin, Whole-Body Response of the Hybrid-III Anthropomorphic Test Device. Final Report, HSRI, February, 1977, 235 p., Report No. UM-HSRI-77-10. Sponsored by GMRL, Biomedical Science Division.
4. R.L. Stalnaker, et al., Validation Studies for Head Impact Injury Model. Final Report, HSRI, June 1976, 541 p., Report No. UM-HSRI-76-14. Prepared for DOT/NHSTA under Contract No. DOT-HS-031-3-749.
5. Third Annual International Workshop on Human Subjects for Biomechanical Research, San Diego, California, November 19, 1975.
6. N.M. Alem, R.L. Stalnaker, and J.W. Melvin, "Measurement of Head Impact Response." Proceedings of the Third International Conference on Impact Trauma, Berlin, Germany, September 7-8, 1977, pp. 152-164. IRCOBI Secretariat, Bron, France.
7. R.L. Stalnaker et al., "Head Impact Response." Proceedings of Twenty-First Stapp Car Crash Conference, New Orleans, La., October 19-21, 1977, pp. 305-335. SAE Paper No. 770921, Society of Automotive Engineers, Warrendale, Pa.
8. N.M. Alem and G.S. Holstein, Measurement of 3-D Motion. HSRI, October 1977, 28 p., Report No. UM-HSRI-77-46. Also Presented at the Fifth Annual International Workshop on Human Subjects for Biomechanical Research, October 1977, New Orleans, La.
9. N.M. Alem, J.W. Melvin, and G.S. Holstein, "Biomechanics Applications of Direct Linear Transformation in Close-Range Photogrammetry." Proceedings of 6th Annual New England Bioengineering Conference, March 1978, Kingston, Rhode Island.

10. Department of Transportation, National Highway Traffic Safety Administration, Docket Number 69-7, Notice 19, "Occupant Crash Protection -- Head Injury Criteria." Part S6.2 of FMVSS 208.
11. C.C. Chou and G.W. Nyquist, "Analytical Studies of the Head Injury Criterion (HIC)." Presented at 1974 SAE Automotive Engineering Congress, Detroit. SAE Paper 740082, Society of Automotive Engineers, Inc., Warrendale, Pa.
12. B.M. Bowman, D.H. Robbins, and R.O. Bennett, MVMA Two-Dimensional Crash Victim Simulation Tutorial System: Self-Study Guide and Audio-Visual Program (two volumes). Prepared for Motor Vehicle Manufacturers Association, Detroit. HSRI, April 1977, 695 p., Report No. UM-HSRI-BI-77-18-1,2.
13. D.R. Foust, B.M. Bowman, and R.G. Snyder, "Study of Human Impact Tolerance Using Investigations and Simulations of Free Falls." Proceedings of the Twenty-First Stapp Car Crash Conference, October 1977. SAE Paper 770915, Society of Automotive Engineers, Inc., Warrendale, Pa.
14. R.G. Snyder, D.R. Foust, and B.M. Bowman, Study of Impact Tolerance Through Free Fall Investigation. Final Report, HSRI, December 1977, 307 p., 307 p., Report No. UM-HSRI-77-8. Sponsored by the Insurance Institute for Highway Safety, Washington, D.C.
15. L.W. Schneider, et al., A Prediction of Response of the Head and Neck of Adult Military Population to Dynamic Impact Acceleration. 12 Months Technical Report, HSRI, May 1976, 163 p., Report No. UM-HSRI-76-10. Sponsored by the Office of Naval Research, Contract No. N00014-75-1077.
16. L.W. Schneider and B.M. Bowman, "Prediction of Head/Neck Dynamic Response of Selected Military Subjects to -Gx Acceleration." Proceedings of Symposium on Biodynamic Models, Dayton, February 1977. Aviation, Space and Environmental Medicine, January 1978.
17. H.J. Mertz and L.M. Patrick, "Strength and Response of the Human Neck." Proceedings of the Fifteenth Stapp Car Crash Conference, November 1971. SAE Paper 710855, Society of Automotive Engineers, Inc., Warrendale, Pa.

